NASA CR-135001

FINAL REPORT

FIBER COMPOSITE FAN BLADE IMPACT IMPROVEMENT

by

J. GRAFF, L. STOLTZE, E.M. VARHOLAK

HAMILTON STANDARD
DIVIDION OF UNITED TECHNOLOGIES CORPORATION
WINDSOR LOCKS, CONNECTICUT 06096

PREPARED FOR

NATIONAL AERONAUTICS AND SPACE ADMINISTRATION

CONTRACT NAS3-17837

NASA LEWIS RESEARCH CENTER
CLEVELAND, OHIO

J. FADDOUL, PROJECT MANAGER

DISCLAIMER NOTICE

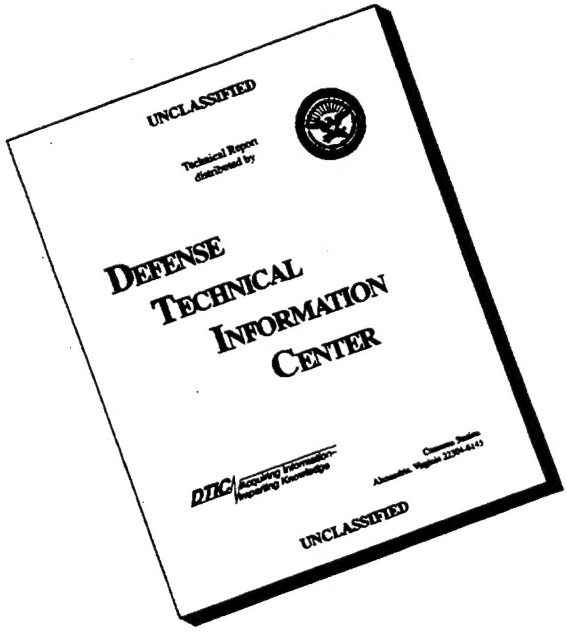

THIS DOCUMENT IS BEST QUALITY AVAILABLE. THE COPY FURNISHED TO DTIC CONTAINED A SIGNIFICANT NUMBER OF PAGES WHICH DO NOT REPRODUCE LEGIBLY.

1. Report No.	2. Government Accession No.	3. Recipient's Catalog No.
NASA CR-135001		

4. Title and Subtitle	5. Report Date
Fiber Composite Fan Blade Impact Improvement	February, 1976
	6. Performing Organization Code

7. Author(s)	8. Performing Organization Report No.
Graff J., Stoltze L., Varholak E. M.	HSER 6968
	10. Work Unit No.

9. Performing Organization Name and Address	11. Contract or Grant No.
Hamilton Standard Division Division of United Aircraft Corp. Windsor Locks, Conn. 06096	NAS3-17837
	13. Type of Report and Period Covered
12. Sponsoring Agency Name and Address National Aeronautics and Space Administration Washington, D.C. 20546	Contractor Final Report
	14. Sponsoring Agency Code

15. Supplementary Notes

Project Manager, J. Faddoul
Materials and Structures Division
NASA Lewis Research Center, Cleveland, Ohio

16. Abstract

This report presents the results of a program conducted between July, 1974 and Nov. 1975 under NASA-Lewis Contract NAS3-17837. The objective of this program was to demonstrate the improved foreign object damage resistance of Hamilton Standard's metal matrix advanced composite fan blade which was developed beginning in 1973. The contract program included the fabrication, whirl impact test and subsequent evaluation of nine advanced composite fan blades of the "QCSEE" type design. The blades were designed to operate at a tip speed of 282 m/sec. (925 fps). The blade design was the spar/shell type, consisting of a titanium spar and boron/aluminum composite airfoils. The blade retention was designed to rock on impact with large birds, thereby reducing the blade bending stresses.

The program demonstrated the ability of the blades to sustain impacts with up to 681 g (24 oz) slices of birds at 0.38 rad with little damage (only 1.4% max weight loss) and 788 g (27.8 oz) slices of birds at 0.56 rad with only 3.2% max weight loss. Unbonding did not exceed 1.1% of the post-test blade area during any of the tests. One test using a fixed retention to preclude rocking confirmed improved FOD performance of the rocking retention. Correlation of the Hamilton Standard FOD analysis with the empirical results (strain gauge data in some tests) was very satisfactory, particularly in the prediction of gross loads.

All blades in the post-test condition were judged capable of operation in accordance with the FAA guidelines for medium and large bird impacts.

17. Key Words (Suggested by Author(s))	18. Distribution Statement
Composites Impact Tests Foreign Object Damage (FOD) Boron-Aluminum Fan Blades	Unclassified - Unlimited

19. Security Classif. (of this report)	20. Security Classif. (of this page)	21. No. of Pages	22. Price*
UNCLASSIFIED	UNCLASSIFIED	82	

* For sale by the National Technical Information Service, Springfield, Virginia 22161

FOREWORD

This final report was prepared by the Advanced Composites Applications Group of the Hamilton Standard Division of United Technologies Corporation and covers the program conducted by Hamilton Standard under NASA Lewis Contract NAS3-17837. The program period was July 1974 to November 1975. Project Manager for the NASA Lewis Research Center was Mr. J. Faddoul. Project Manager for Hamilton Standard was Mr. L. Stoltze. Fabrication of the test blades was under the direction of Mr. E. Varholak and Mr. R. Walters. Testing was under the direction of Mr. J. Graff.

Other individuals making significant contributions to this program were:

Design	Mr. E. Rothman, Mr. C.E.K. Carlson
Analysis	Dr. R. Cornell, Mr. N. Houtz, Mr. J. Marti
Fabrication	Mr. E. Havens, Mr. G. Charette, Mr. H. Nutter
NDI	Mr. E. Carlson
Materials	Mr. E. Delgrosso
Testing	Mr. A. Fletcher, Mr. J. Korecki, Mr. R. Scalise

TABLE OF CONTENTS

LIST OF ILLUSTRATIONS

LIST OF ILLUSTRATIONS (CONTINUED)

LIST OF TABLES

SUMMARY

This report presents the results of a program conducted between July, 1974, and November, 1975, under NASA-Lewis Contract NAS3-17837. The objective of this program was to demonstrate the improved foreign object damage resistance of Hamilton Standard's metal matrix advanced composite fan blade which was developed beginning in 1973. The contract program included the fabrication, whirl impact test and subsequent evaluation of nine advanced composite fan blades of the Quiet Clean Short-haul Experimental Engine ("QCSEE") type. The blades were designed using advanced FOD analytical techniques recently developed by Hamilton Standard. The design was also supported by numerous materials systems evaluations to define the optimum blade constituents. The blades, 22 per stage in the Hamilton Standard design, were designed to operate at 282 m/s (925 fps.). The blade span was 46.2 cm (18.2 in). The blade construction consisted of a Ti-6Al-4V titanium spar which provided retention feature and extended into the airfoil. This spar was adhesively bonded to titanium foil covered Borsic® /Al shells which formed the airfoils. The cavities fore and aft of the spar, between the Borsic/aluminum airfoils contained aluminum honeycomb. An Inconel 625 leading edge sheath provided resistance to damage from hard objects as well as from birds. The blade retention used a ball type bearing similar to that used in variable pitch propellers. The retention was sized to function normally except when the blade was impacted by a large mass. In this circumstance, the bending moment generated by the impact would, by exceeding the centrifugal restoring moment, cause the blade to rock thereby reducing the blade bending stresses. Adhesive bond joints were used in this blade design. However, the use of metal matrix composite shells in place of previously used epoxy matrix was expected to significantly increase the interlaminar shear strength of the blade structure, and, thereby, significantly increase the impact capability of the blade.

The nine blades fabricated in this program were subjected to eleven tests ranging from impacts with 5.08 cm iceballs to 1400 g real and simulated birds. The blade impact location was the 0.8 span. The blades were evaluated at two impact angles, 0.38 rad (22°) and 0.56 rad (32°), to determine the blade impact resistance at simulated takeoff and climb conditions. In one test at 0.56 rad impact angle, the retention was modified to prevent rocking; in all other tests, the flexible retention design was utilized. Four of the test blades were instrumented to measure blade impact strains for correlation with the FOD analysis predictions.

The 5.08 cm (2 in) iceball tests at both impact angles resulted in slight leading edge denting. No other damage due to impact was detected. At the 0.38 rad (22°) impact angle, the blades were impacted with bird slices weighing up to 681 g (24 oz). No weight loss was sustained with slices weighing up to 372 g (13.1 oz) and only minor weight loss (1.4%) occurred as the result of slices in excess of 681 g (24 oz). When weight loss did occur it was at the tip trailing edge of the blade. In all cases, the leading edge was slightly dented but otherwise structurally sound. At the 0.56 rad (32°) impact angle,

only minor weight loss (2%) occurred as the result of impact with bird slices weighing up to 440 g (15.5 oz). The damage to those blades was similar to that of the blades tested at 0.38 rad (22°), i.e., trailing edge only. Additional tests at 0.56 rad (32°) included bird slices up to 788 g (27.8 oz). The resulting damage to these blades in addition to trailing edge damage included material separation from the leading edge outboard of the blade midspan. Total material loss was always less than 3.2%. Unbonds were predominantly local to the impact site or near the inboard end of the shell, but did not exceed 1.1% after any of the tests. The rigid retention test (1400 g bird) resulted in slightly more damage at the impact site (4.7% weight loss) but appeared similar to the other large bird impacts. All blades in the post-test condition were judged capable of operation in accordance with the FAA medium and large bird impact requirements.

Both real and modified gelatin simulated birds were used in this program. Blade damage resulting from impact with both impact objects appeared very similar demonstrating the adequacy of the modified gelatin simulation.

Correlation of the FOD analysis with the experimental blade impact test results was satisfactory particularly in the prediction of gross blade loads.

This program demonstrated the improvement in composite fan blade technology realized over the last three years. This technology has resulted in the development of large composite fan blades which are lighter than, and which are judged to match the FOD resistance of, conventional titanium blades.

INTRODUCTION

In 1972 - 1973, Hamilton Standard and two other blade manufacturers conducted a program for NASA Lewis to establish the foreign object damage (FOD) resistance of then current off the shelf composite fan blade designs selected for their applicability to the fan stage of Q-Fan type engines. Hamilton Standard conducted its program under NASA-Lewis contract NAS3-16778 (NASA CR-134521). The Hamilton Standard test blade design was a boron/epoxy shell, titanium spar blade similar in configuration to that used in noise and aerodynamic studies in a previous NASA Lewis contract. Based on the impact tests conducted, Hamilton Standard concluded that current fan blade configurations could withstand impact with a 280 g (10 oz) slice of a bird with moderate damage. The blades survived iceball, stone, bolt, nut and rivet impact with little damage.

Subsequent to the NAS3-16778 contract, Hamilton Standard continued its efforts to develop Q-Fan blade configurations capable of withstanding impact with large birds. These efforts comprised a multi-faceted program and included analytical and experimental development of fan blade impact design techniques, materials evaluation to determine optimum FOD resistant blade materials, the design of a QCSEE type fan blade, blade tool design, tool manufacture and blade manufacturing process development.

The program reported herein was funded by NASA and was a continuation of the work initiated under the Hamilton Standard program to develop fan blades which conform to FAA requirements (Ref. 1). Under NASA contract, FOD evaluations were made of 9 fan blades designed to be structurally representative of QCSEE type fan jet engine blades. The design incorporated the latest state-of-the-art advances in metal matrix advanced composites. The NASA program was conducted in three phases: fabrication, testing and evaluation of the blades to determine the effects of impact on structural integrity. The nine contract fan blades that were fabricated were subjected to eleven tests. These tests consisted of striking whirling blades with foreign objects ranging from 5.08 cm (2 in) iceballs to simulated and real birds weighing 300 g (10.6 oz) to 1400 g (49.3 oz). Testing was conducted in a whirl cell at Hamilton Standard designed to inject foreign objects in a repeatable fashion. High speed film was utilized to verify and record the impacts.

Examination of the blades tested herein firmly supports the judgement that this spar-shell design is capable of withstanding impact of medium and large bird sizes in accordance with FAA acceptance criteria. As such, blades impacted with birds 890 g (32 oz) or less were judged capable of supporting continued engine operation at 75% power level. The blades impacted with birds up to 1576 g (55.5 oz) were judged to be in a condition permitting a controlled engine shut-down.

DISCUSSION

FAN BLADE DESIGN

General

The primary objective of this contract was to demonstrate via test a composite blade with the structural characteristics necessary to sustain impact with medium and large size birds in conformance with the requirements of the FAA. These are interpreted to include the ability to continue operation at reduced power for a specified period after impact with a medium size bird (900 g or less) and to allow a controlled shutdown after impact with a large bird (1400 g or larger). The chosen fan blade design was sized to conform approximately to the requirements of current QCSEE variable pitch fans. The selected fan stage design contains 22 circular arc airfoil blades and is 1.78 m, (70 in) in diameter. The blade is comparable in length to the 1.83 m, (6 ft) Q-Fan blade tested under NAS3-16778 in 1973 and width and thickness ratios for both blades are presented in Figures 1 and 2. Fan tip speed is 282 m/s, (925 fps). Pressure ratio is 1.325. FOD analytical techniques being developed by Hamilton Standard under IR&D programs, were employed extensively in the design of the fan blade. These techniques will be discussed in detail later in this report.

The fan blade design consists of three primary elements: a spar, a leading edge sheath and a shell set. The blade is shown conceptually in Figures 3 and 4. A complete blade is shown in Figure 5. As shown in Figure 3, the airfoil has been rotated slightly producing approximately a 0.087 rad (5°) sweep of the blade leading edge to the spar. This modification was made to reduce the overhang of the leading edge over the spar and, thereby, reduce the blade airfoil stresses at the impact sight. The airfoil rotation modification was selected to minimize the effects on tooling activity in progress when improvements in the FOD analysis permitted more reliable analysis of the blade stresses at the impact sight. This analysis predicted excessive local blade stressing for the 1400 g bird impact condition. The effect of this modification on blade performance, other than FOD, was minimal. The spars were machined from Ti-6Al-4V titanium. The spar inboard end was machined to provide a circular rocking retention and variable pitch capability. The retention was designed to rock up to 0.279 rad (16°) in reacting to the impact load of a three-pound bird and is shown conceptually in Figure 6. The essential components of this retention are the outer race, inner race, wire ring and anti-torque lever. Normally, balls are used instead of the wire ring for pitch change operation. However, the wire ring was used in this program to reduce cost and lead time. The anti-torque lever simulated the link between the blade and the variable pitch actuator. For test purposes, the lever was restrained in a narrow slot machined in the retention sleeve. The lever was pinned to the base of the blade to allow blade rocking. The angle between the lever pin and the impact station was selected to allow rocking of the blade during impact while restraining the torsional motion in the blade retention. The entire sleeve assembly was turned in the test hub to set blade angle.

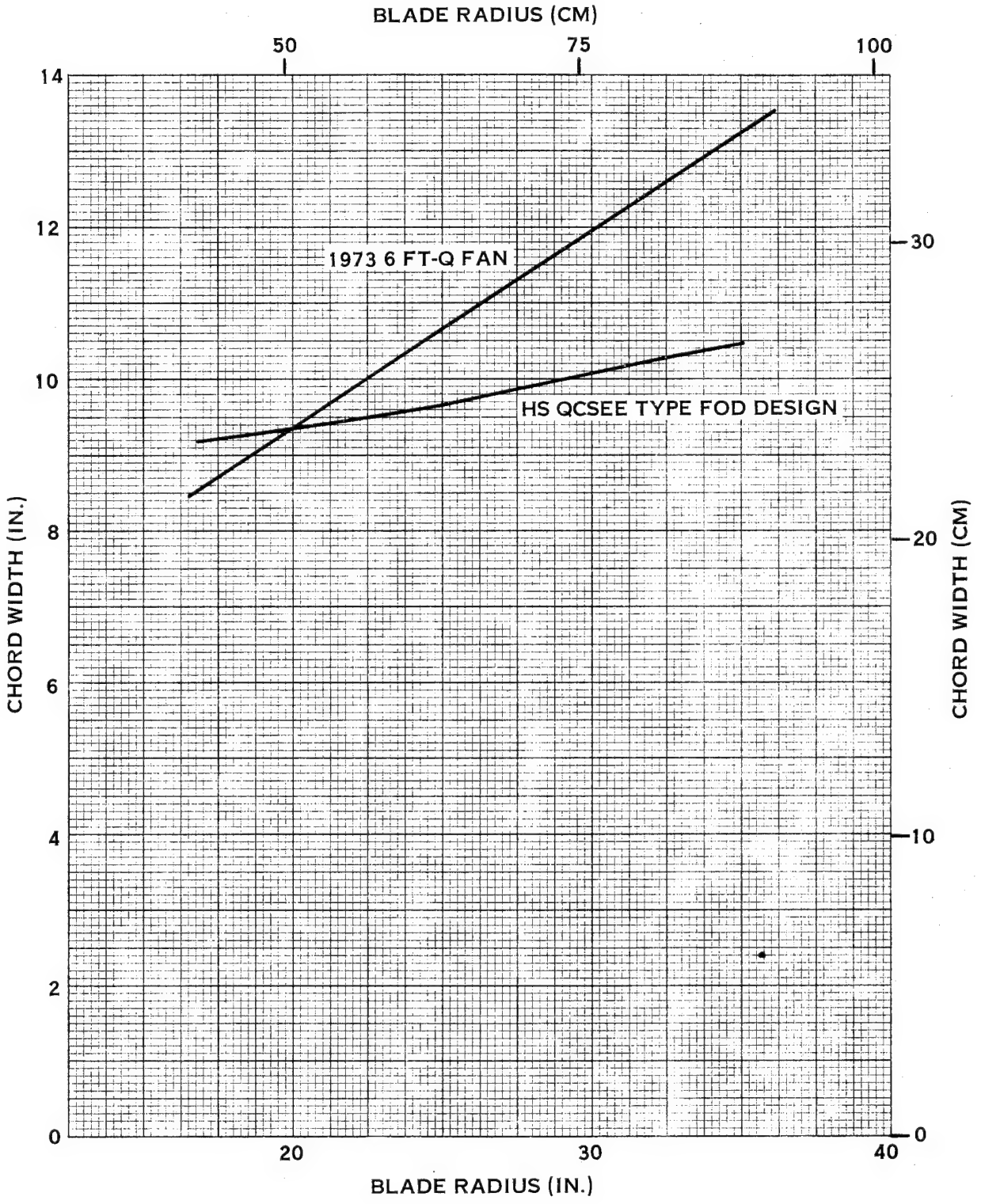

FIGURE 1. HAMILTON STANDARD QCSEE TYPE FOD BLADE CHORD WIDTH VS RADIUS

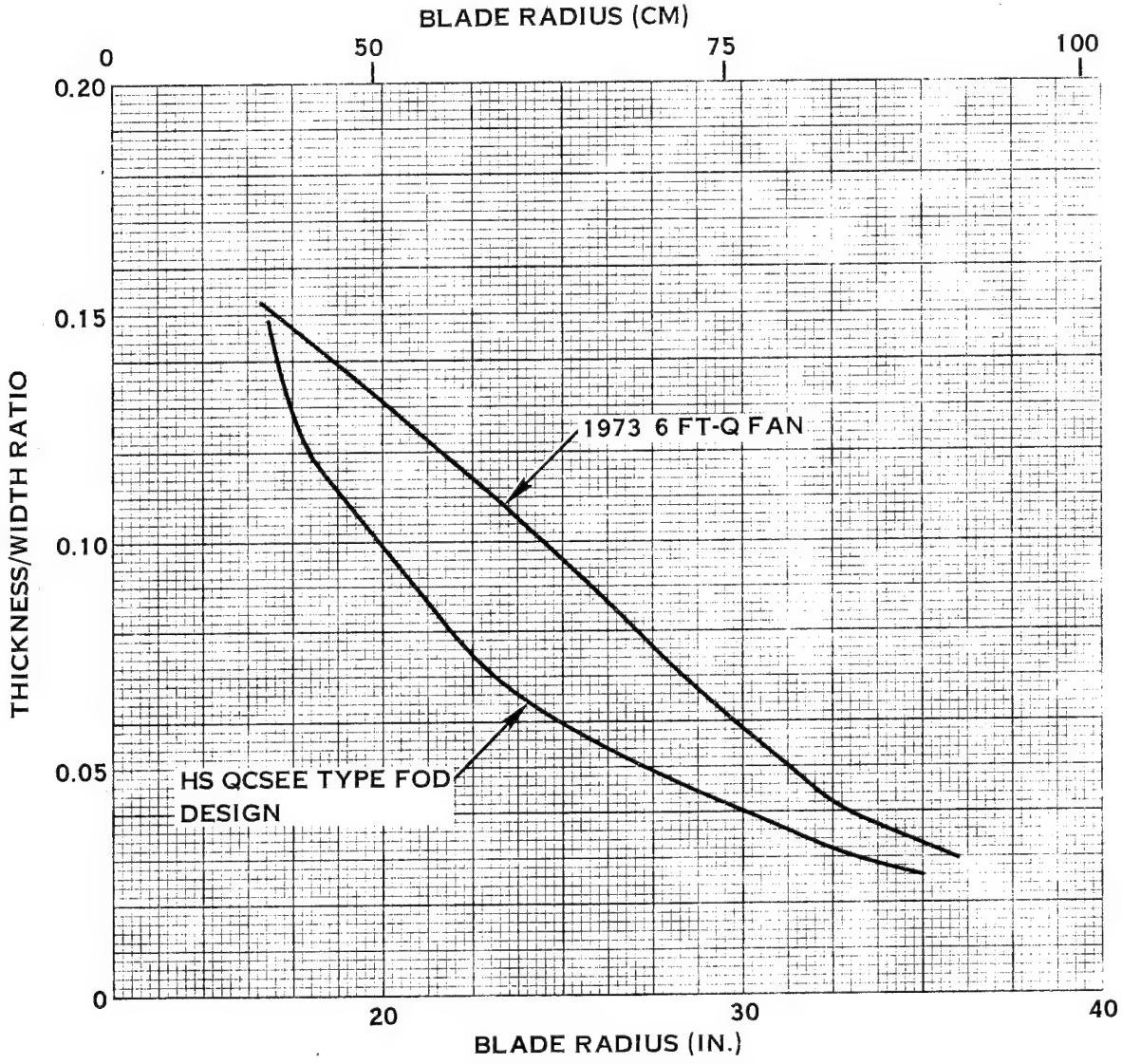

FIGURE 2. HAMILTON STANDARD QCSEE TYPE FOD BLADE THICKNESS RATIO VS BLADE RADIUS

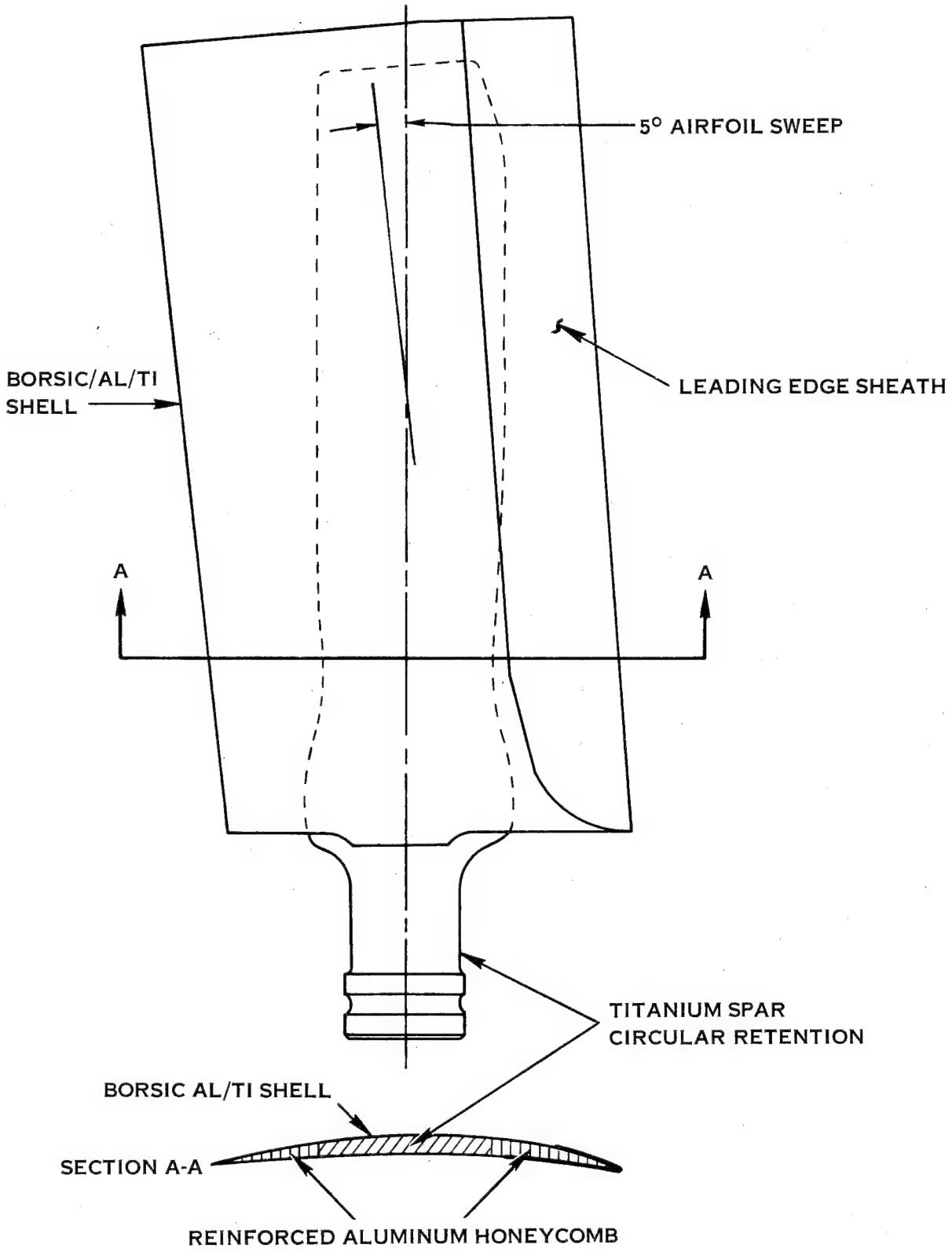

FIGURE 3. HAMILTON STANDARD QCSEE TYPE FOD FAN BLADE DESIGN CONFIGURATION

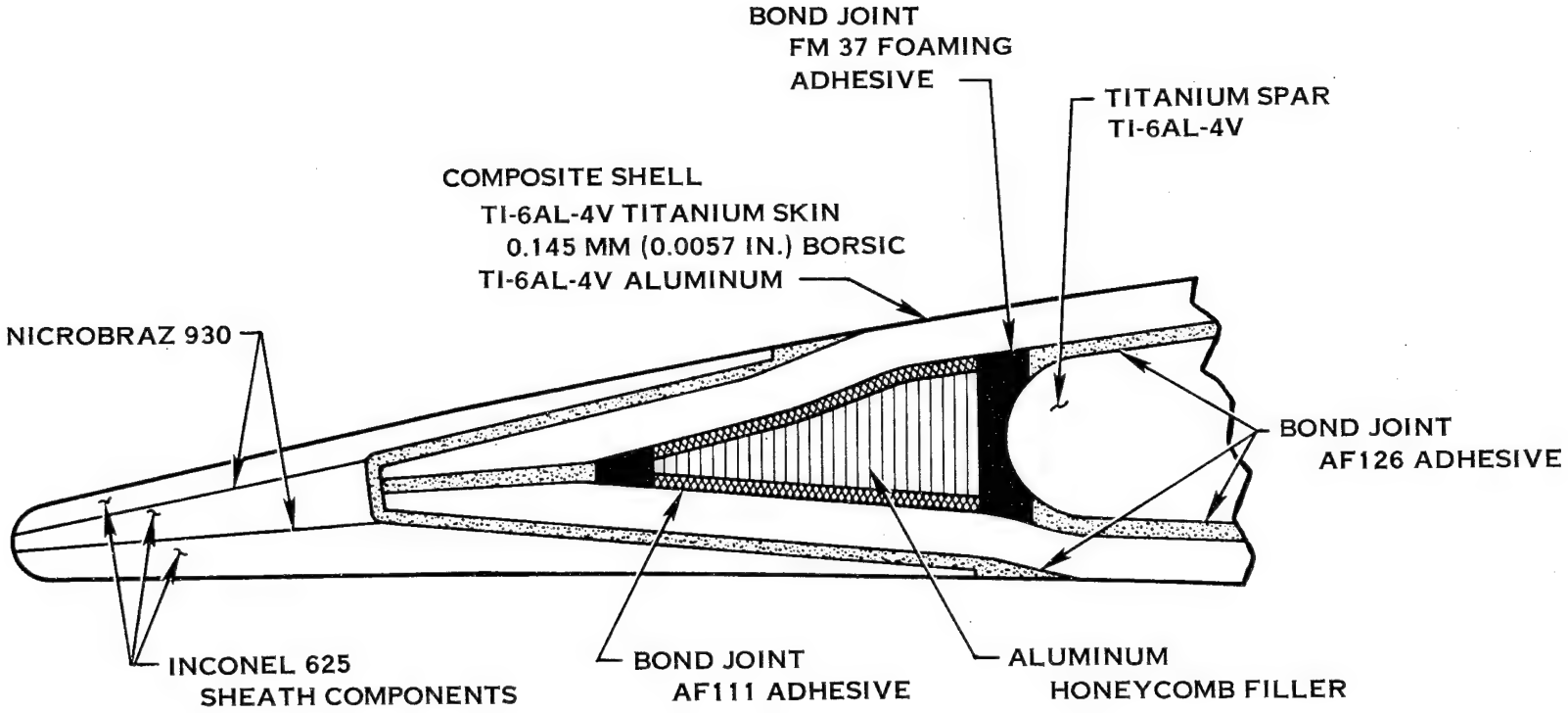

FIGURE 4. TYPICAL FAN BLADE LEADING EDGE CROSS-SECTION SCHEMATIC

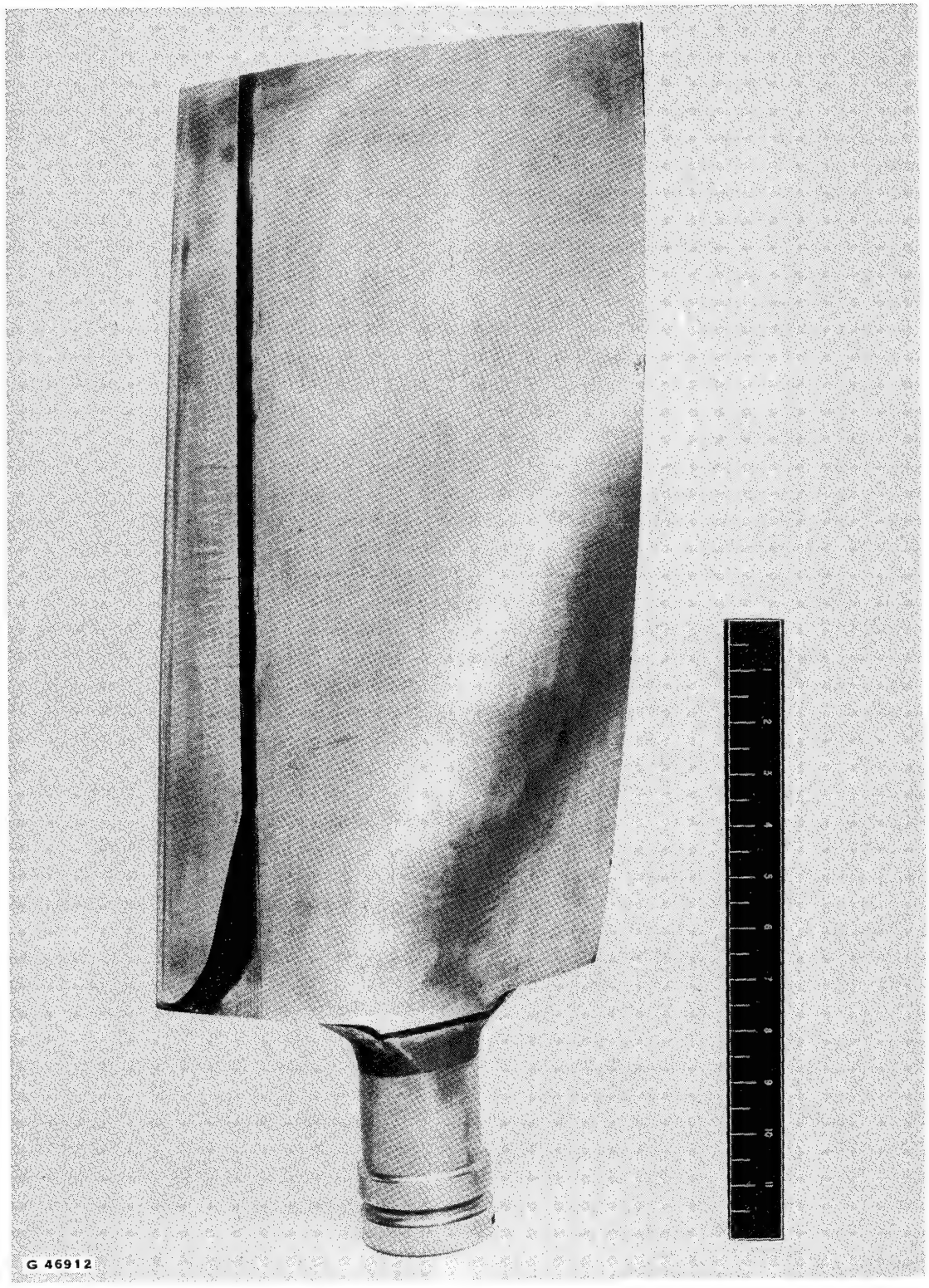

FIGURE 5. HAMILTON STANDARD QCSEE TYPE FOD FAN BLADE

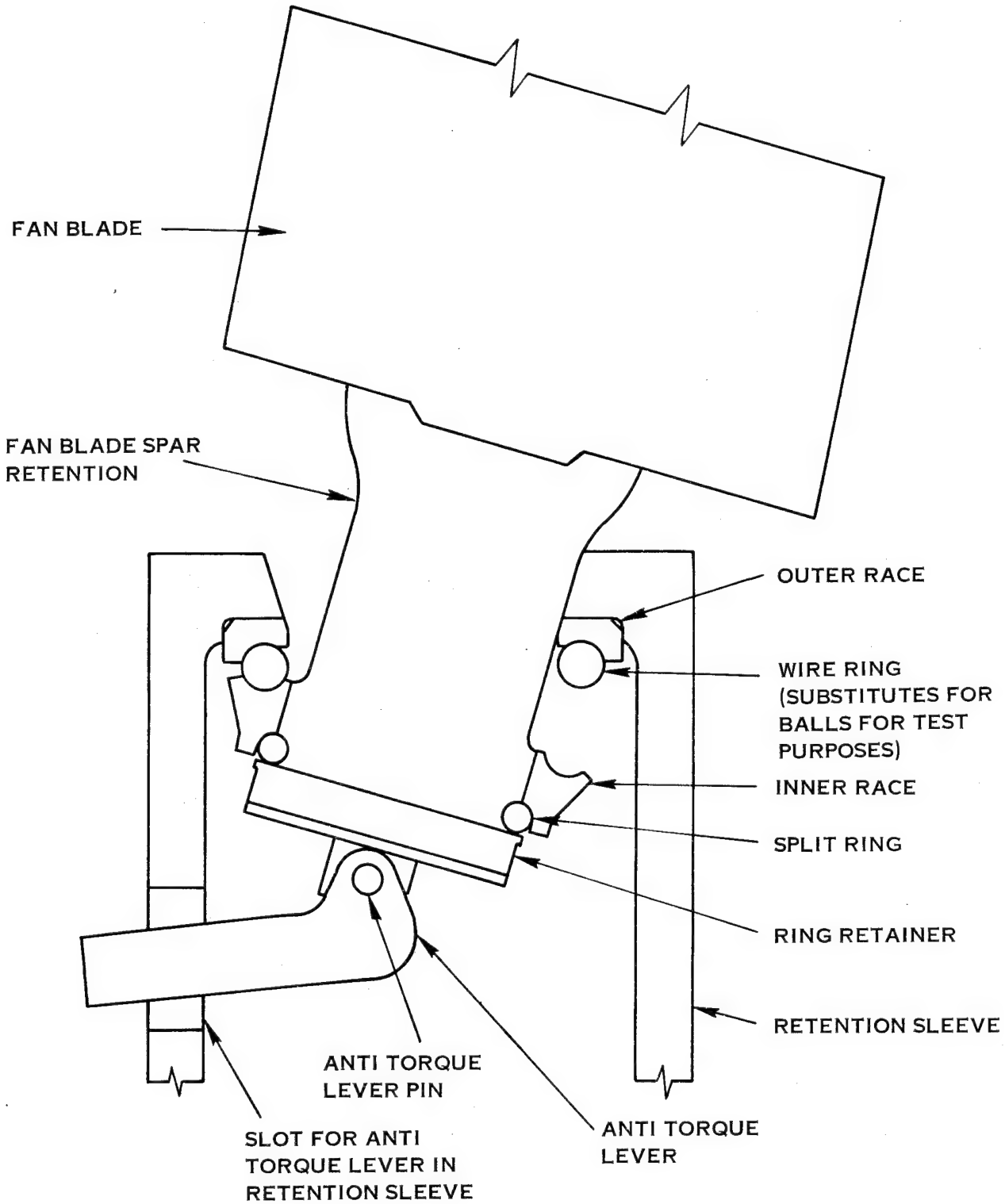

FIGURE 6. QCSEE TYPE FOD FAN BLADE RETENTION SCHEMATIC (IN ROCKED POSITION)

The blade shell structure consists of layers of 0.145 mm, (5.7 mil) Borsic® filament in a 6061 aluminum matrix. An integrally bonded layer of AMS4901 (commercially pure) titanium foil forms the outside shell surface and served to provide surface erosion and corrosion protection. The shells were fabricated using an air diffusion bonding process. A schematic representation of the shell ply thickness distribution is shown in Figure 7. Ply orientations for the shell layup were at ± 0.79 rad, (± 45°) and 1.57 rad, (90°) to the radial axis of the blade. Several other shell ply orientations were evaluated in the Hamilton Standard development program. Of the orientations that showed high impact resistance, the selected orientation was most compatible with the blade shell inboard ending requirements. The shells were bonded to each other and to the spar with AF-126-2 adhesive, an adhesive selected for its superior peel resistance. The cavities forward and aft of the spar, between the shells, were filled with aluminum honeycomb, 609 kg/m^3 (38 lb/ft^3) density and bonded with AF-111 adhesive, a low viscosity adhesive having favorable wetting and filleting characteristics. The leading edge sheath was made from Inconel 625 nickel stainless steel. This material was selected from a number of candidates on the basis of its overall balance of properties. Evaluations for this selection included the modulus of resilience and modulus of rupture, measures of recoverable distortion and energy absorption before rupture, respectively. The chordwise width of the sheath on the pressure side (face) is greater than that on the suction side (camber) in recognition of normal service erosion patterns and the leading edge is solid for maximum durability in small, hard object impact with stones, bolts, rivets, etc., and to provide blendability for local repairs of nicks that may occur.

Blade Structural Characteristics

The fan blade calculated weight is 5.18 kg (11.4 lb) with a solid titanium spar. Based on test results, however, the blade could be reduced primarily by spar redesign to approximately 3.63 kg (8.0 lb). For comparison, a solid titanium blade of the same geometry, less part span shrouds, was calculated to weigh 7.00 kg (15.4 lb). Therefore, a weight saving of at least 48% is anticipated in the Hamilton Standard design.

The centrifugal load of the blade was calculated to be 351,000 N, (79,000 lb) at 348 rad/s (3323 rpm), 10% overspeed. Since the impact tests were to be conducted in a partially evacuated test chamber, estimates of the aerodynamic loads occurring at this pressure condition were made and used in a steady state stress analysis. These stresses are plotted in Figure 8. Calculated spar stresses were low since vibratory stress was minimal. The higher spar stress in the shank region near the retention was due to a decrease in section area to promote rocking. The shell stress was slightly higher than the spar stress due to its higher modulus. For clarity, only maximum calculated shell stress is presented in Figure 8. Frequencies and critical speeds were calculated and are shown in Figure 9. The 317 rad/s (3030 rpm) line represents the desired blade tip speed of 282 m/s (925 fps). A Campbell diagram also is presented in Figure 9 to show that the critical speeds are adequately separated from the operating speed.

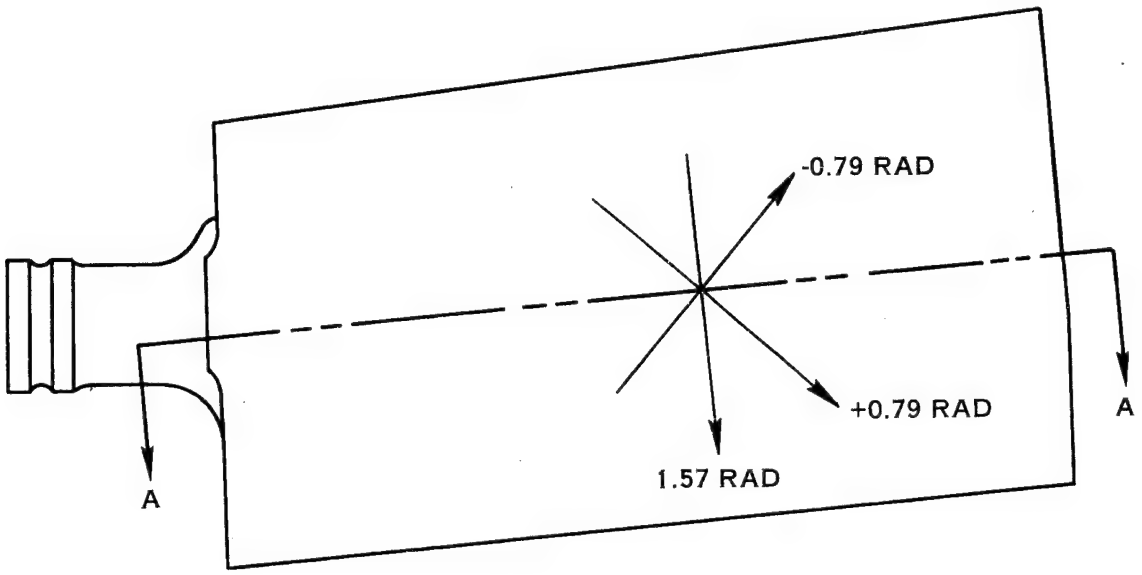

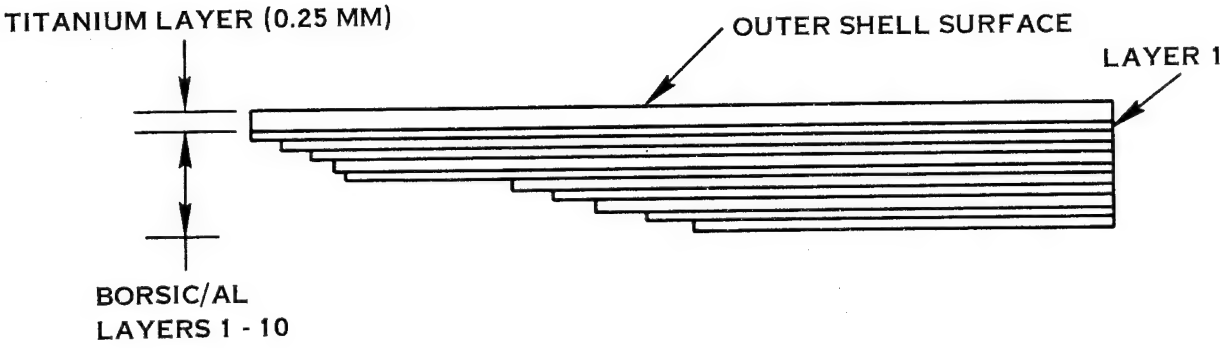

SECTION A-A

COMPOSITE LAYER NO.	1	2	3	4	5	6	7	8	9	10
FIBER ORIENTATION (RADIANS)	1.57	1.57	1.57	+0.79	-0.79	+0.79	-0.79	1.57	1.57	1.57

MATERIAL : 0.145 MM/6061/BORSIC ALUMINUM AND UNALLOYED TITANIUM FOIL

CONDITIONS FOR SHELL DIFFUSION BONDING:
AIR BOND, 811-839° K AT 345 N/M^2

FIGURE 7. SHELL DETAILS - ORIENTATION AND BONDING

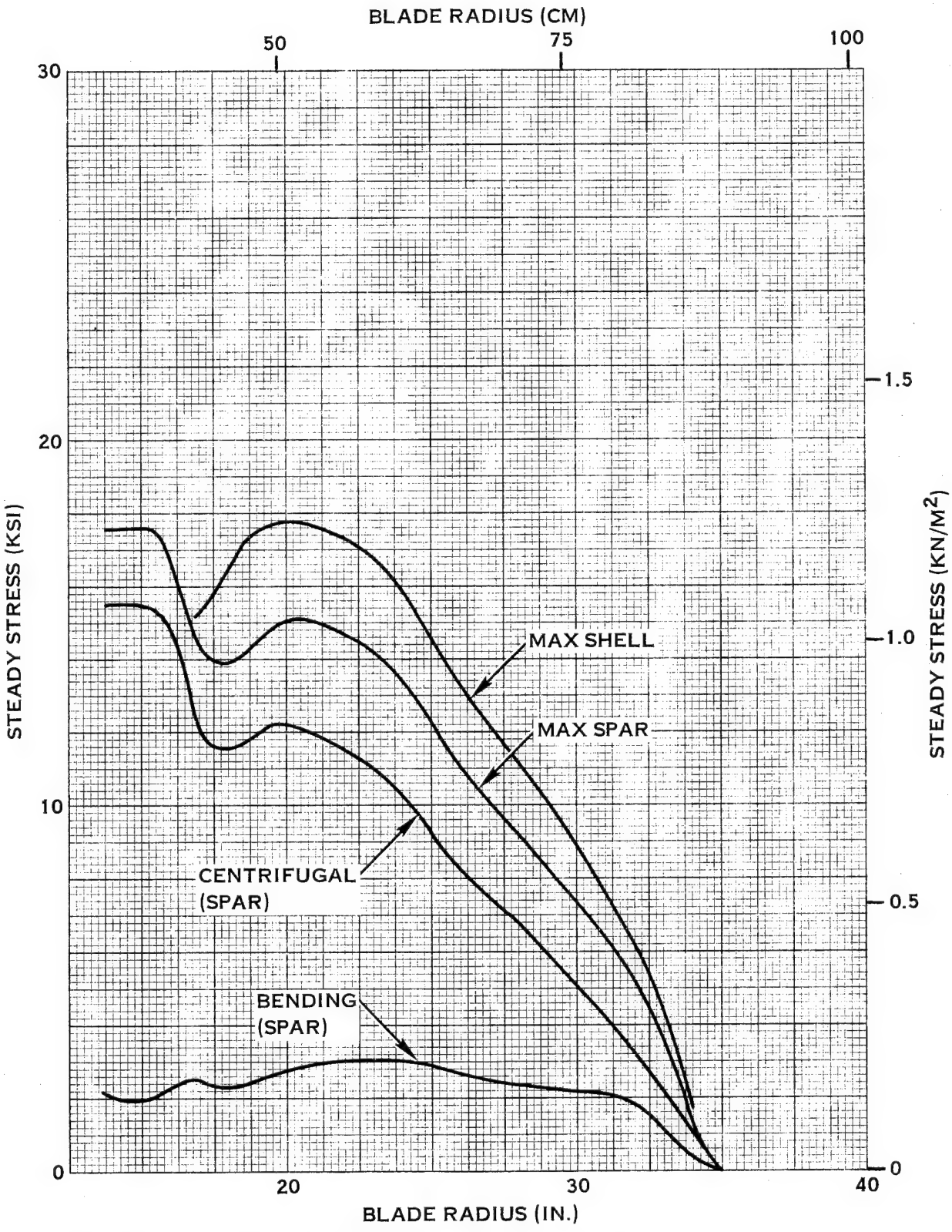

FIGURE 8. QCSEE TYPE FOD FAN BLADE STEADY STRESS VS BLADE RADIUS (110% NORMAL SPEED)

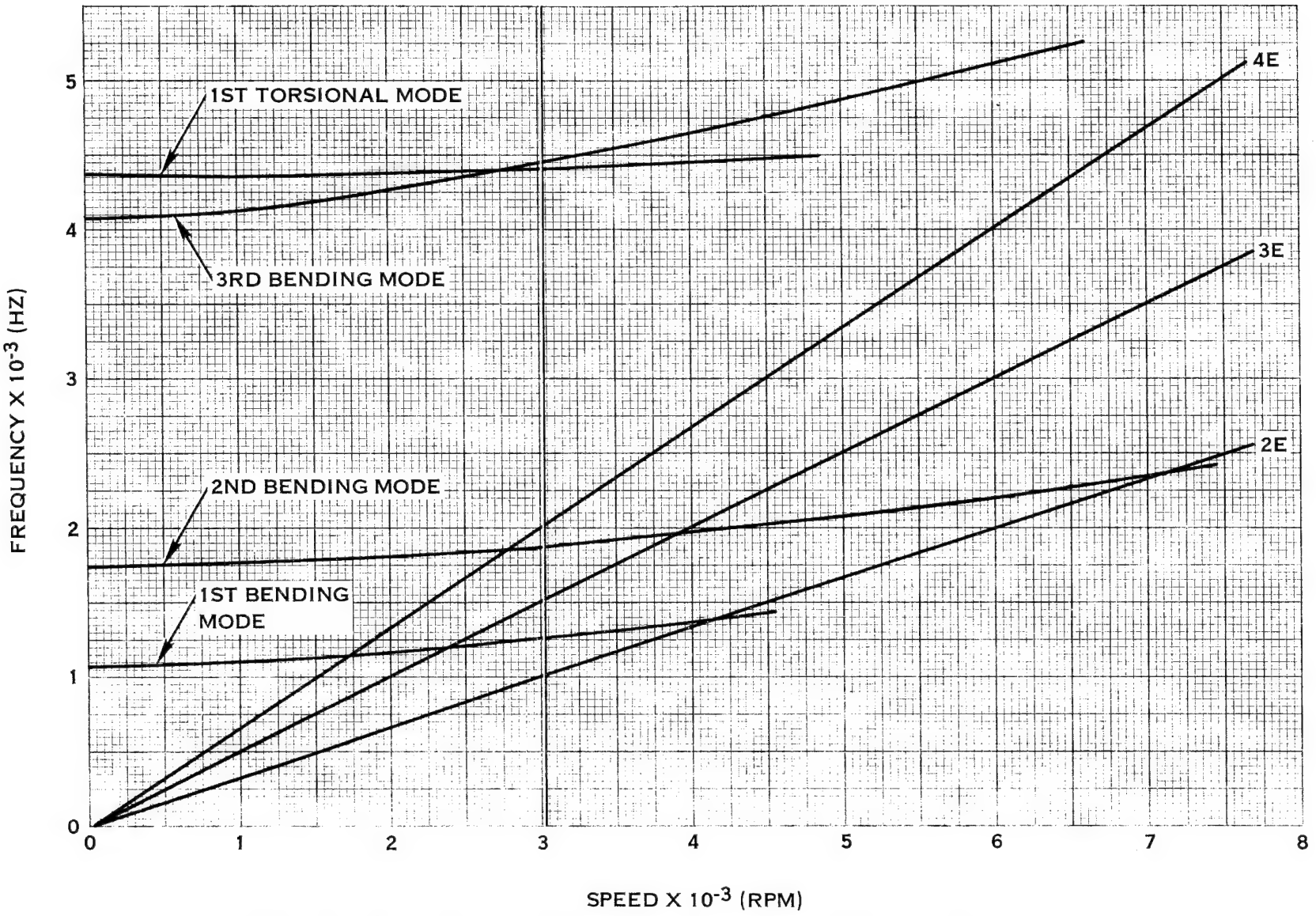

FIGURE 9. QCSEE TYPE FOD FAN BLADE FREQUENCY VS SPEED
BLADE ANGLE = 0.79 RAD @ 0.75R RET. STIFF. = 56.5 nN•M/RAD

Borsic/Aluminum Material Evaluation

Prior to use, the 5.7/6061 Borsic/aluminum material was evaluated by panel fabrication and test to determine the acceptability of the material for use in this program. Minimum allowable 0 and 1.57 rad (0° and 90°) unidirectional tensile strength was 110,320 and 6,895 N/m^2 (160,000 and 10,000 psi), respectively. The results of these tests are shown below:

BORSIC®/ALUMINUM COMPOSITE TAPE VERIFICATION*

		Ultimate Tensile Strength		Tensile Modulus	
Panel No.	Fil. Orient.	$N/m^2 \times 10^{-3}$	psi $\times 10^{-3}$	$N/m^2 \times 10^{-6}$	psi $\times 10^{-6}$
1174A	0 rad.	132	192		
	(0°)	118	171	22.5	32.6
	1.57 rad.	8.7	12.6		
	(90°)	12.5	18.1	13.2	19.2
1174B	0 rad.	159	231		
	(0°)	156	227	22.1	32.1
	1.57 rad.	10.4	15.1		
	(90°)	13.2	19.1	12.8	18.6

*8 ply unidirectional panels, 0.145 mm (5.7 mil) Borsic filament in 6061 aluminum matrix.

3448 N/m^2 (5000 psi) bonding pressure, 30 minutes 839°K (1050°F) vacuum processing.

All other materials were procured and certified in accordance with established Hamilton Standard procurement procedures.

IMPACT TEST PROCEDURES

Impact Object Description

The FOD test fan blades were impact tested using iceballs, simulated birds and real birds. The iceballs were 5.08 cm (2 in) diameter spheres prepared in accordance with Appendix A. The simulated birds were made with gelatin, water and phenolic micro-balloons to produce a specific gravity of approximately 0.69. This density is within the range indicated for real birds in several studies. The simulated birds were cylindrical in configuration and the bird length was twice the bird diameter. Based on these same studies, the 2:1 length to diameter ratio appeared to be reasonable for simulating the proportions of real birds. The configurations of the three simulated bird sizes used and the preparation of the bird simulation material are described in Figure 10. As shown, the gelatin mixture was molded into low density foam casings which stabilized the gelatin during injection into the plane of rotation of the blade.

The real birds used were maintained in a frozen condition until needed. At least 24 hours at room temperature were allowed to insure complete thawing of the bird prior to use in the real bird tests. Photographs of the two birds used (both wild ducks) are shown in Figure 11. These birds were installed in the 1400 g size simulated bird foam casings to keep the bird in the desired strike position during test. They were installed with the breast up and head tucked in over the breast. The feet were secured to the casing to restrain the unstruck section of the bird from subsequently moving into the blade path.

The impact slice size was determined by weighing the bird or bird simulations before and after the impact test. In the case of double hits, the individual slice weights were estimated by movie analysis and by visual examination of the foam collar surrounding the bird. This collar was found in large sections of clearly identifiable thickness after each test and was reconstructed to show the size of the slice through the bird.

Test Facility

The impact tests were conducted in Hamilton Standard's G-5 whirl impact test facility shown in Figure 12. This facility consists of a sealed chamber and a 500 HP electric motor drive to rotate the fan. The chamber was evacuated to approximately 1.7 N/m^2 (2.5 psi) during whirl test to minimize power requirements, blade heatup and windage effects on bird injection timing. The test hub was originally made for four blades but was fitted with only one blade retention adapter into which the test blade was installed. The other blade positions were fitted with balancing counterweights which were sufficiently short to prevent impact with the "foreign object" during fan rotation.

Photographic documentation of the impact tests was accomplished using Fastex and Hycam high speed movie cameras capable of 7000 and 11000 frames per second camera speed, respectively. In most tests, these two cameras were used to obtain views of the blade camber side and the blade tip during the impact event; the tip view was provided by use of a mirror. Lighting of the cell during test required 21 kW of power.

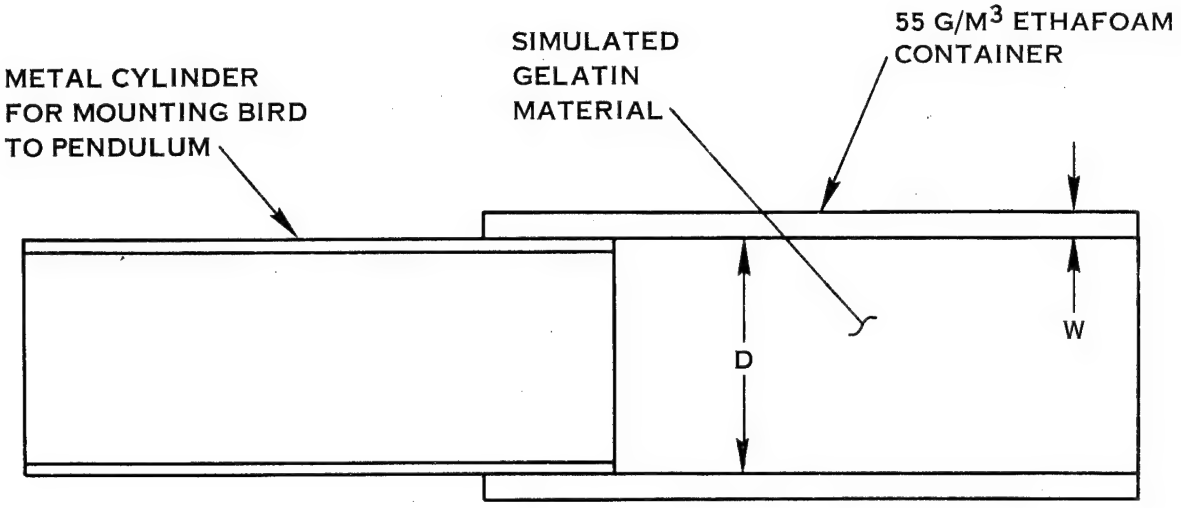

BIRD TYPE	D CM/IN	W CM/IN
300 G SIMULATED	6.50/2.56	0.635/0.250
700 G SIMULATED	8.66/3.41	0.635/0.250
1400 G SIMULATED	10.90/4.29	0.952/0.375
REAL BIRD	10.90/4.29	0.952/0.375

1. THE GELATIN MASS WILL CONSIST OF 18.0% BY WEIGHT INDUSTRIAL GELATIN, SPECIFICATION 275 BLOOM, ATLANTIC INDUSTRIAL GELATIN, MIXTURE WITH 72.0% BY WEIGHT TAP WATER AND 10.0% BY WEIGHT OF 12#/CU. FT. PHENOLIC MICRO BALLOON MATERIAL TYPE BJO 0930 OBTAINABLE FROM ALLIED RESIN CORP., WEYMOUTH INDUSTRIAL PARK, PLEASANT STREET, EAST WEYMOUTH, MA. 02189.

2. SPECIFIC GRAVITY OF THE MASS IN THE "CURED" STATE WILL BE APPROXIMATELY 0.69.

FIGURE 10. SIMULATED BIRD CONFIGURATION

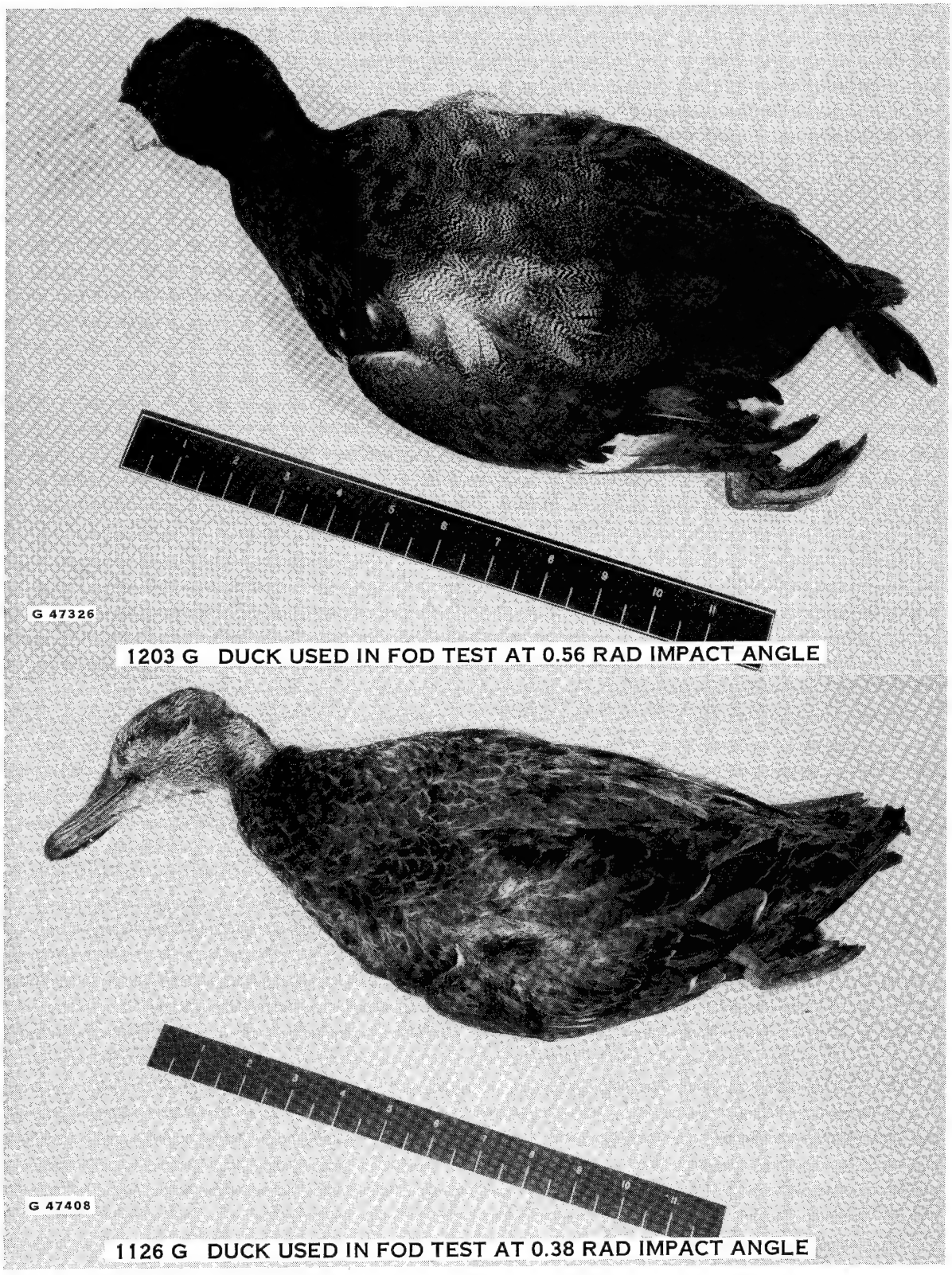

FIGURE 11. REAL BIRDS USED IN FOD TESTS

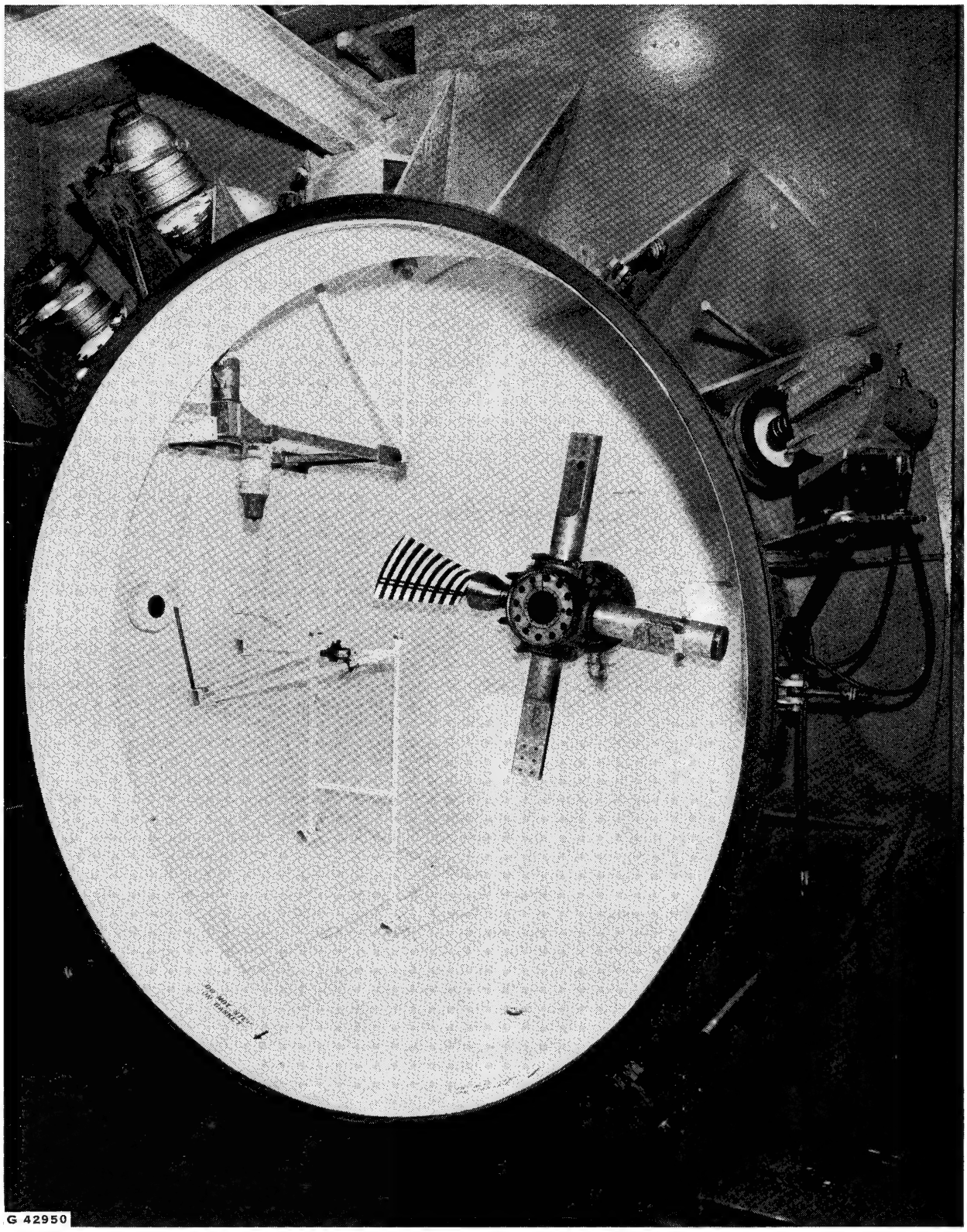

FIGURE 12. WHIRL IMPACT TEST FACILITY SET UP FOR BIRD IMPACT

A chute injection system was used for injection of the 5.08 cm (2 in) diameter iceballs as shown in Figure 13. Prior to injection, the iceball was contained at the top of the chute in a section cooled with dry ice to keep the temperature below 273°K (32°F). Injection was achieved by electrically opening the restraining plate allowing the iceball to gravity drop down the chute into the blade plane of rotation. Iceball injection was random, i.e., not synchronized, to blade position.

A pendulum injection system was used to inject the simulated and real birds into the test blade. This setup is shown in Figure 12. As shown, the bird was attached to a pendulum which was held in the armed position by an electromagnet prior to injection. Pendulum injection was synchronized electronically with blade position so that the bird swung into the plane of rotation as the blade arrived at the strike position. Dry run drops were accomplished prior to each impact test to establish the drop time calibration required for the electronics to obtain bird/blade entry synchronization. After the first entry, the pendulum and bird rebounded out of the plane of rotation and were restrained from secondary impact by a clutching system.

Non-Destructive Investigation Techniques

Several evaluation techniques were employed in this program to establish the pre- and post-test condition of the fan blades. A description of these techniques and their applicability to the NDI of the fan blades is discussed below.

1. X-ray was used to examine filament orientation and alignment and filament continuity in impacted areas. It was also used to detect any cracking in the sheath, spar and honeycomb filler materials.

2. Fokker Bond Test was used to examine the integrity of the bonds between the various components of the blade, i.e. spar to shell, shell to honeycomb filler, shell to shell edge bonds, and leading edge sheath to shell.

3. Holography was used to examine the integrity of the bonds between the various components of the blade as was the Fokker Bond Test. Figure 14 shows the setup of the holographic equipment for the fan blade.

4. Tap testing is a method of NDI which consists of striking the blade lightly with a small steel ball welded to a slender rod handle and interpreting the structural integrity of the bonds on the basis of the sounds emitted. The tones emitted from the unbond areas are different from those emitted from bonded areas. Interpretation of these tones by trained inspectors provides a good indication of the structural integrity of the bonds.

5. Dimensional inspections were made to determine the extent of deformation of the blade resulting from the impact. Manual inspections were made with airfoil templates for airfoil fit and edge and face alignments were measured for gross blade deformation evaluation.

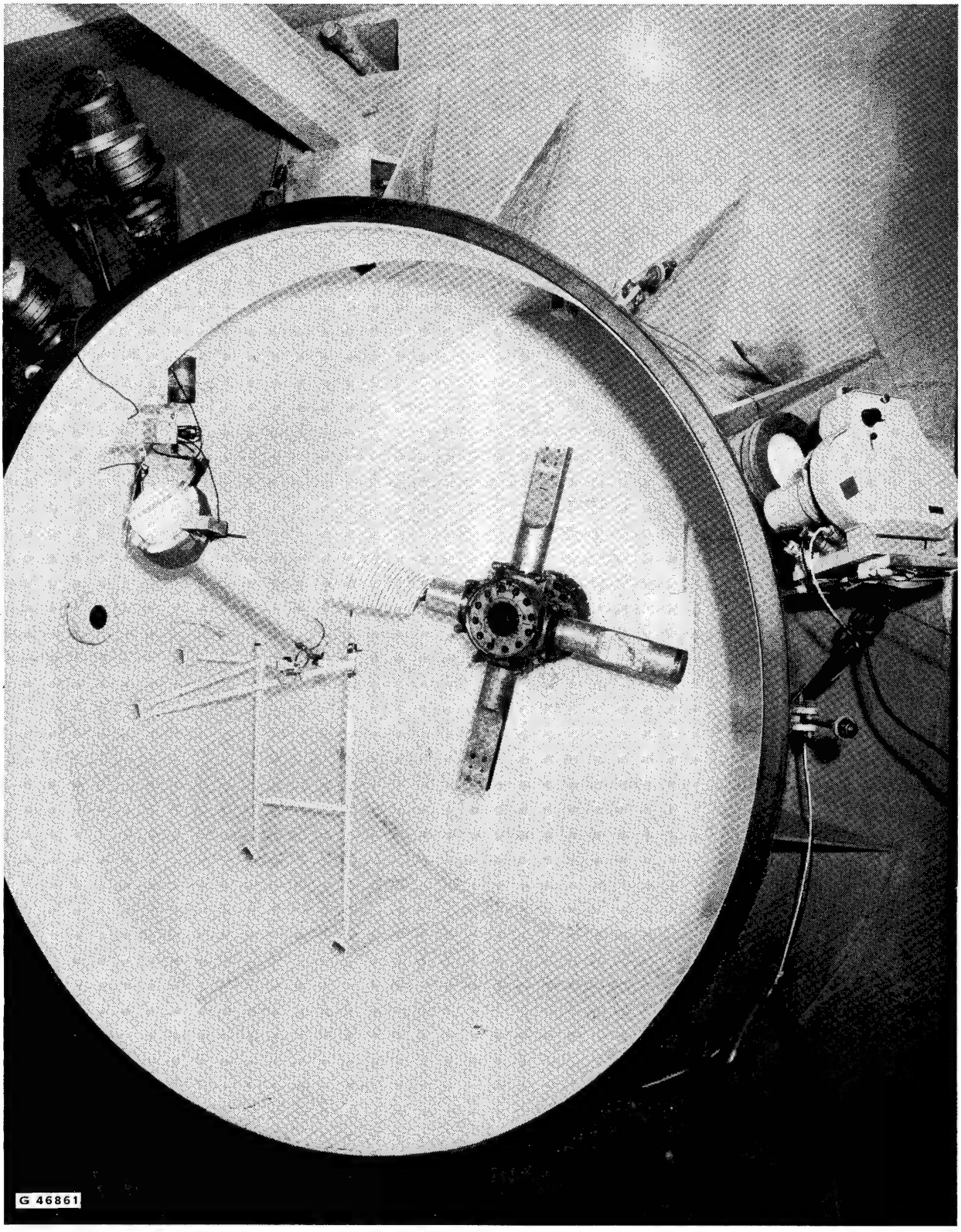

FIGURE 13. WHIRL IMPACT TEST FACILITY SET UP FOR ICEBALL IMPACT TEST

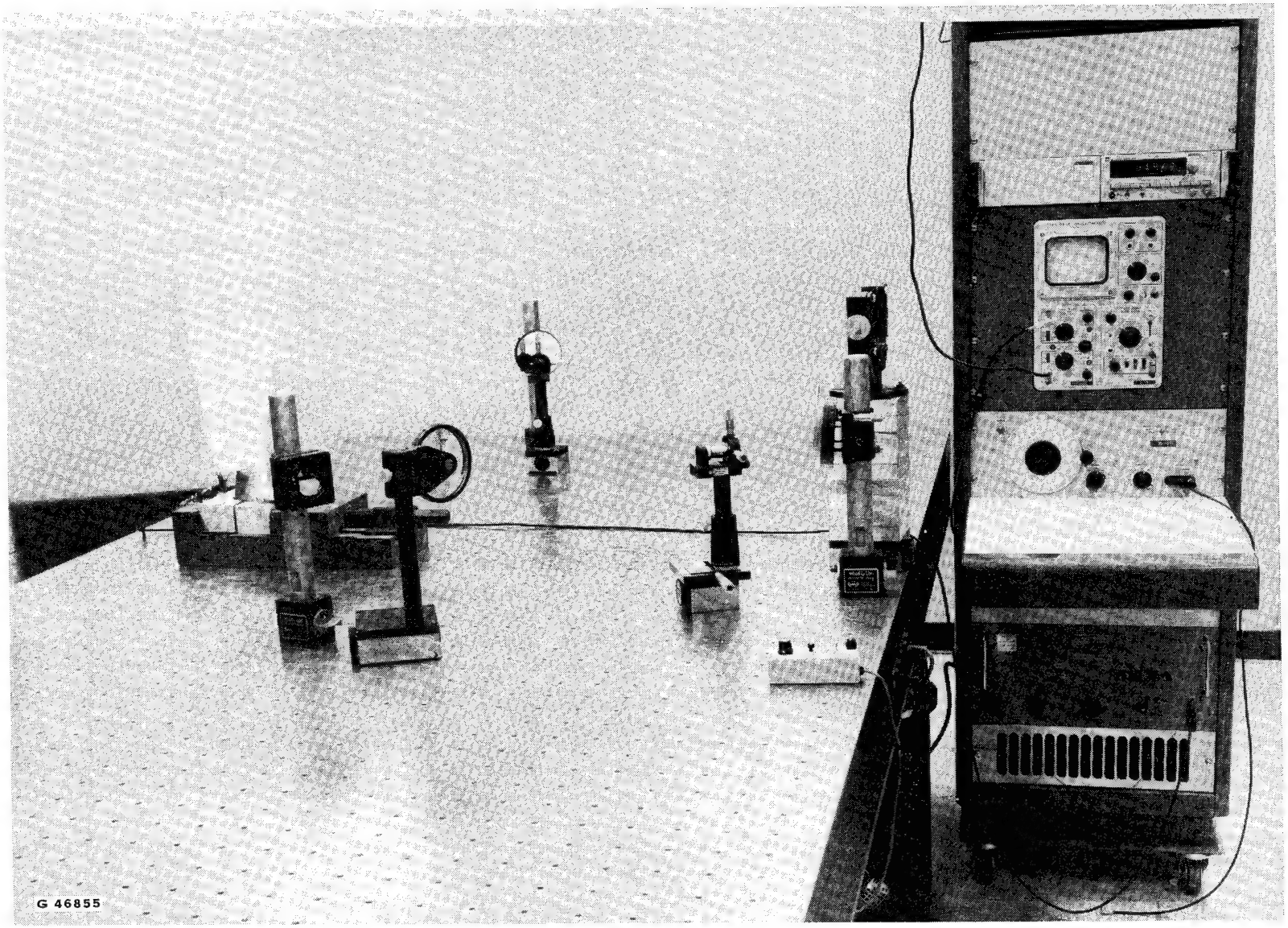

FIGURE 14. HOLOGRAPHIC SETUP FOR FAN BLADE NDI

Blade Impact Test Program

The impact test program presented in Table 1 consisted of eleven impact tests on the nine blades manufactured in this program. Included in the program were evaluations of blades impacted with 5.08 cm (2 in) iceballs, simulated birds and real birds. The impact materials were targetted to strike the blade at the 0.8 span. The specified angles of incidence were also as measured at the 0.8 span. Generally, the tests were conducted using the flexible blade retention hardware. In one test, however, the retention hardware was modified to rigidize the retention thereby eliminating the blade rocking features of the design. This was accomplished to assess the improvements in FOD resistance associated with the flexible retention concept.

The blade angles of incidence used in the program, i.e. 0.38 rad (22°) and 0.56 rad (32°), were selected from the NASA Lewis specified ranges of 0.38 to 0.44 rad (22 to 25°) and 0.56 to 0.63 rad (32 to 36°). The angles selected were those which occur during aircraft takeoff and climb. The 0.38 rad (22°) angle occurs at 114 m/s (222 kts) and the 0.56 rad (32°) angle occurs at 65 m/s (125 kts).

The fan blade design speed is 317 rad/s (3030 rpm). The two flight speeds to be simulated in the tests were 125 and 222 kts. The resultant speed at the impact station (0.8 span) would then be 261 and 278 m/s (857 and 912 fps) respectively. Since the test rig bird injection speed is very low (approximately 12 kts), the rig test fan rpm is usually increased to obtain the desired resultant speed at the impact station. Thus test fan speed would be raised to 3128 or 3327 from the 3030 design rpm to simulate the 125 or 222 kts flight conditions, respectively. However, these higher fan speeds would result in substantial increases in the moment necessary to start blade rocking, a function of centrifugal load, and thereby limit the effectiveness of the flexible retention design. Moreover, the test slice thickness of 10.9 cm (4.29 inches) for the 1400 gm bird is substantially larger than can occur at the flight condition values corresponding to these angles of impact. As shown in Figure 15, the expected penetration values are 5.64 cm (2.22 inches) at 65 m/s (126 kts) using an incidence angle of 0.56 rad and 9.40 cm (3.70 inches) at 114 m/s (222 kts) using an incidence angle of 0.38 rad. Table II presents the calculated impact loads predicted for the flight conditions and for the whirl rig conditions. The data shown was derived by means of the three degrees of freedom gross blade response analysis described later in the FOD analysis section of the report. The table shows that the impact forces generated during the rig tests would be at least as severe as those generated during the flight conditions even if conducted at the 317 rad/s (3030 rpm) design speed. In fact, the loads generated in the 0.56 rad (32°) impact angle rig tests would far exceed the loads of the corresponding flight conditions. This results because the target slice size is a constant 10.9 cm (4.29 inches) for the rig tests whereas the slice size varies with flight speed and would be only 5.64 cm (2.22 inches) at the 0.56 rad (32°) impact angle. In view of these considerations, it was concluded that conducting the rig tests at 317 rad/s (3030 rpm) design speed would provide a conservative approach toward defining the impact resistance of these fan blades.

TABLE I

FAN BLADE IMPACT TEST CONDITIONS
(ALL SLICE SIZES TARGETED FOR 50% OF OBJECT)

Test No.	Blade No.	Object	Impact Incidence Angle		Object Size
			Radians	Degrees	
1	1	Iceballs	0.38	22	5.08 cm dia.
2	5	Iceballs	0.56	32	5.08 cm dia.
3	1	Sim. Bird (Retest)	0.56	32	300 g
4	4	Sim. Bird	0.56	32	700 g
5	2	Sim. Bird	0.56	32	1400 g
6	5	Sim. Bird (Retest)	0.38	22	300 g
7	3	Sim. Bird	0.38	22	700 g
8	7	Sim. Bird	0.38	22	1400 g
9	6	Real Duck	0.38	22	1126 g
10	9	Real Duck	0.56	32	1203 g
11	8	Sim. Bird (Fixed Root)	0.56	32	1400 g

Note: Impact at 0.8 span. Angle of incidence at 0.8 span. Tip speed 282 m/s (925 ft/sec)

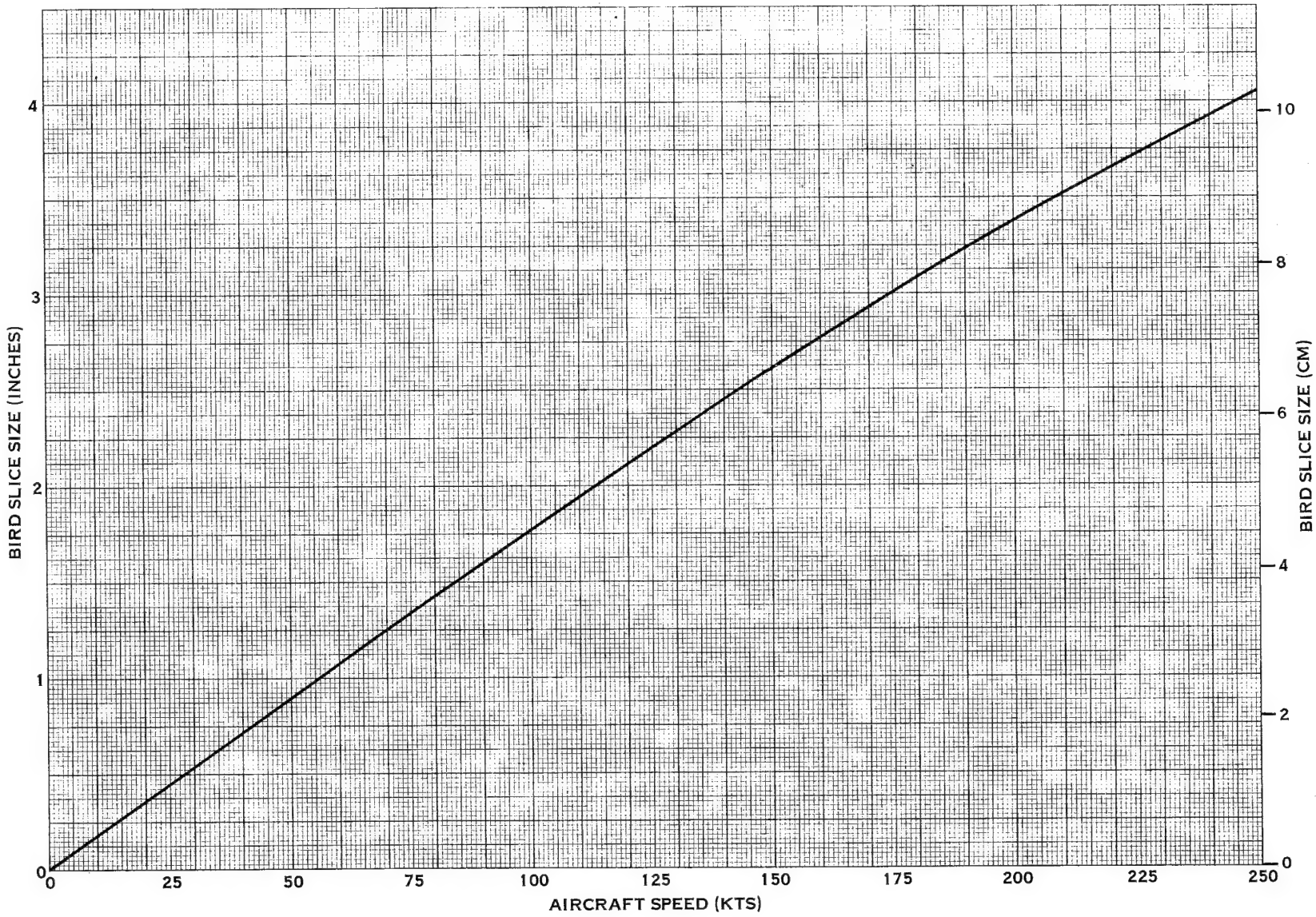

FIGURE 15. BIRD SLICE SIZE VS AIRCRAFT SPEED QCSEE TYPE FOD FAN BLADE HEAD–ON BIRD IMPACT

TABLE II

THEORETICAL COMPARISON OF FLIGHT AND WHIRL RIG IMPACT CONDITIONS
INTERNATIONAL SYSTEM OF UNITS

Impact Description	Fan Speed (rad/s)	Ingestion Velocity (m/s)	Resultant Imp. Velocity (m/s)	Incidence Angle (rad)	Sliced Bird Wt. (g)	Slice Thick (cm)	Rigid Bld. Imp. Force ($N \times 10^{-3}$)	Max. Bld Resp. Force ($N \times 10^{-3}$)	Max. Bld Resp. Torque (m-N)
Whirl Rig*	348	0	279	0.38	700	10.9	209	42.4	6590
Adjusted Bld Speed	328	0	261	0.56	700	10.9	262	56.7	8800
Flight	317	114	279	0.38	604	9.4	180	36.9	6720
	317	65	261	0.56	362	5.6	135	28.0	7750
Whirl Rig	317	0	253	0.38	700	10.9	173	39.2	5930
Design Bld Speed	317	0	253	0.56	700	10.9	246	55.4	8560

U.S. CUSTOMARY UNITS

Impact Description	Fan Speed (rpm)	Ingestion Velocity (kts)	Resultant Imp. Velocity (fps)	Incidence Angle (deg.)	Sliced Bird Wt. (oz)	Slice Thick (in.)	Rigid Bld. Imp. Force (lb.)	Max. Bld Resp. Force (lb.)	Max. Bld Resp. Torque (in.-lb.)
Whirl Rig*	3327	0	911.6	22	24.7	4.29	47,000	9,530	58,300
Adjusted Bld Speed	3128	0	857.1	32	24.7	4.29	58,800	12,749	77,900
Flight	3030	222	911.6	22	21.3	3.70	40,500	8,301	59,500
	3030	126	857.1	32	12.8	2.22	30,400	6,291	68,600
Whirl Rig	3030	0	830.3	22	24.7	4.29	39,000	8,823	52,500
	3030	0	830.3	32	24.7	4.29	55,200	12,450	75,800

*Fan rpm increased to obtain velocity at impact station (resultant impact velocity column in table) equivalent to the resultant of operating speed and flight speeds shown in the flight condition heading.

IMPACT TEST RESULTS

General

Generally, the actual slice size ranged from 46 to 63% of the total bird size versus a 50% slice size target. For the real bird tests, the target slice was 50% of 1400 g. One exception to this slice accuracy occurred during the 1400 g simulated bird test at 0.38 rad (22°) impact angle. Two slices, 18% and 21% were impacted instead of one large slice when the injection system prematurely released.

A summary of the actual blade conditions and blade results are presented in Tables III and IV and Figures 16 and 17. The summaries include impact induced weight loss and unbond as well as frequency change and leading edge deformation data. The general physical appearance of the blades is also shown. Additional data and photographs of the blades in the post impact condition are presented later in this report. The unbond calculations were based on the holographic and tap test evaluations of the blade. The percentage determination is based on the total blade airfoil surface area remaining after test. Frequency change and weight loss determinations were made by comparing pre and post test results in each case.

The effect of the impact on blade static frequencies was mixed. Unbonding resulted in some frequency reduction (approx. 1% for each percent of unbonds) in the torsional mode and almost none in the 1st and 2nd bending modes whereas weight loss resulted in a frequency increase. The greatest effect of weight loss on frequency increase was on the torsion frequency. Frequency increased approximately 4% for each percent of weight loss. First bending frequency increased approximately 2% and second bending frequency approximately 1% for each percent of weight loss. The frequency increase is attributed to the location of the material which was lost from the blade, i.e., the material weight loss at the tip reduced blade mass sufficiently to increase the blade stiffness in the three reported bending modes. The changes in frequencies were small and would not likely jeopardize the short term operation of the engine.

Except for the three large bird tests at 0.56 rad (32°), (Blade S/N 2, 9 and 8) the blade leading edge survived the impacts intact. Weight loss was from the blade trailing edge tip region and included shell and fill material but did not affect the spar. The first gelatin impact test (the 300 g bird test at 0.56 rad) resulted in a weight loss of 2% due to a material loss from the trailing edge tip. This was considered unacceptable for this relatively small slice size and a design modification was therefore made. The remaining blades were reworked to remove a portion of the tip, approximately 1.8 cm (0.7 in) wide at mid chord, to reduce the enertia of the blade in the tip area. This was done so that the blade could deflect at impact more readily thereby reducing the tip damage. Blade hit station and tip speed were adjusted to comply to the specified test parameters. The tip cutoff appeared to improve the blade performance, however, the trailing edge area of the tip continued as the principal problem area of the blade in subsequent larger impacts.

TABLE III

FOD IMPACT TEST RESULTS

Impact Media	Bld S/N	Bld. Incidence Angle (deg.)	Bld. Incidence Angle (rad.)	Bld. Tip Speed (fps)	Bld. Tip Speed (m/s)	Impact Slice Size* (lb.)	Impact Slice Size* (oz.)	Impact Slice Size* (g)	% Unbonds	% Wt. Loss	FREQUENCY CHANGE 1B%	FREQUENCY CHANGE 2B%	FREQUENCY CHANGE 1T%
5.08 cm Iceball	1	22.5	0.39	925	282	0.11	1.7	48	0.0	0.0	0.87	-2.90	0.75
300 g (1)	5	21.7	0.38	924	282	0.42	6.7	190	0.0	0.0	-0.14	-1.23	-0.61
700 g (1)	3	22.4	0.39	925	282	0.82	13.1	372	0.0	0.0	0.65	-0.56	-1.93
1400 g (1)	7	22.1	0.39	926	282	0.57/0.66	9.1/10.6	258/300	0.7	0.0	-0.46	0.83	-2.81
1126 g (2)	6	22.2	0.39	925	282	1.50	24.0	681	0.2	1.4	4.65	-0.92	10.22
5.08 cm Iceball	5	32.9	0.57	930	283	0.11	1.7	48	0.0	0.0	0.10	0.80	-0.30
300 g (1)	1	31.9	0.56	927	283	0.36	5.7	163	0.0	0.9	3.20	0.60	2.90
700 g (1)	4	32.4	0.57	926	282	0.97	15.5	440	0.0	2.0	4.55	2.46	14.06
1400 g (1)	2	32.5	0.57	925	282	1.68	26.9	763	0.3	3.0	7.26	-0.70	16.00
1203 g (2)	9	31.9	0.56	925	282	1.74	27.8	788	1.1	3.2	6.34	5.14	8.20
1400 g (3)	8	32.6	0.57	926	282	1.43	22.9	650	0.9	4.7	10.30	7.50	13.40

* Two numbers indicates a double hit.

(1) Simulated bird
(2) Real duck
(3) Simulated bird, blade retention fixed

TABLE IV

BLADE LEADING EDGE DEFORMATION RESULTING FROM IMPACT

Impact Media	Blade S/N	Dent Span (cm)	Dent Span (in.)	Dent Depth (cm)	Dent Depth (in.)
0.38 rad. Impact Angle					
5.08 cm Iceball	1	6.4	2.5	0.46	0.18
300 g Sim. Bird	5	7.6	3.0	0.33	0.13
700 g Sim. Bird	3	7.8	3.1	0.25	0.10
1400 g Sim. Bird	7	7.6	3.0	0.48	0.19
1126 g Duck	6	8.5	3.3	1.00	0.39
0.56 rad. Impact Angle					
5.08 cm Iceball Inboard	5	3.8	1.5	0.20	0.08
5.08 cm Iceball Outboard	5	5.3	2.1	0.49	0.19
300 g Sim. Bird	1	8.6	3.4	1.15	0.45
700 g Sim. Bird	4	9.4	3.7	0.60	0.24
1400 g Sim. Bird	2	Leading edge section removed			
1203 g Duck	9	Leading edge section removed			
1400 g Sim. Bird/Fixed Root	8	Leading edge section removed.			

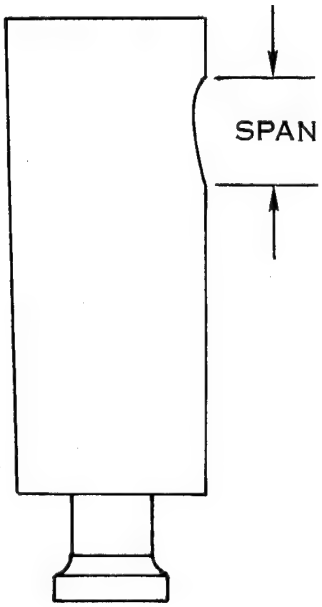

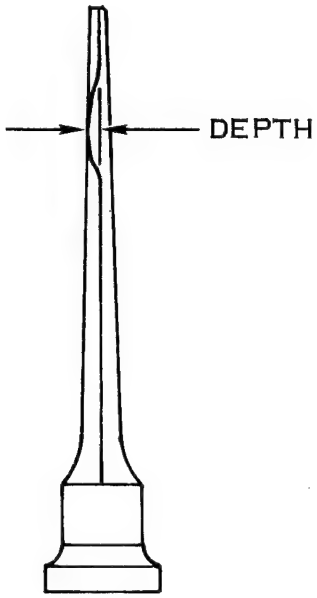

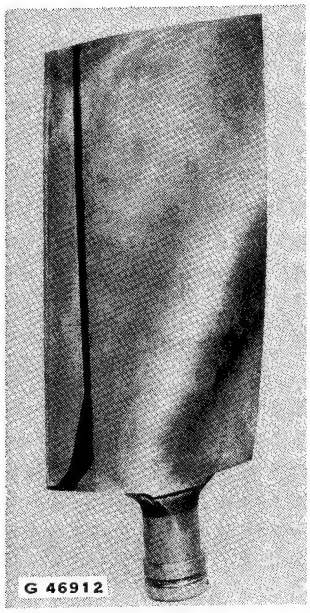

PRETEST

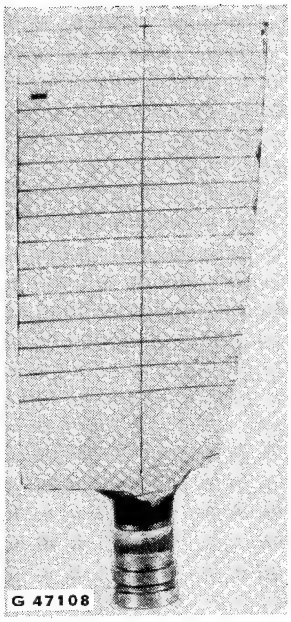

190 G (6.7 OZ.)
SLICE (GELATIN)

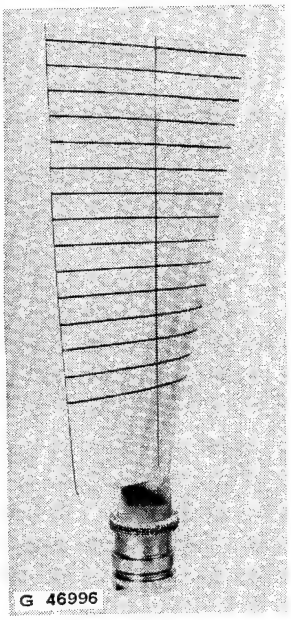

372 G (13.1 OZ.)
SLICE (GELATIN)

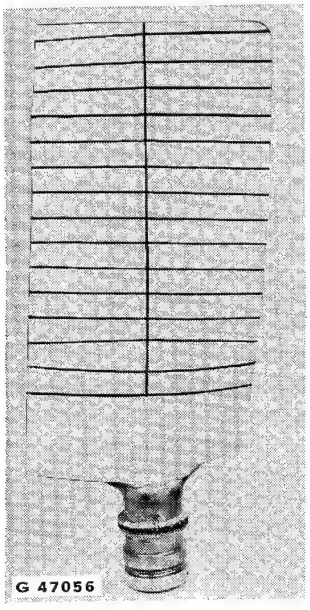

258 & 300 G
(9.1 & 10.6 OZ)
SLICES (GELATIN)

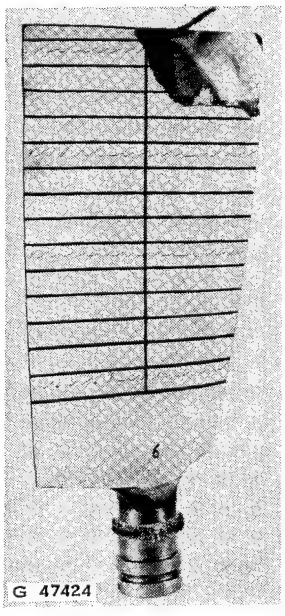

681 G (24 OZ.)
SLICE (REAL BIRD)

FIGURE 16. QCSEE TYPE FOD FAN BLADE TEST RESULTS
IMPACT ANGLE 0.38 RAD (22°) TIP SPEED 282 M/S (925 FPS)

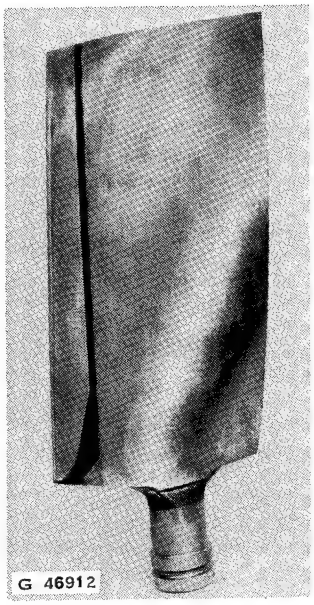

PRETEST

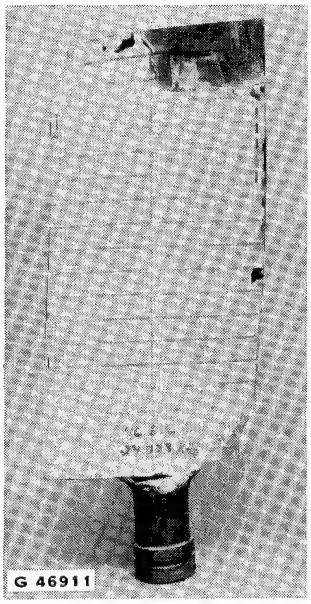

163 G (5.7 OZ.)
SLICE (GELATIN)

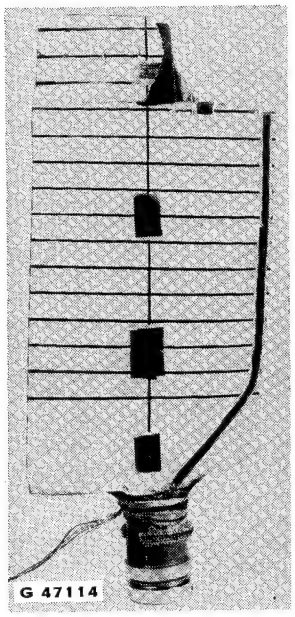

440 G (15.5 OZ.)
SLICE (GELATIN)

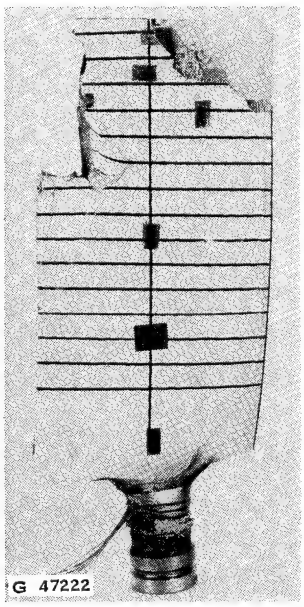

763 G (26.9 OZ.)
SLICE (GELATIN)

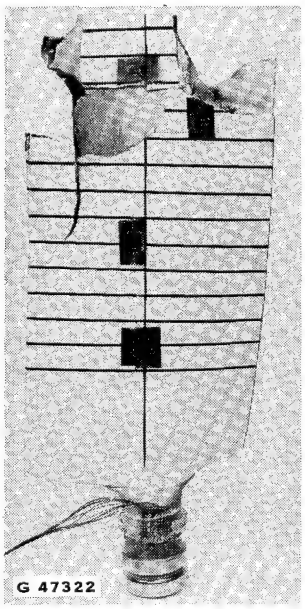

788 G (27.8 OZ.)
SLICE (REAL BIRD)

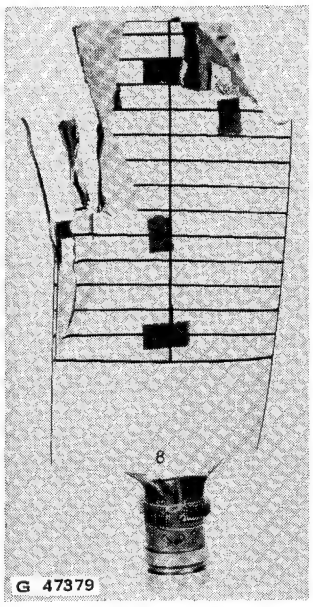

650 G (22.9 OZ.)
SLICE (GELATIN,
FIXED ROOT)

FIGURE 17. QCSEE TYPE FOD FAN BLADE TEST RESULTS
IMPACT ANGLE 0.56 RAD (32°) TIP SPEED 282 M/S (925 FPS)

The trailing edge damage after a 440 g (15.5 oz) slice at 0.56 rad. impact angle was very similar to the damage on the blade after 681 g (24 oz) slice at 0.38 rad (22°), Figure 18. In general, the high speed movie documentation indicates that the blades sliced through the birds at 0.38 rad impact angle whereas at 0.56 rad impact angle, the more pronounced impact mode was a slapping action.

Figure 19 shows the calculated bird slice weight which could be removed from a 1400 g bird by this fan design during aircraft operation. Head on penetration is assumed as is a bird length to diameter ratio of 2. Bird attitudes other than head on are possible but the head on entry is equivalent to that attitude used in the rig FOD tests. As shown, the slice weight at the 0.56 rad (32°) impact angle (65 m/s aircraft speed) is 363 g (12.8 oz) and at the 0.38 rad (22°) impact angle (114 m/s aircraft speed) is 590 g (20.8 oz). The impacts that approximate these conditions are 440 g (15.5 oz) slice at 0.56 rad (32°) and 681 g (24 oz) slice at 0.38 rad (22°), Figure 18. In each case, the leading edge was completely intact after impact and only small sections of the blade trailing edge tip were removed. More severe impacts up to 790 g (27.8 oz) slices were evaluated at 0.56 rad (32°). To impact slice sizes of this weight, the blade would have to strike a bird much larger than 1400 g (50 oz). However, even at the most severe impact condition material weight losses remained low (3.2%) and the damage on the leading edge, though significant, would not be expected to greatly effect the short term operation of the aircraft.

The blade impact tests conducted in the 1973 program, using a boron/epoxy shell structure, produced interlaminar failure in layers adjacent to the epoxy adhesive bond joints. This mode of failure, in effect, established the limit of impact load capability for the resin matrix blade structure. Subsequent laboratory test specimens made to load the composite under impact in a similar manner showed that a 2.6 fold increase in strength was realized by incorporation of an aluminum matrix. The actual increase in full scale blade impact capability was not readily quantifiable since peel and shear loads were not clearly separable. However, it was observed in the test program reported herein that the adhesive bond strength was not taxed to a level of incipient interlaminar failure. Distress in the adhesive joint was found only in areas of high local damage in the immediate vicinity of impact.

Figure 20 shows the blade weight loss as a function of bird slice weight. The figure shows (1) that the 0.56 rad (32°) impact angle tests conditions are much more severe than the 0.38 rad (22°) impact angle test conditions. (2) That the gelatin/phenolic microballoon bird is a good simulation of a real bird (see Figures 39 & 41, 760 gm (26.9 oz) gelatin vs 790 g (27.8 oz) slice real bird) and (3) that in this evaluation the flexible retention blades sustained less weight loss than the fixed retention blade. The weight losses resulting from the tests were all local to the impact site. It had been anticipated that the retention design would reduce gross damage but have little effect on damage at the impact site.

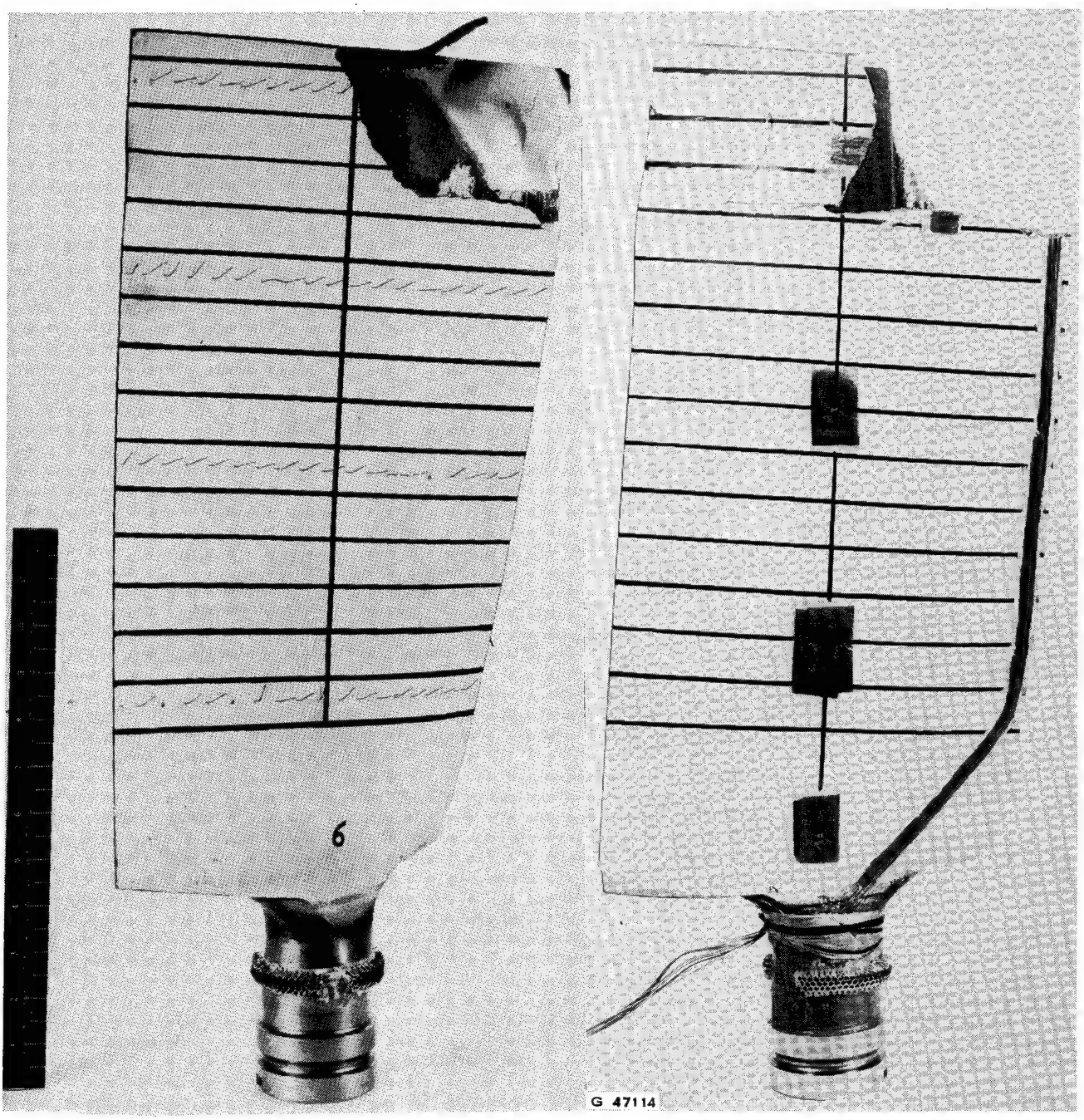

0.38 RAD IMPACT ANGLE
681 G (24 OZ.) SLICE

0.56 RAD IMPACT ANGLE
440 G (15.5 OZ.) SLICE

FIGURE 18. IMPACT TEST CONDITIONS PRODUCING COMPARABLE BLADE DAMAGE AT THE TWO TEST INCIDENCE ANGLES

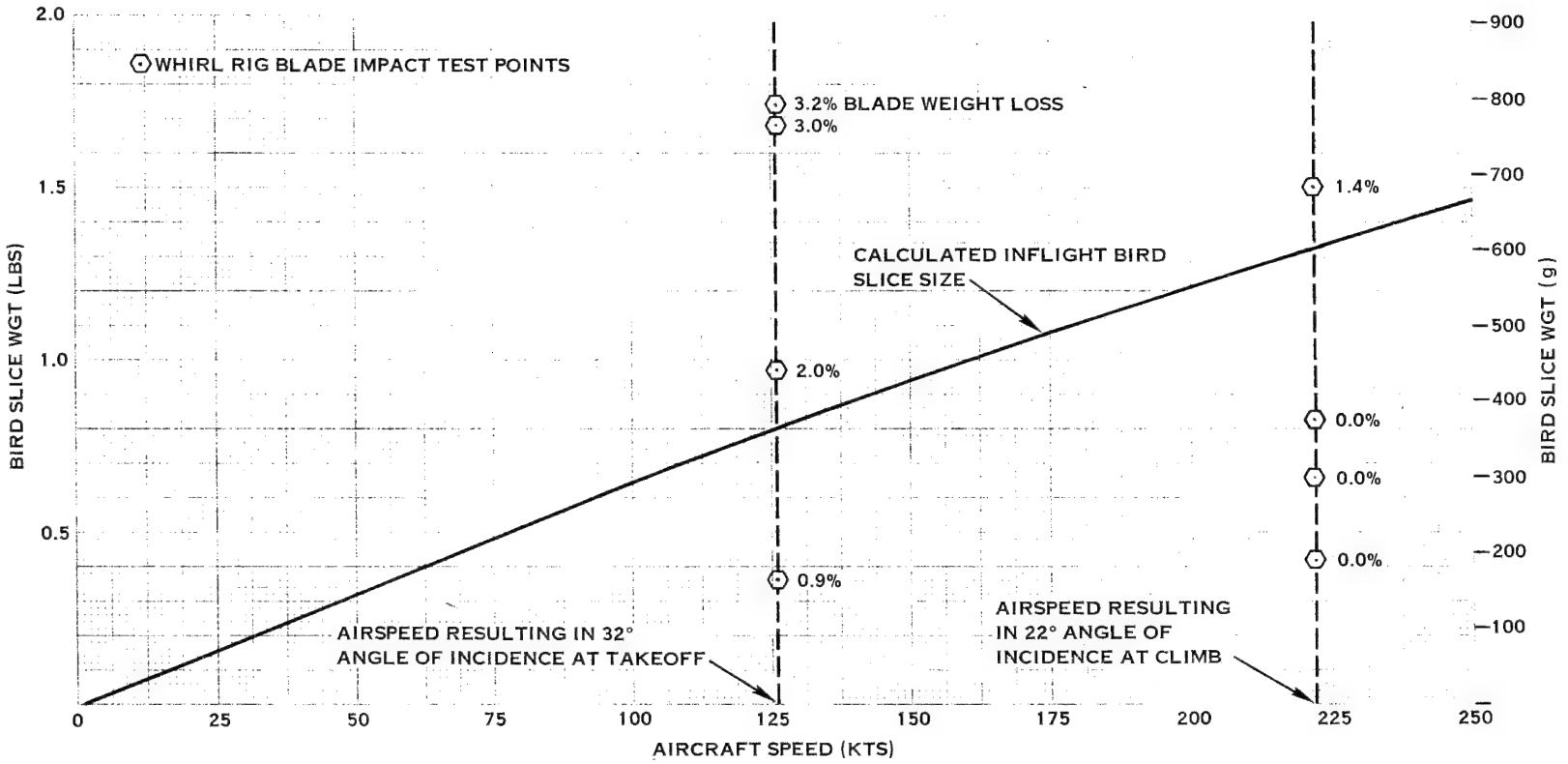

FIGURE 19. CALCULATED BIRD SLICE SIZE IMPACTED BY QCSEE TYPE FOD BLADE VS AIRCRAFT SPEED FOR 1400g (3 LB) BIRD ASSUMING HEAD-ON ENTRY

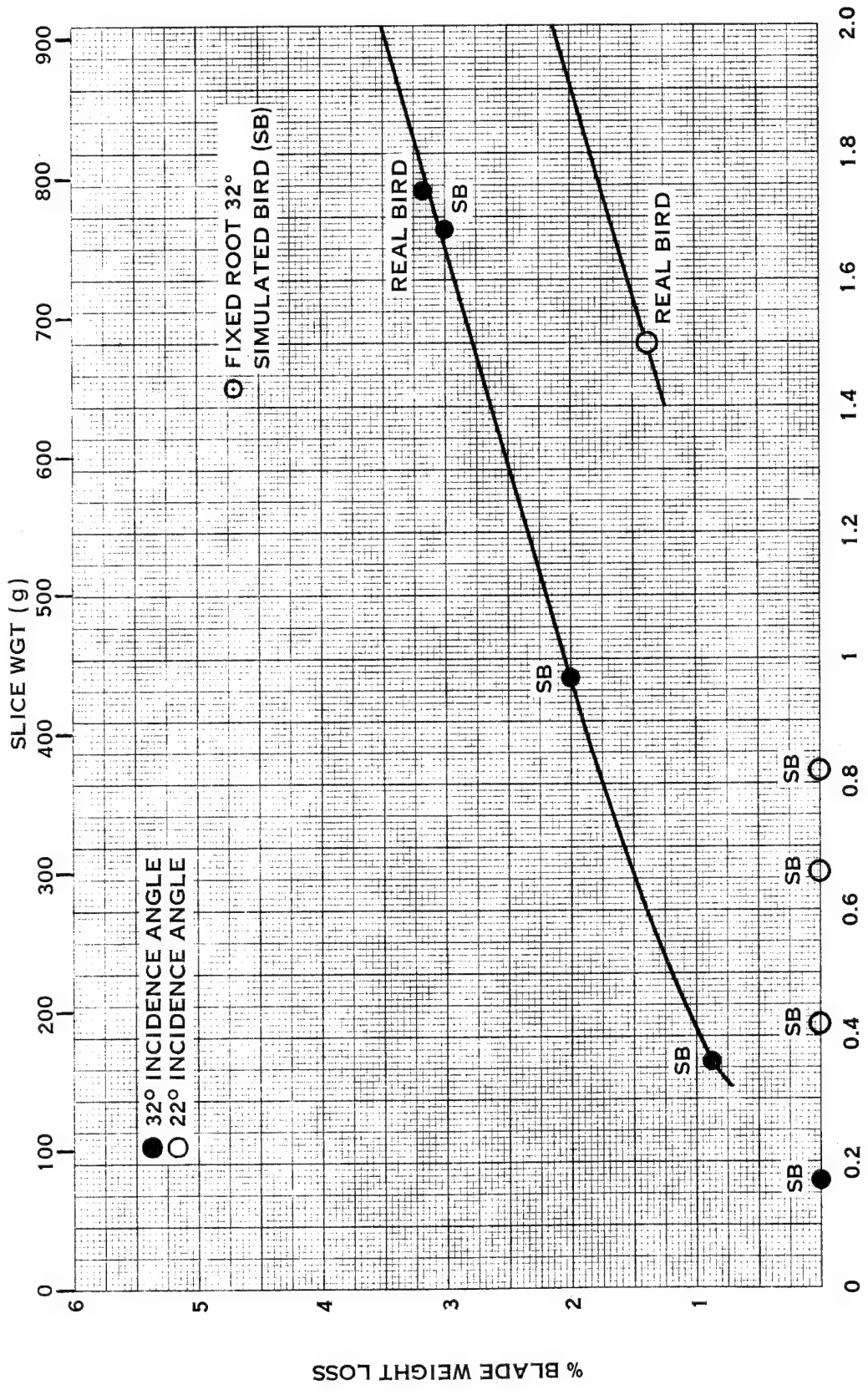

FIGURE 20. PERCENT WEIGHT LOSS VS SLICE SIZE WHIRL IMPACT TESTS OF QCSEE TYPE FAN BLADE

Individual Test Results

Table V indicates the test conditions and provides an index of the appropriate figures relating the blade post test condition. Some blades had evidence of cracking in the composite shell and in the honeycomb fill. No evidence of cracking was detected on any of the titanium spars. When debonding occurred, it was in general between the titanium surface foil and the composite shell. The composite layers remained bonded to each other. The fabrication process for compacting the composite shells included air bonding to facilitate manufacture. Although, the air bond process was successful for compaction of boron/aluminum composite, the bonding of the titanium foil to the composite proved more difficult. These bonds were sometimes marginal in quality particularly at the edges which were exposed most to the air. On impact, these marginal areas sometimes debonded though the integrity of the remaining composite structure was intact.

Figure 21 shows the vast improvement of FOD tolerance that has been achieved by the boron/aluminum blades used in this program compared to the boron/epoxy blades of the 1973 program. The bare spar is a 1973 vintage boron/epoxy shell blade configuration after impact with an 312 g (11 oz.) slice. This blade was impact tested under NASA Contract NAS3-16778, reference 2. The other blade is a 1975 vintage boron/aluminum shell blade impacted during this program. The blade was impacted by a 440 g (16 oz.) slice with little damage and represents a major advancement in blade FOD resistance technology over the three year period.

ANALYTICAL AND EXPERIMENTAL STRUCTURAL RESULTS

General

The design of the fan blade utilized several analytical techniques developed by Hamilton Standard under IR&D programs. These analyses provided the first in-depth capability to predict the impact performance of a fan blade. The following sections present a general review of these analytical methods, and demonstrate the correlation of the analytically predicted stresses with those obtained experimentally in this program.

Description of Analytical Methods

The blade impact analysis covers three aspects of the blade impact; gross blade response, local blade response, and local chordwise stressing.

The gross blade response dynamic analysis yields the maximum bending and torsion deflections and the stresses that occur at the respective times of maximum deflections. The stresses in the shank region of the blade are believed maximum at these times, but stresses in other parts of the blade, particularly near the impact site, reach peak values at earlier times. The gross blade response analysis therefore gives peak stresses in the shank region of the blade and gives accurate deflections at or near the respective times of maximum bending and torsional deflections.

TABLE V

FAN BLADE TEST CONDITIONS AND INDEX OF REFERENCE FIGURES

Impact Media	Blade S/N	Figures For Photographs	Figures For NDI
0.38 rad. Impact Angle			
5.08 cm Iceball	1	22	(4)
300 g (1)	5	23	(4)
700 g (1)	3	24	(4)
1400 g (1)	7	25	26
1126 g (2)	6	27	28
0.56 rad. Impact Angle			
5.08 cm Iceball	5	29	(4)
300 g (1)	1	30	31
700 g (1)	4	32	33
1400 g (1)	2	34	35
1203 g (2)	9	36	37
1400 g (3)	8	38	39

(1) Simulated bird

(2) Real duck

(3) Simulated bird, fixed root

(4) No damage indicated by NDI

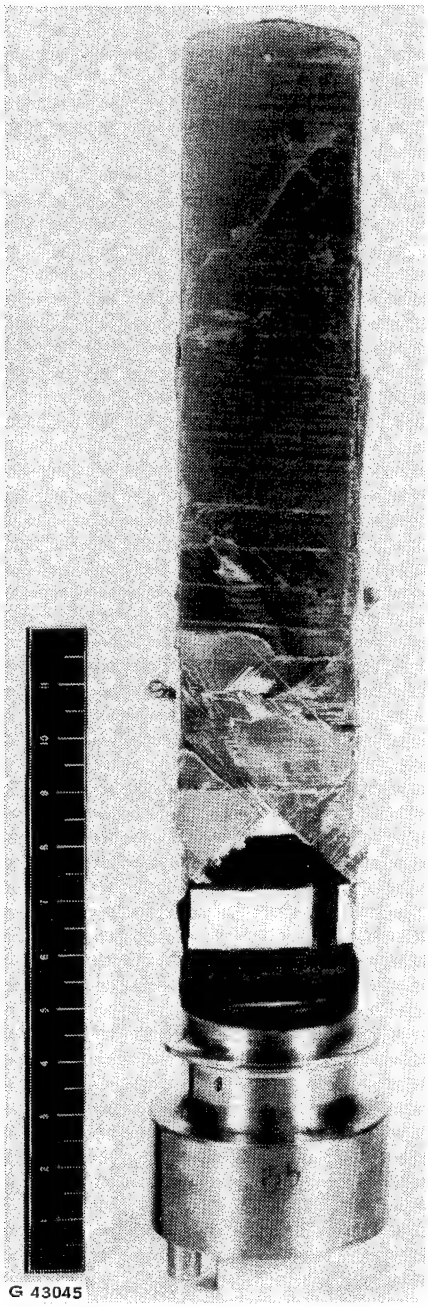

1973 DESIGN
(BORON/EPOXY SHELL)
312 G (11 OZ.) SLICE

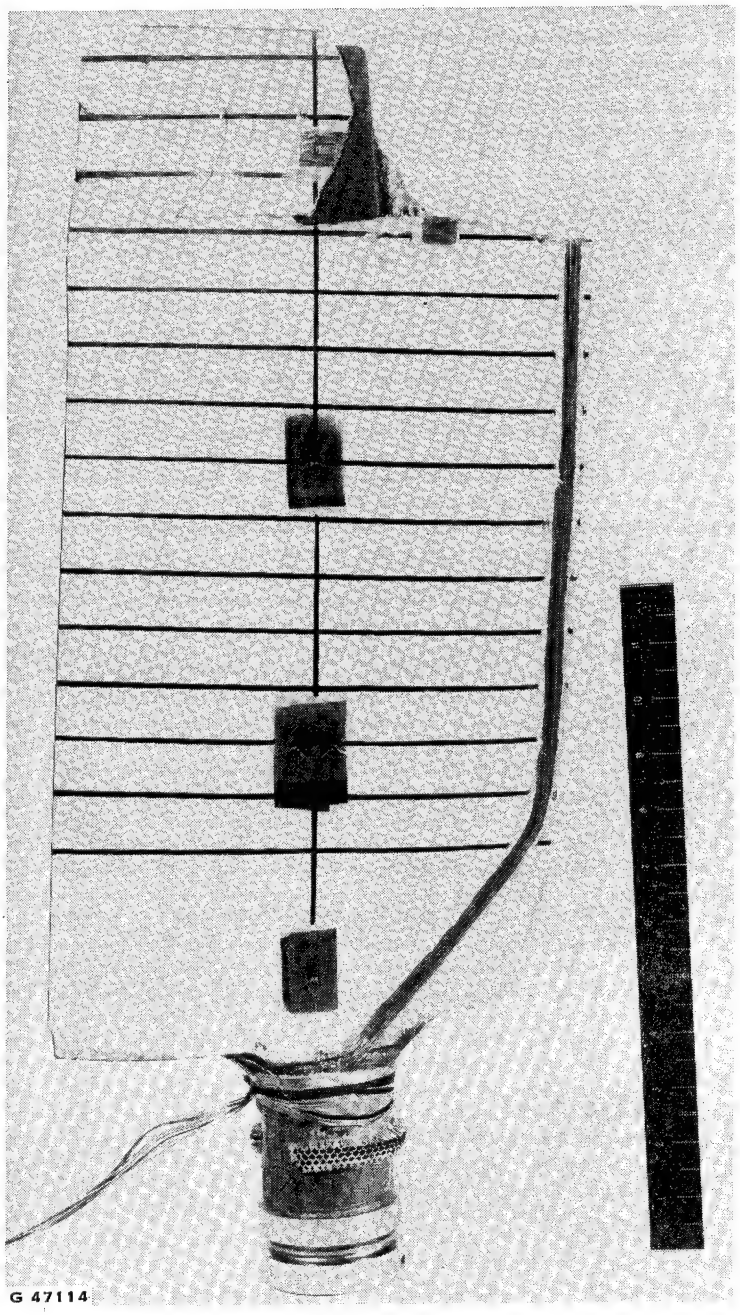

1975 DESIGN
(BORSIC/AL SHELL)
440 G (16 OZ.) SLICE

FIGURE 21. COMPARATIVE FOD 1973 BLADE DESIGN VS 1975

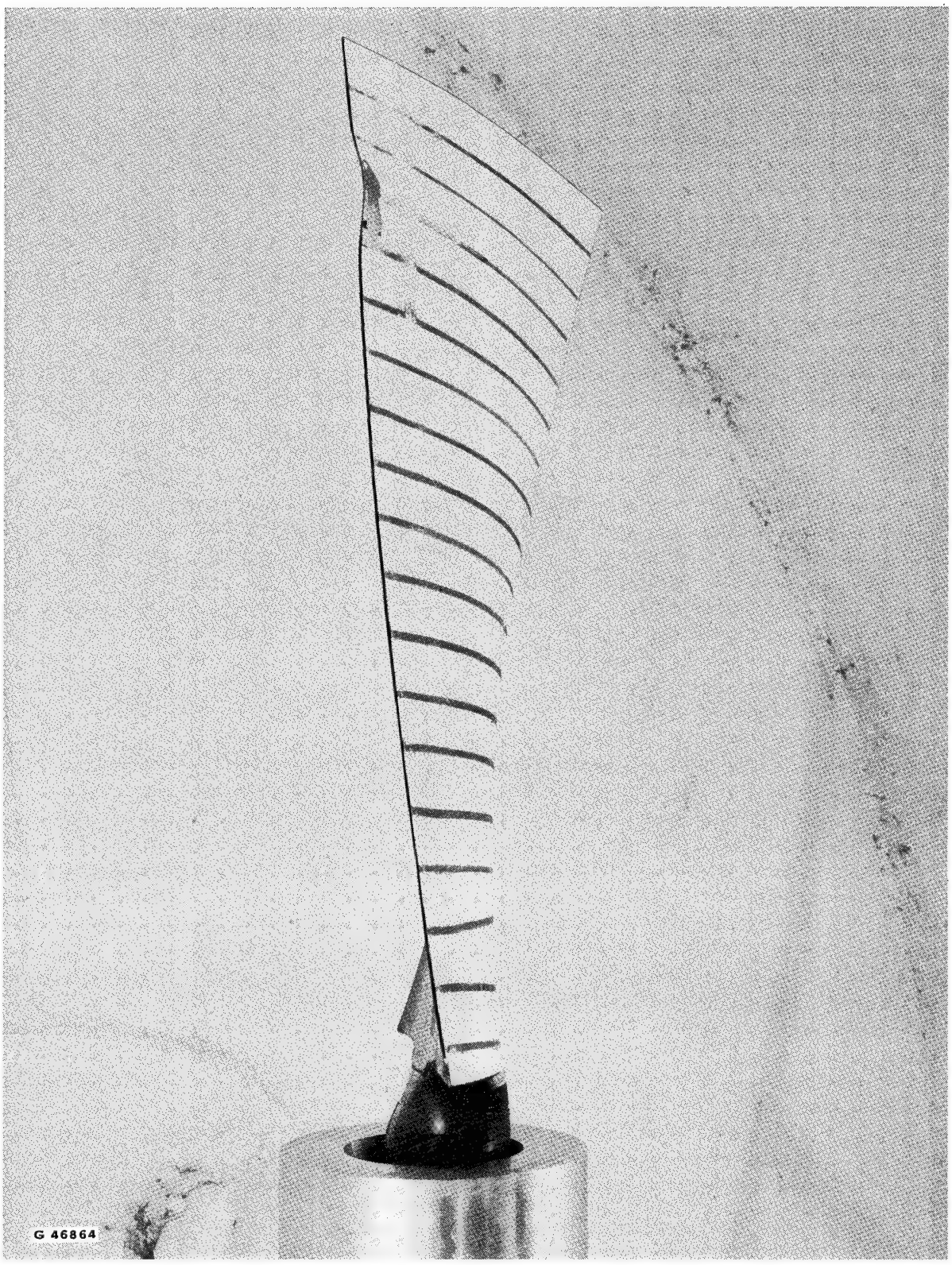

FIGURE 22. 5.08 CM ICEBALL/0.38 RAD S/N 1 BLADE POST TEST CONDITION IMPACT ANGLE 48G (1.7 OZ.) SLICE

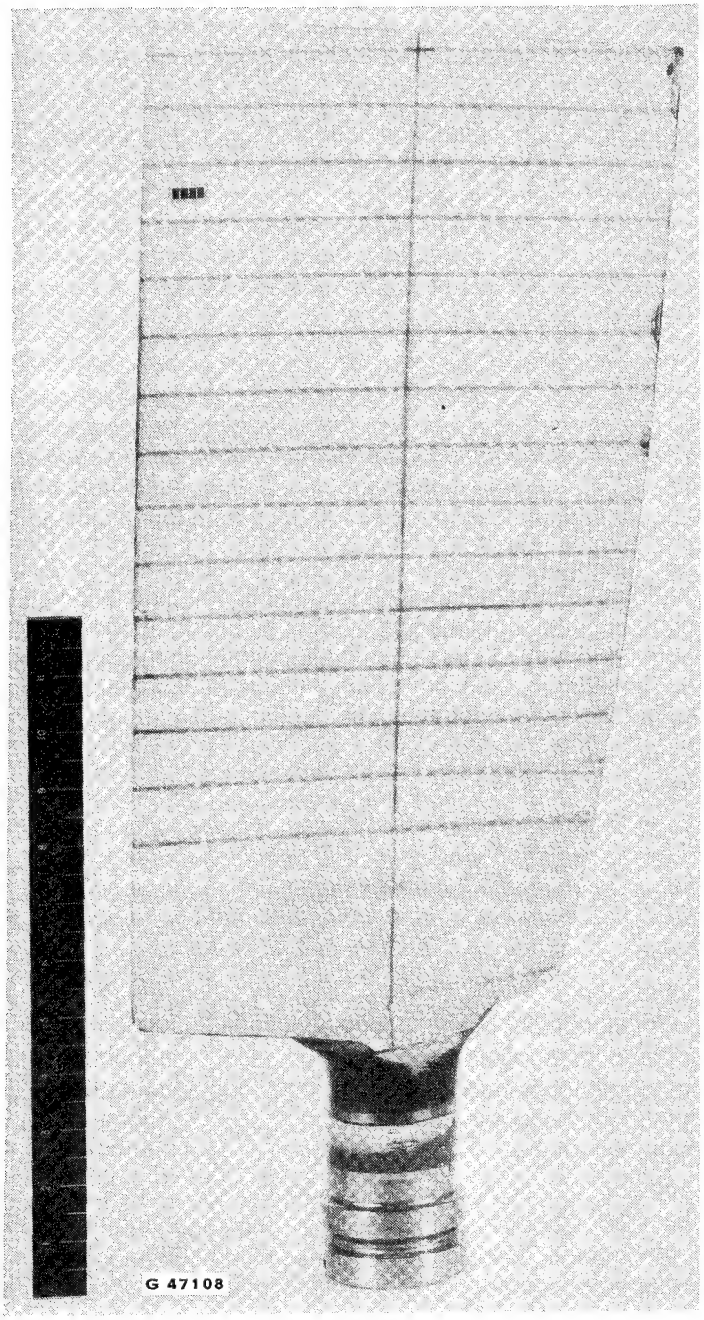

FIGURE 23. 300 G SIMULATED BIRD/0.38 RAD S/N 5 BLADE POST TEST CONDITION IMPACT ANGLE 190 G (6.7 OZ) SLICE

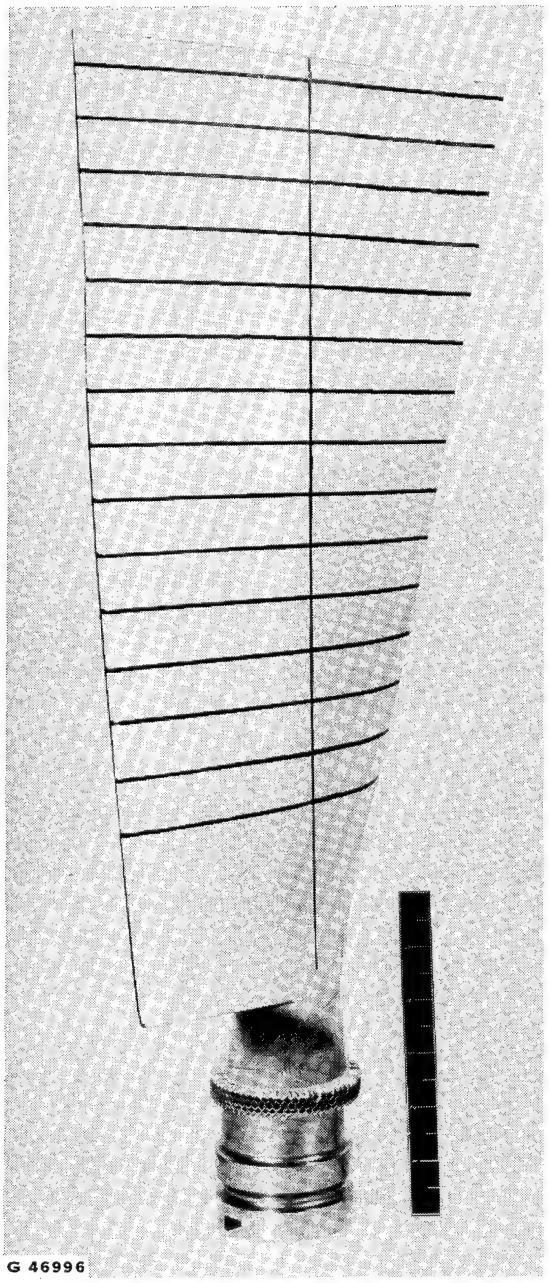

FIGURE 24. 700G SIMULATED BIRD/0.38 RAD SN/3 BLADE POST TEST CONDITION IMPACT ANGLE 372 G (13.1 OZ) SLICE

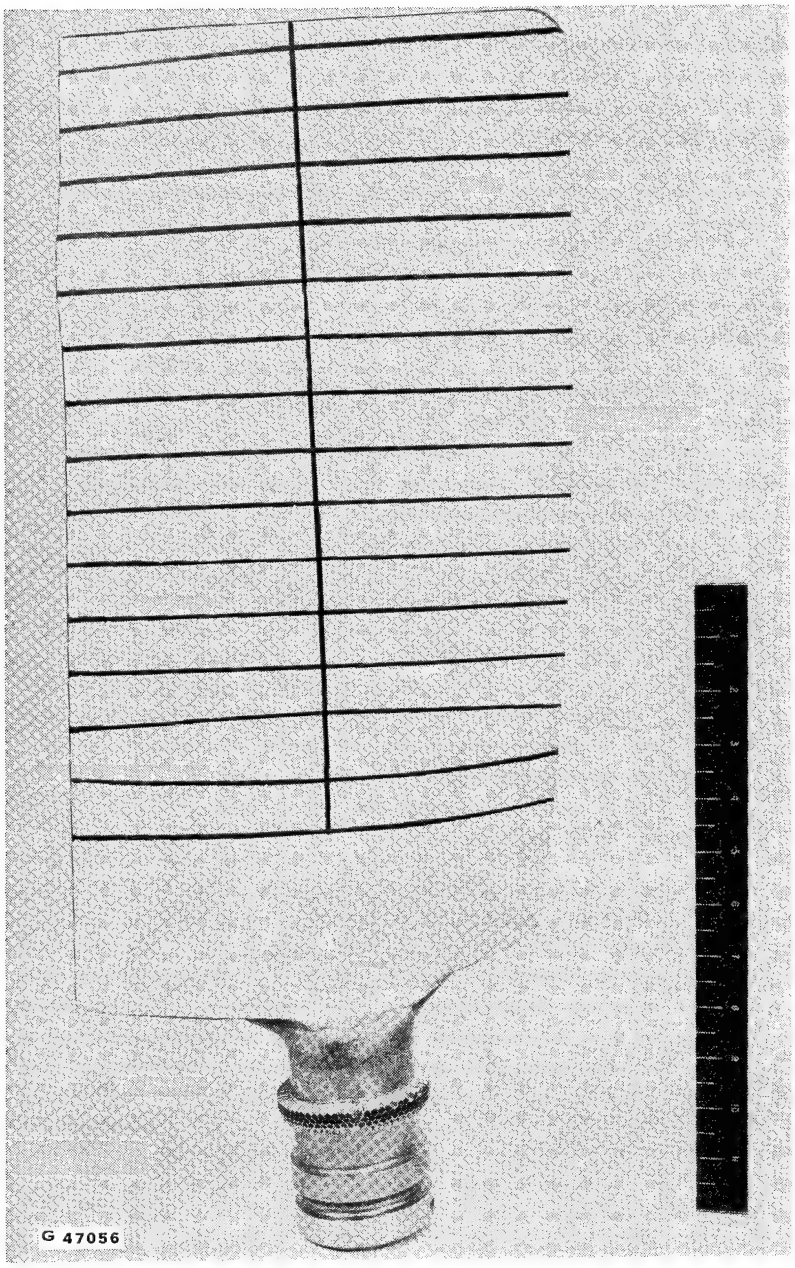

FIGURE 25. 1400G SIMULATED BIRD/0.38 RAD S/N 7 BLADE POST TEST CONDITION IMPACT ANGLE 258/300 G (9.1/10.6 OZ) SLICES (DOUBLE HIT)

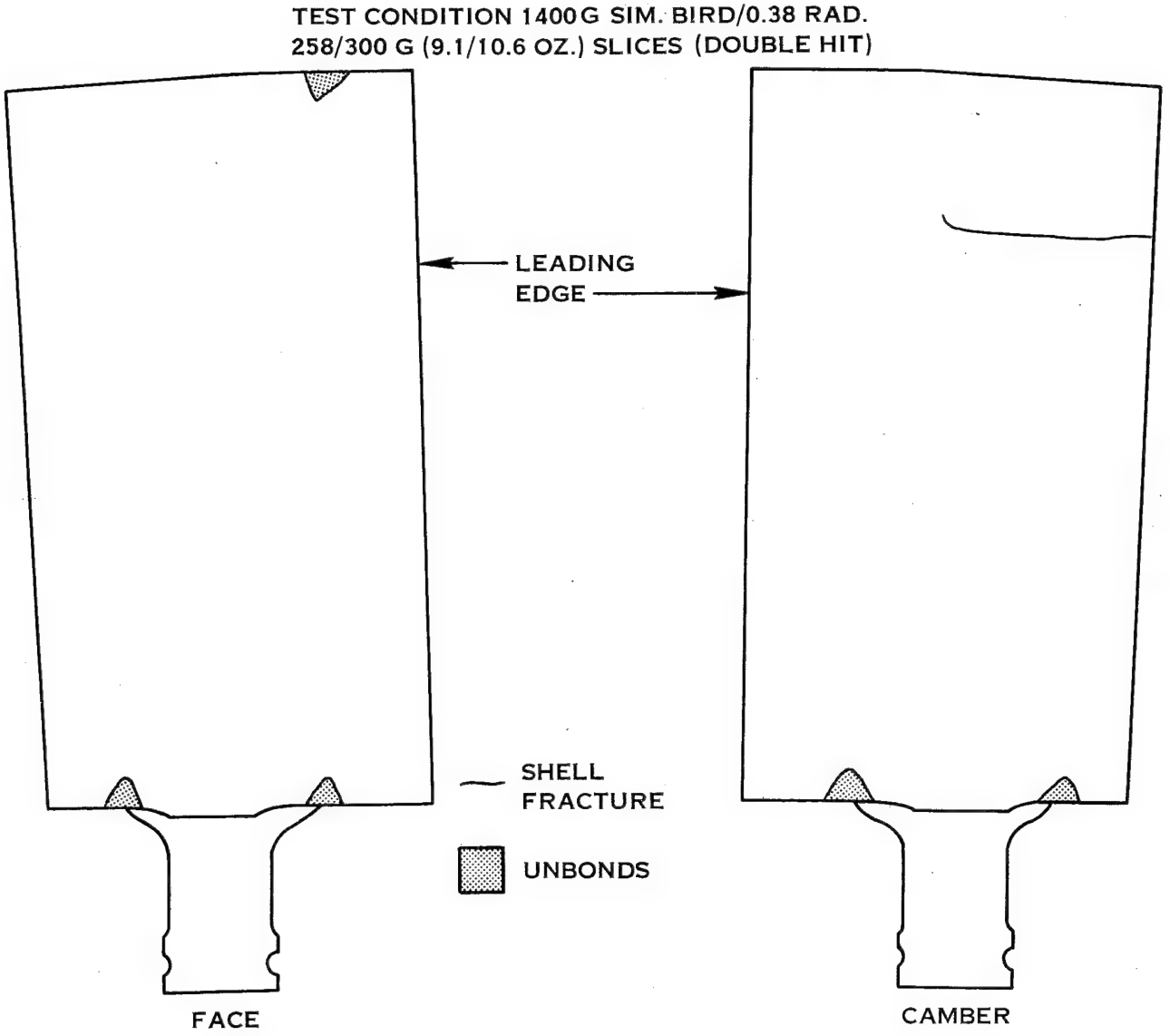

FIGURE 26. S/N 7 BLADE POST TEST CONDITION

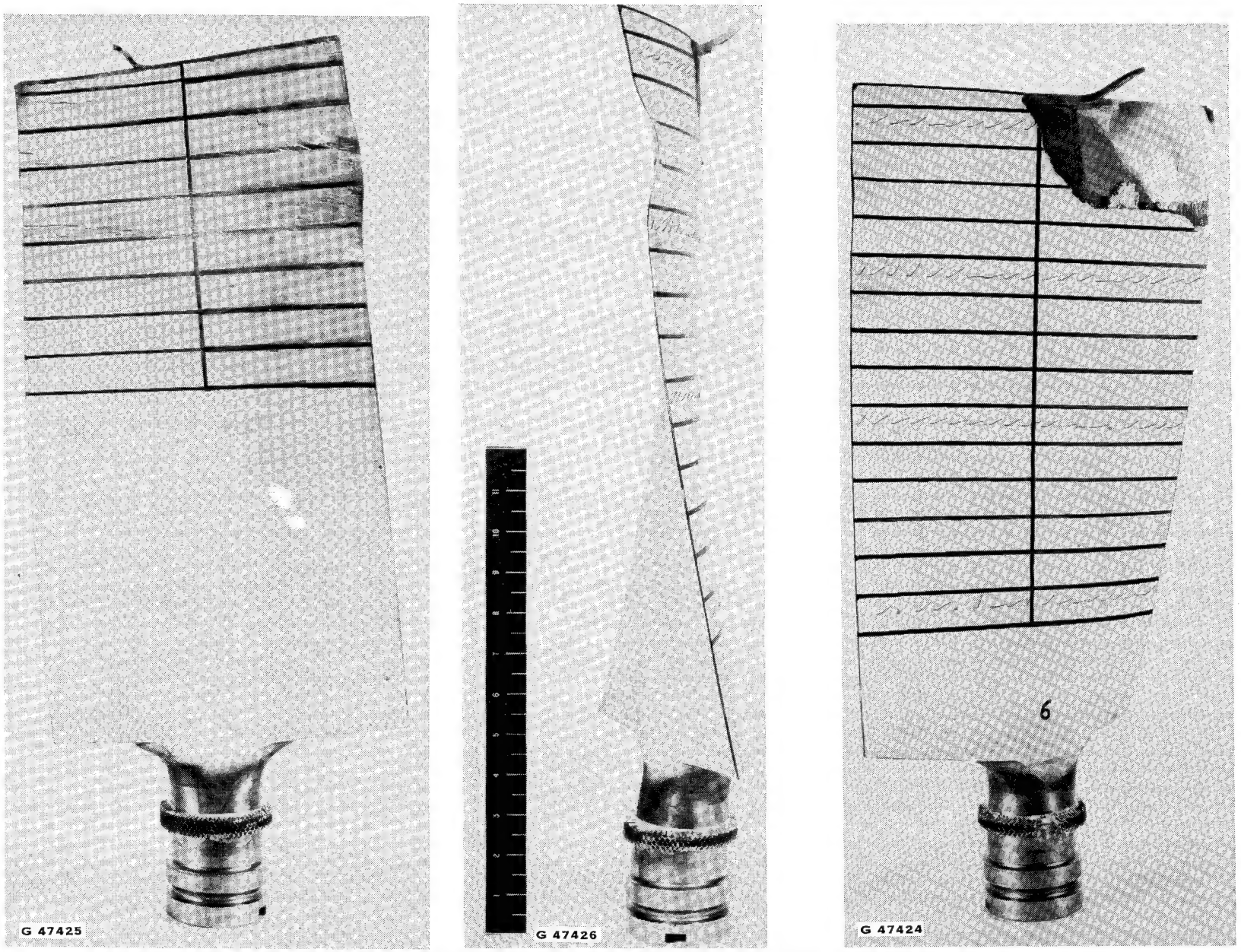

FIGURE 27. 1126G REAL BIRD/0.38 RAD S/N 6 BLADE POST TEST CONDITION
IMPACT ANGLE 681 G (24 OZ) SLICE

TEST CONDITION 1126G REAL BIRD/0.38 RAD.
681 G (24 OZ.) SLICE

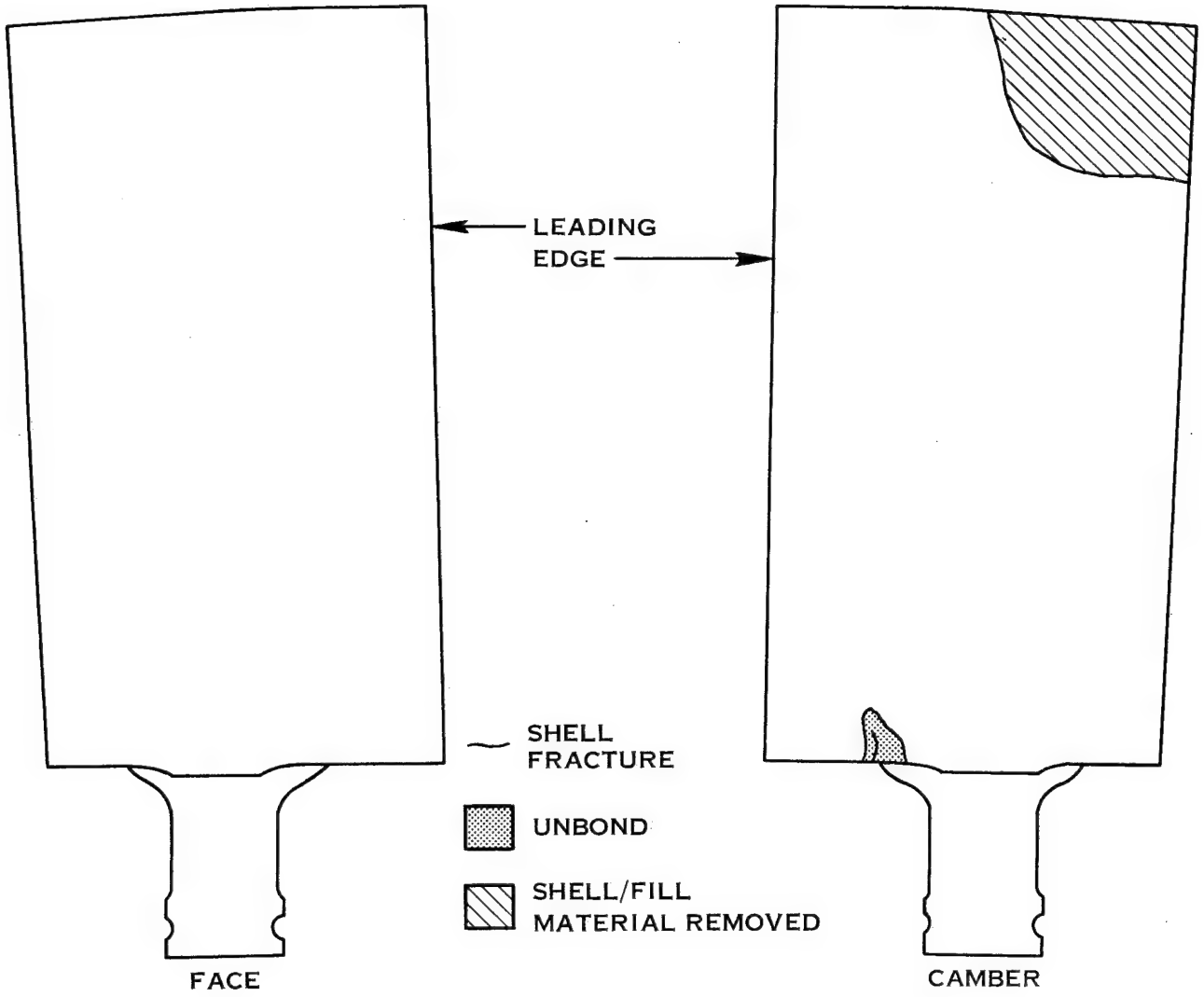

FIGURE 28. S/N 6 BLADE POST TEST CONDITION

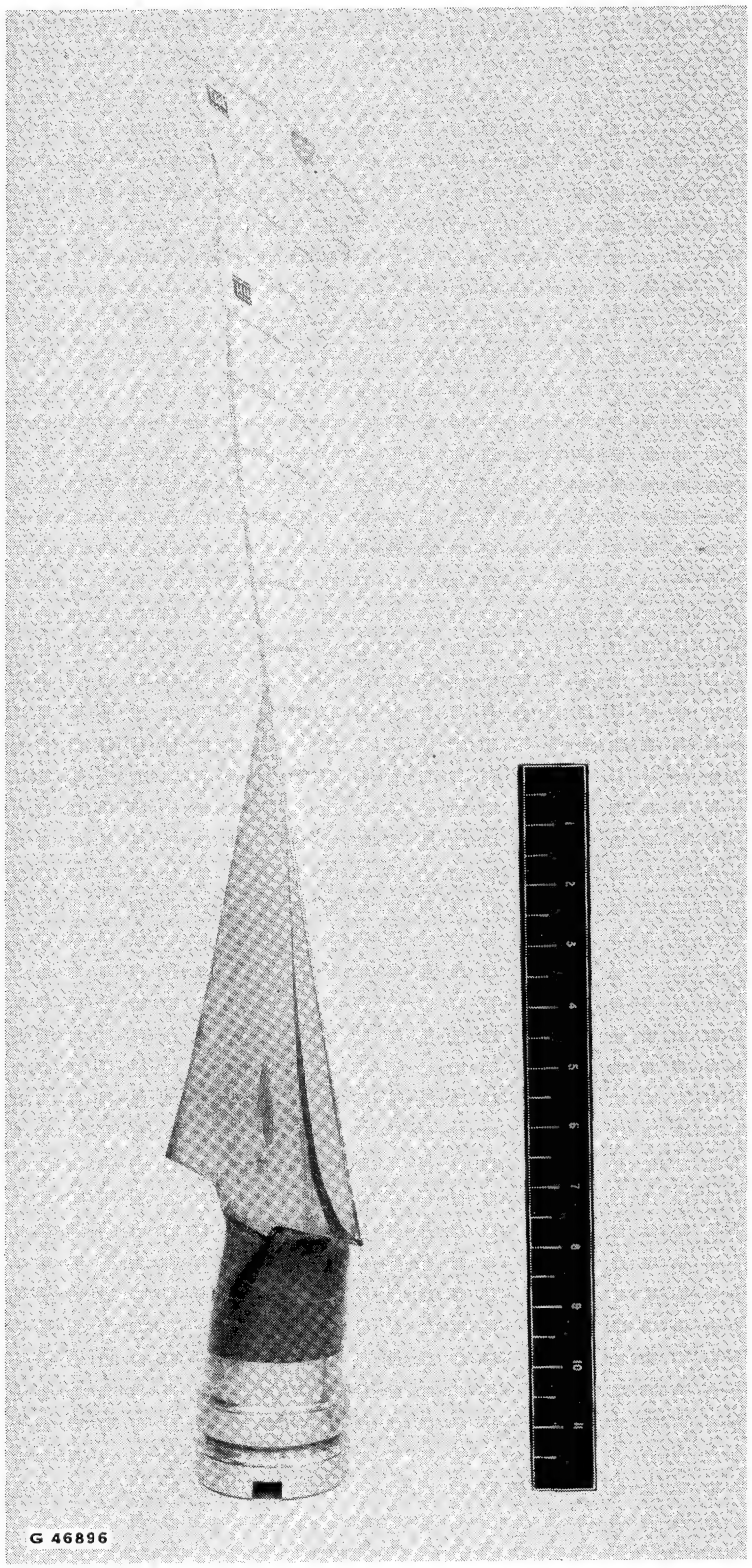

FIGURE 29. 5.08 CM ICEBALL/0.56 RAD S/N 5 BLADE POST TEST CONDITION IMPACT ANGLE 48G (1.7 OZ) SLICE

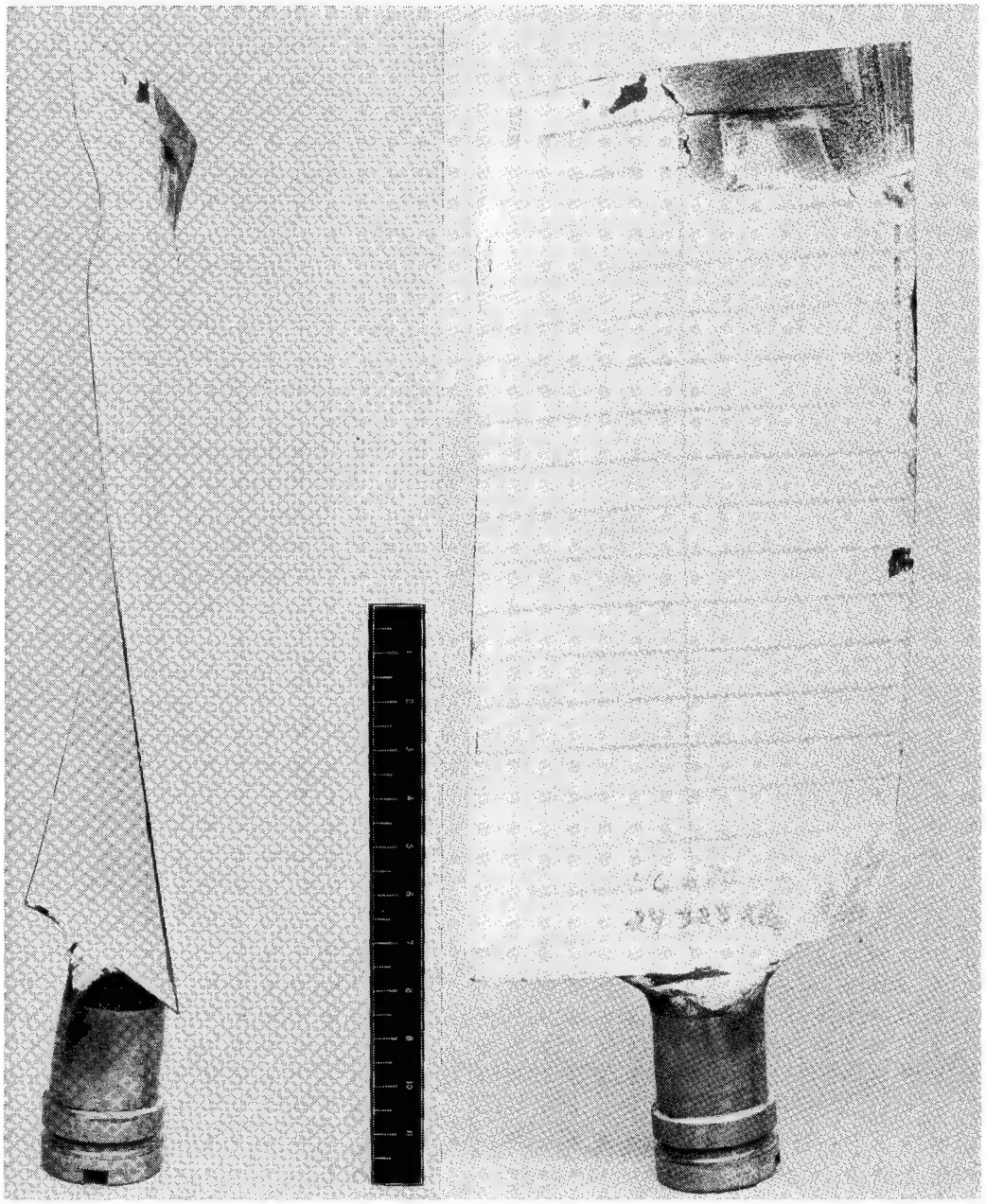

G 46910 G 46911

FIGURE 30. 300G SIMULATED BIRD/0.56 RAD S/N 1 BLADE POST TEST CONDITION IMPACT ANGLE 163 G (5.7 OZ) SLICE

TEST CONDITION 300G SIM BIRD/0.56 RAD
163 G (5.7 OZ) SLICE

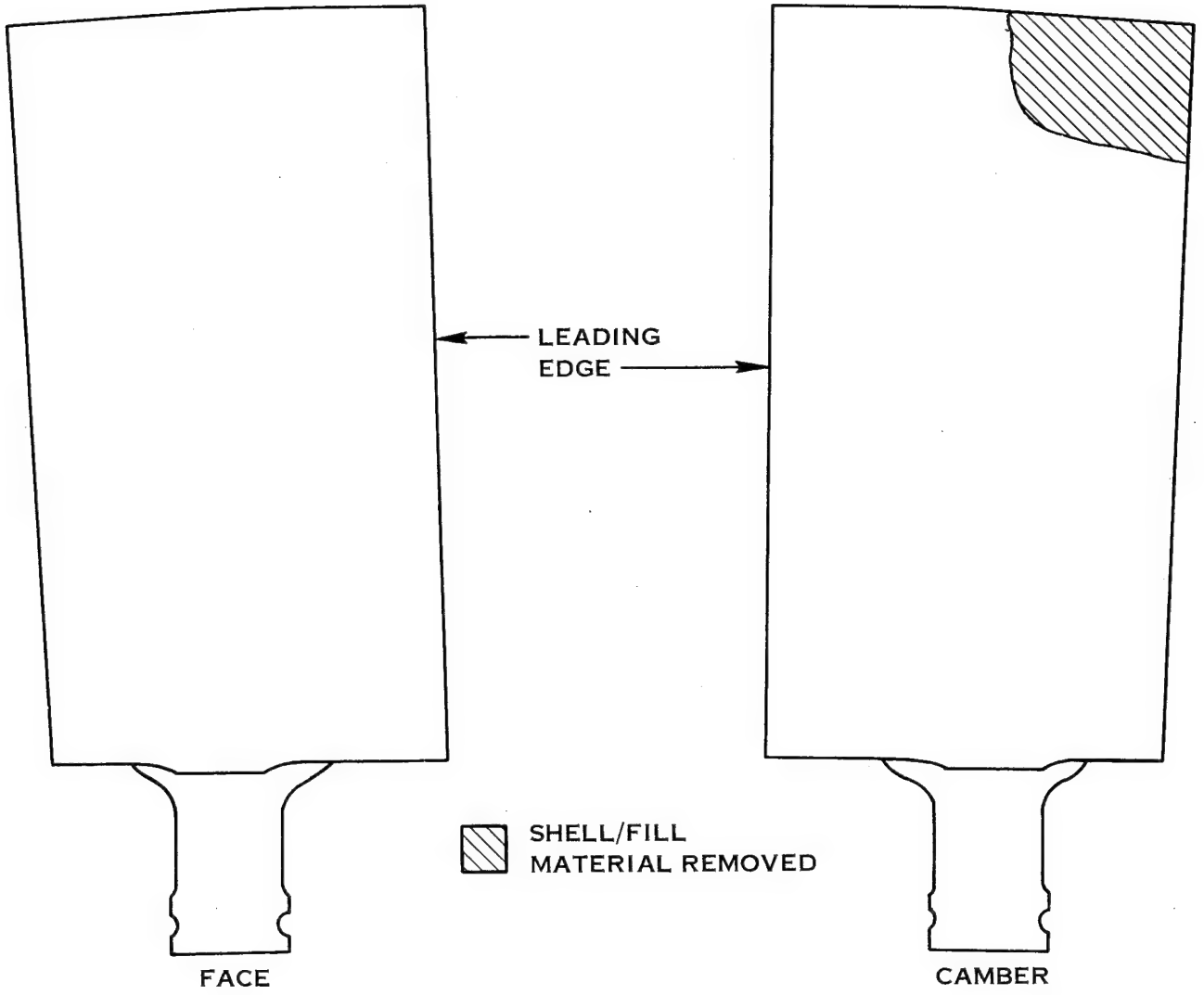

FIGURE 31. S/N 1 BLADE POST TEST CONDITION

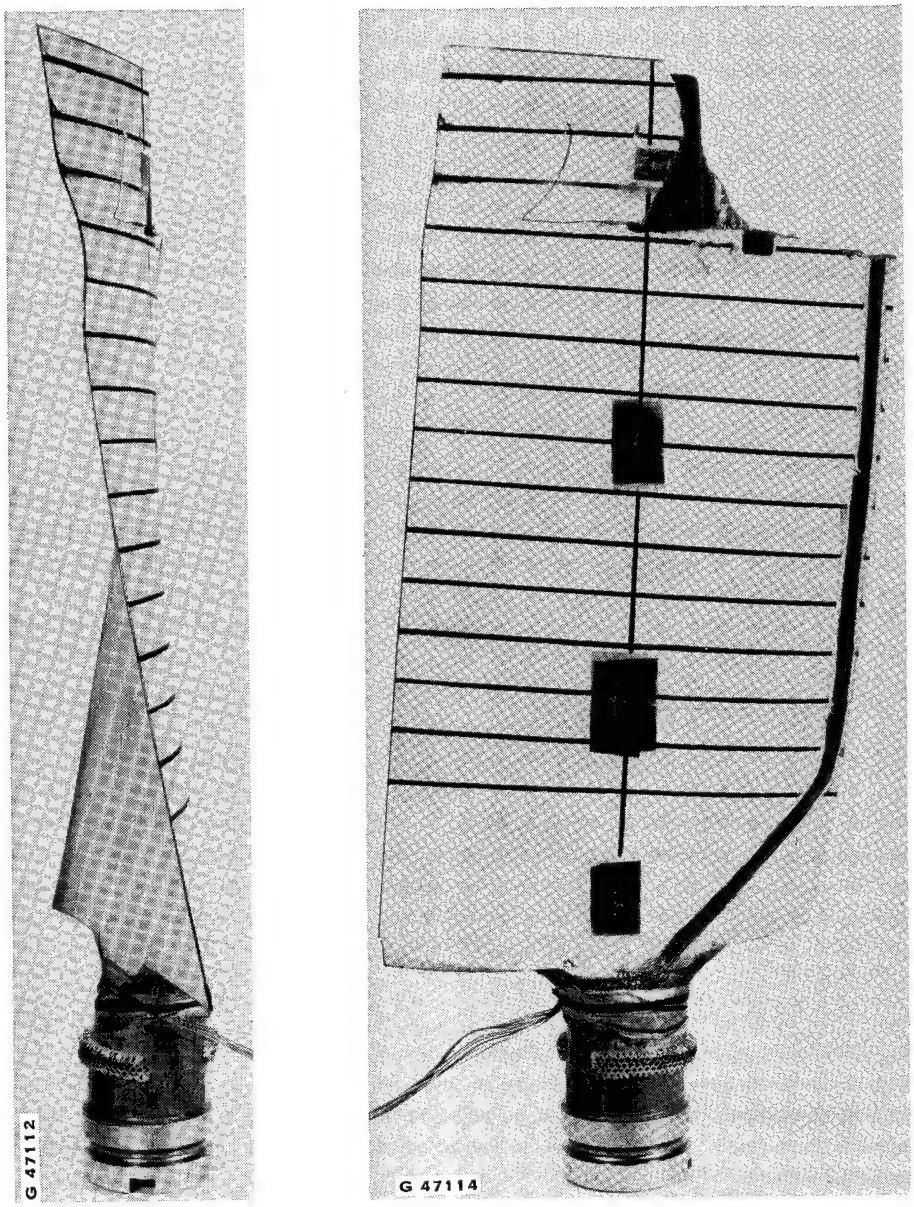

FIGURE 32. 700G SIMULATED BIRD/0.56 RAD S/N 4 BLADE POST TEST CONDITION IMPACT ANGLE 440 G (15.5 OZ) SLICE

TEST CONDITION 700G SIM. BIRD/0.56 RAD
440 G (15.5 OZ.) SLICE

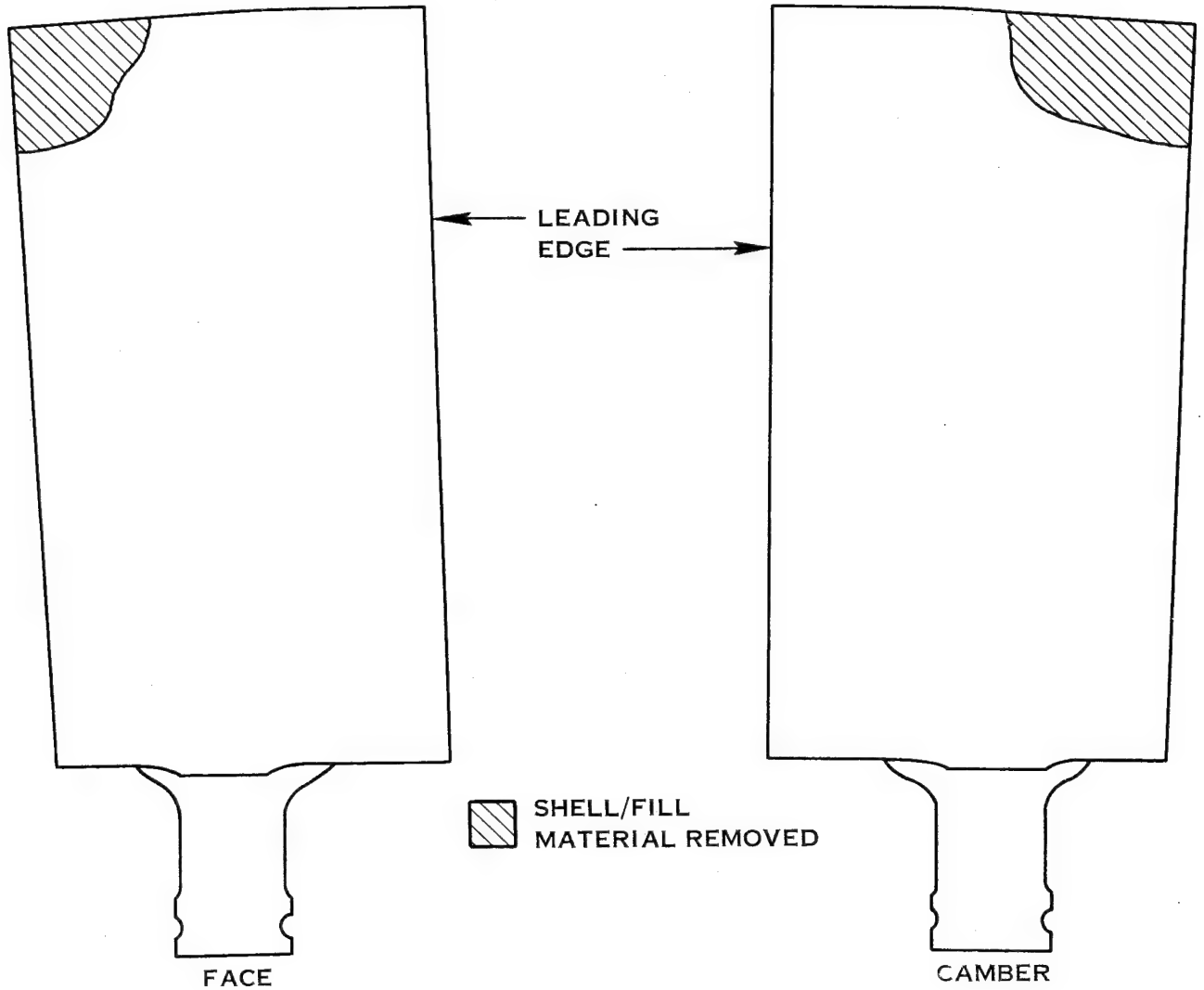

FIGURE 33. S/N 4 BLADE POST TEST CONDITION

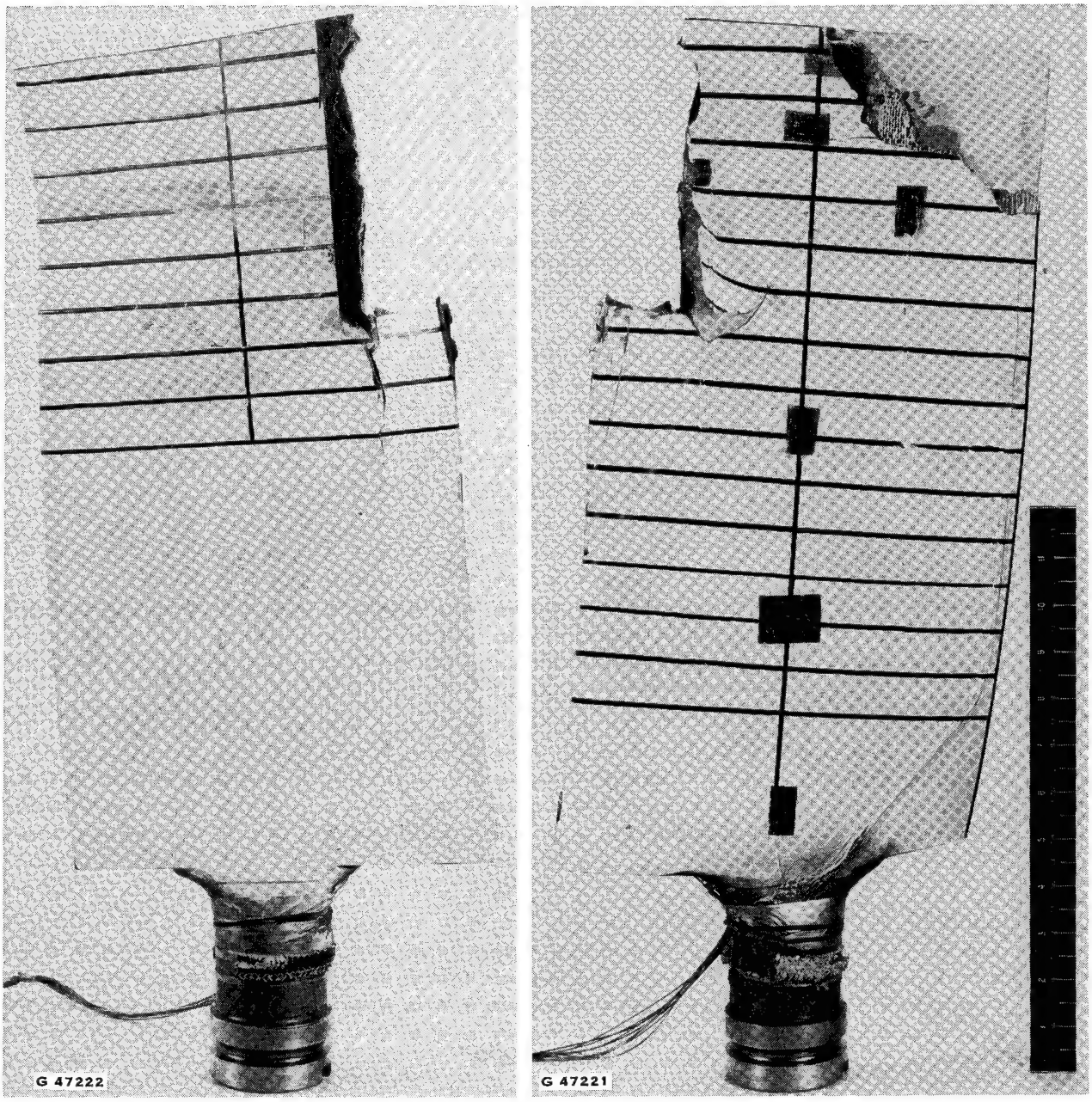

FIGURE 34. 1400G SIMULATED BIRD/0.56 RAD S/N 2 BLADE POST TEST CONDITION IMPACT ANGLE 763 G (26.9 OZ.) SLICE

TEST CONDITION 1400 G SIM. BIRD/0.56 RAD.
763 G (26.9 OZ.) SLICE

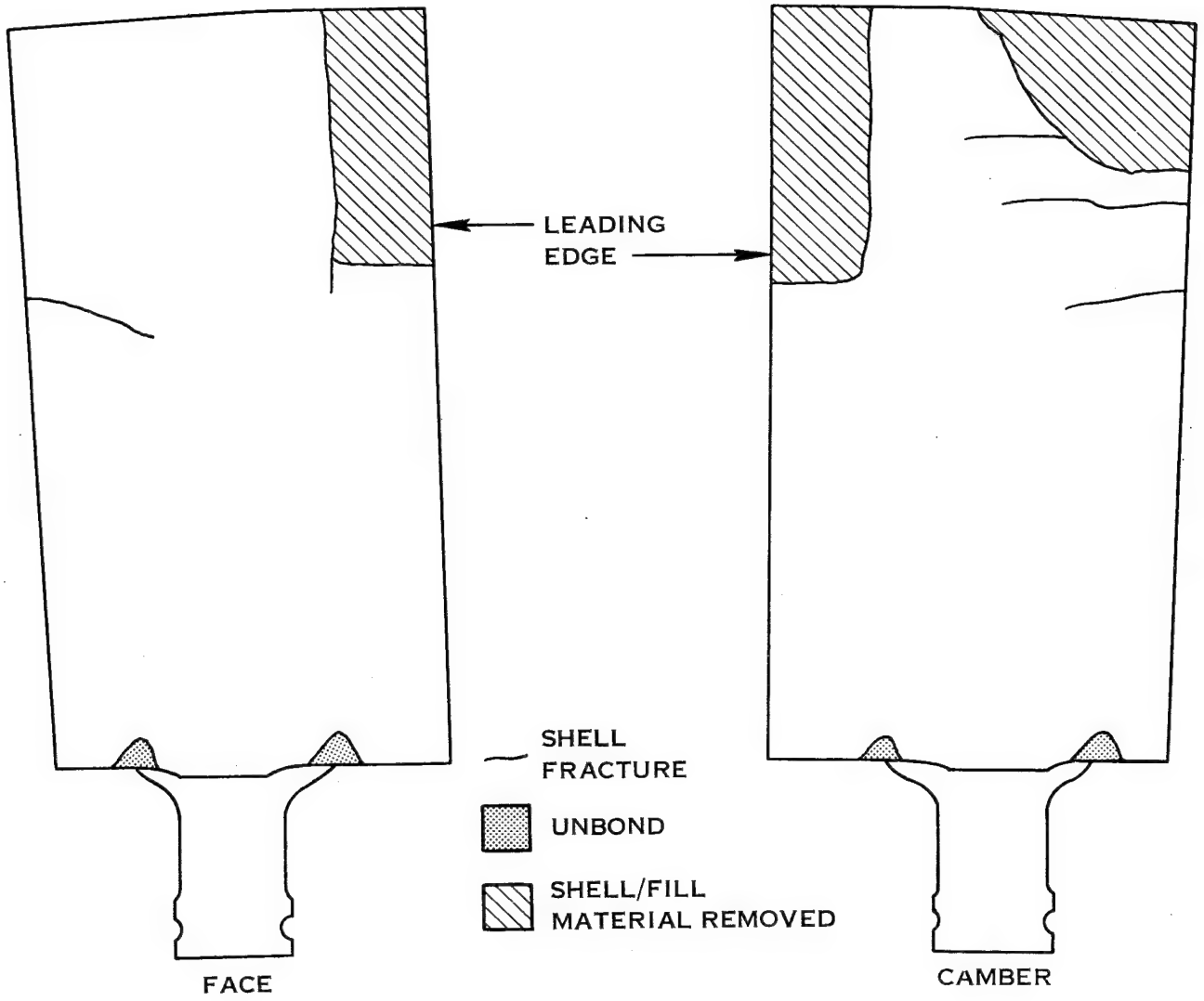

FIGURE 35. S/N 2 BLADE POST TEST CONDITION

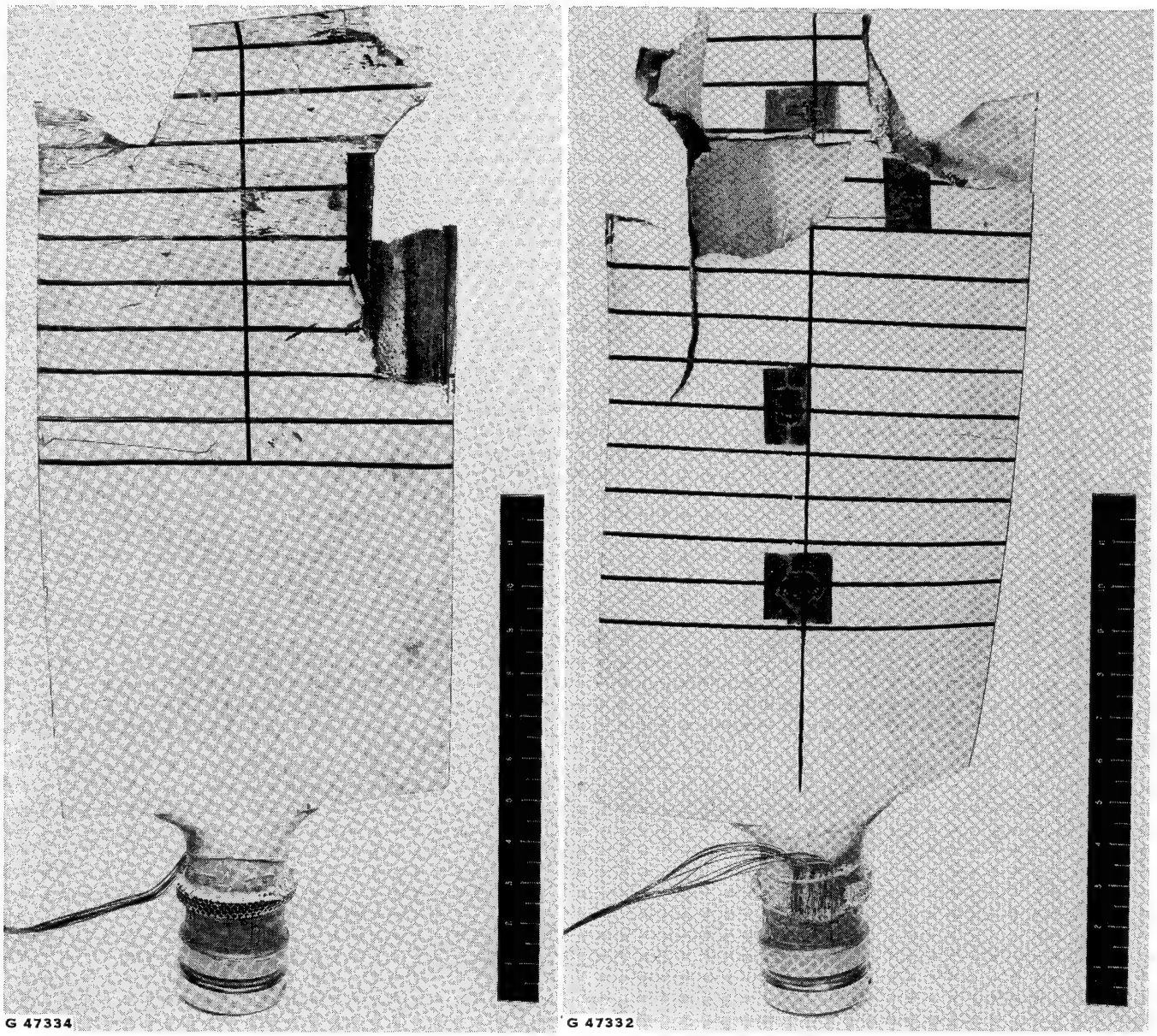

FIGURE 36. 1203G REAL BIRD/0.56 RAD IMPACT S/N 9 BLADE POST TEST CONDITION ANGLE 788 G (27.8 OZ.) SLICE

TEST CONDITION 1203G REAL BIRD/0.56 RAD.
788 G (27.8 OZ.) SLICE

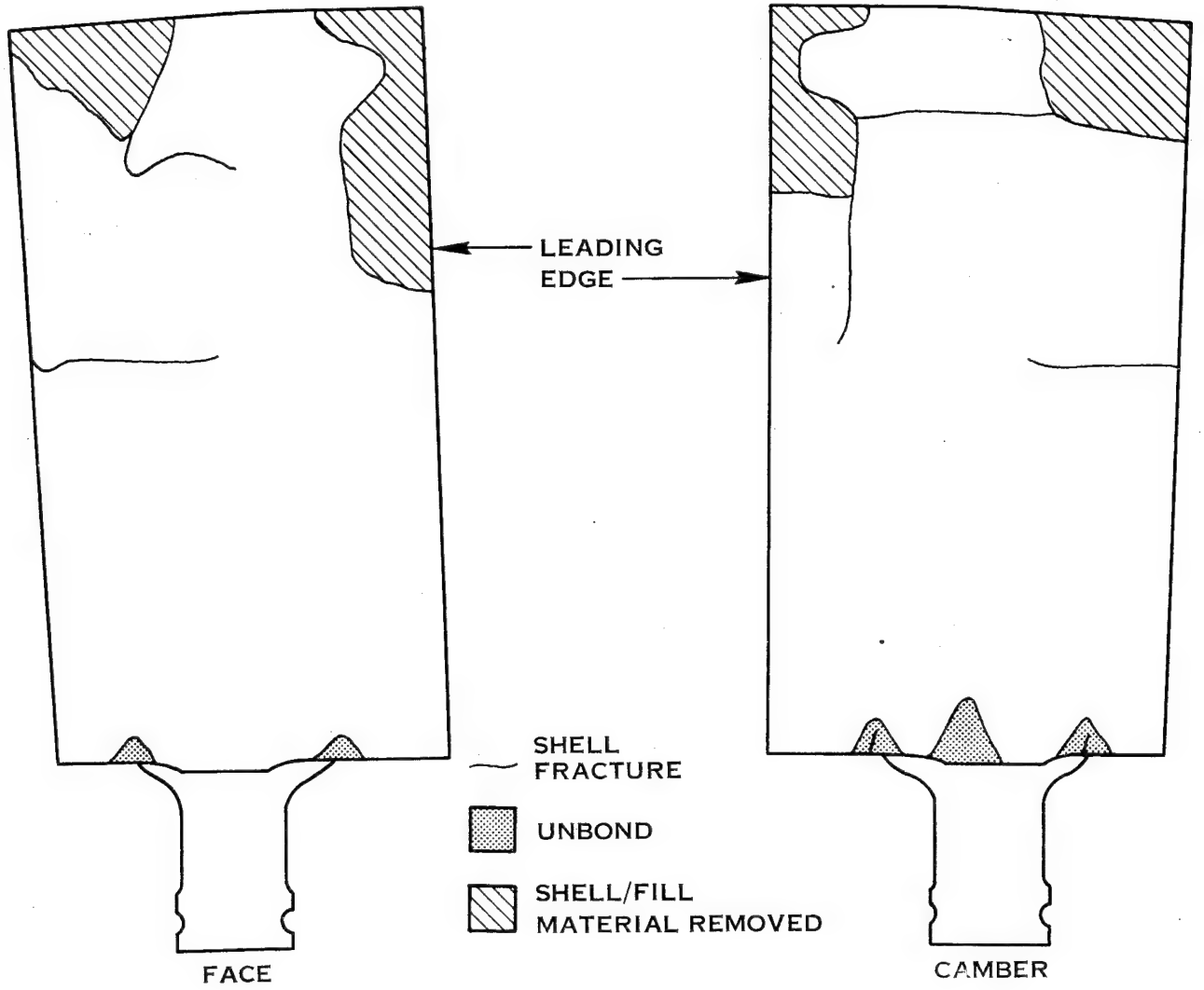

FIGURE 37. S/N 9 BLADE POST TEST CONDITION

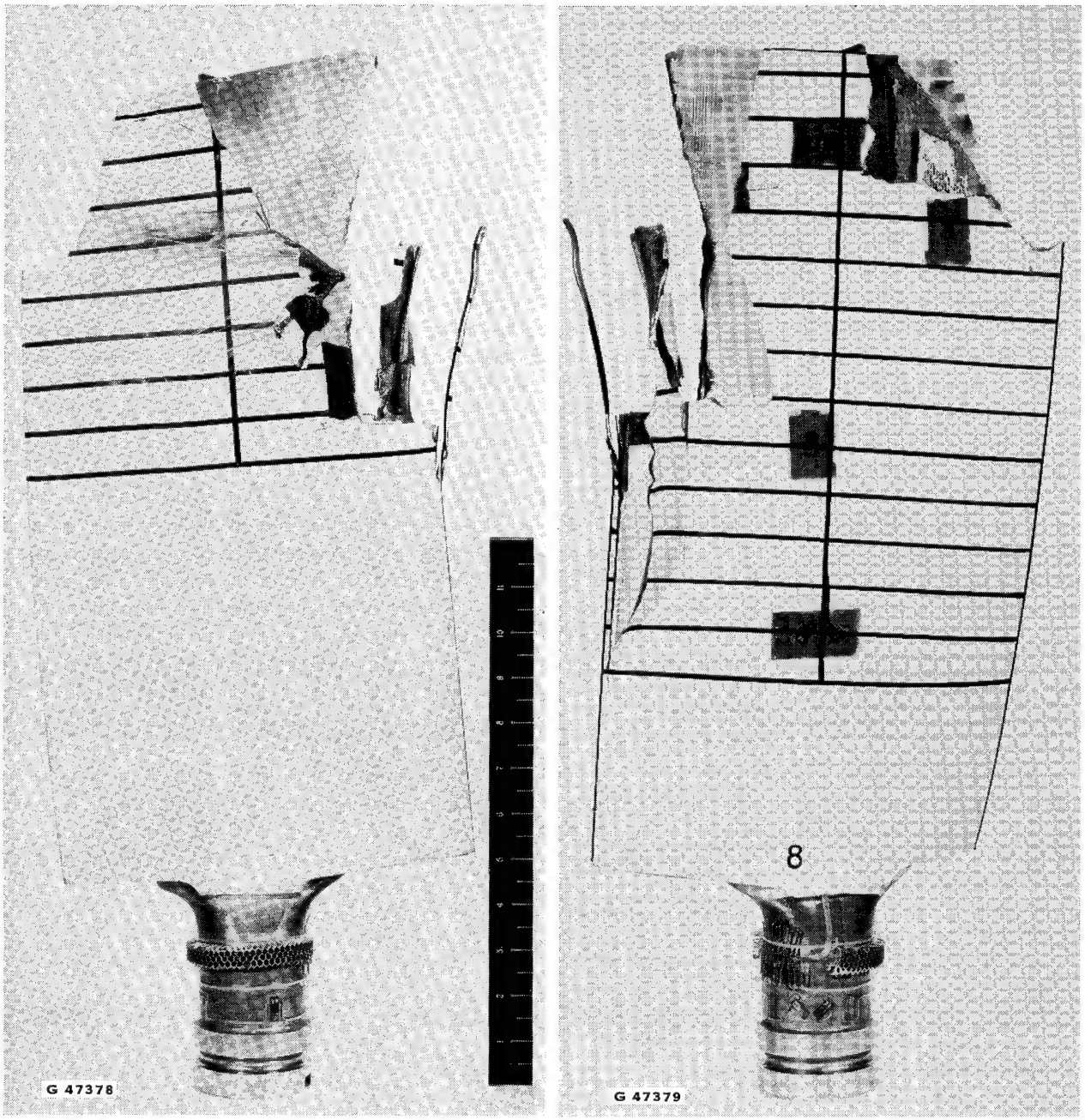

FIGURE 38. 1400G SIMULATED BIRD/0.56 RAD S/N BLADE POST TEST CONDITION IMPACT ANGLE/FIXED RETENTION 650 G (22.9 OZ.) SLICE

TEST CONDITION 1400G SIM. BIRD/0.56 RAD/FIXED ROOT
650 G (22.9 OZ.) SLICE

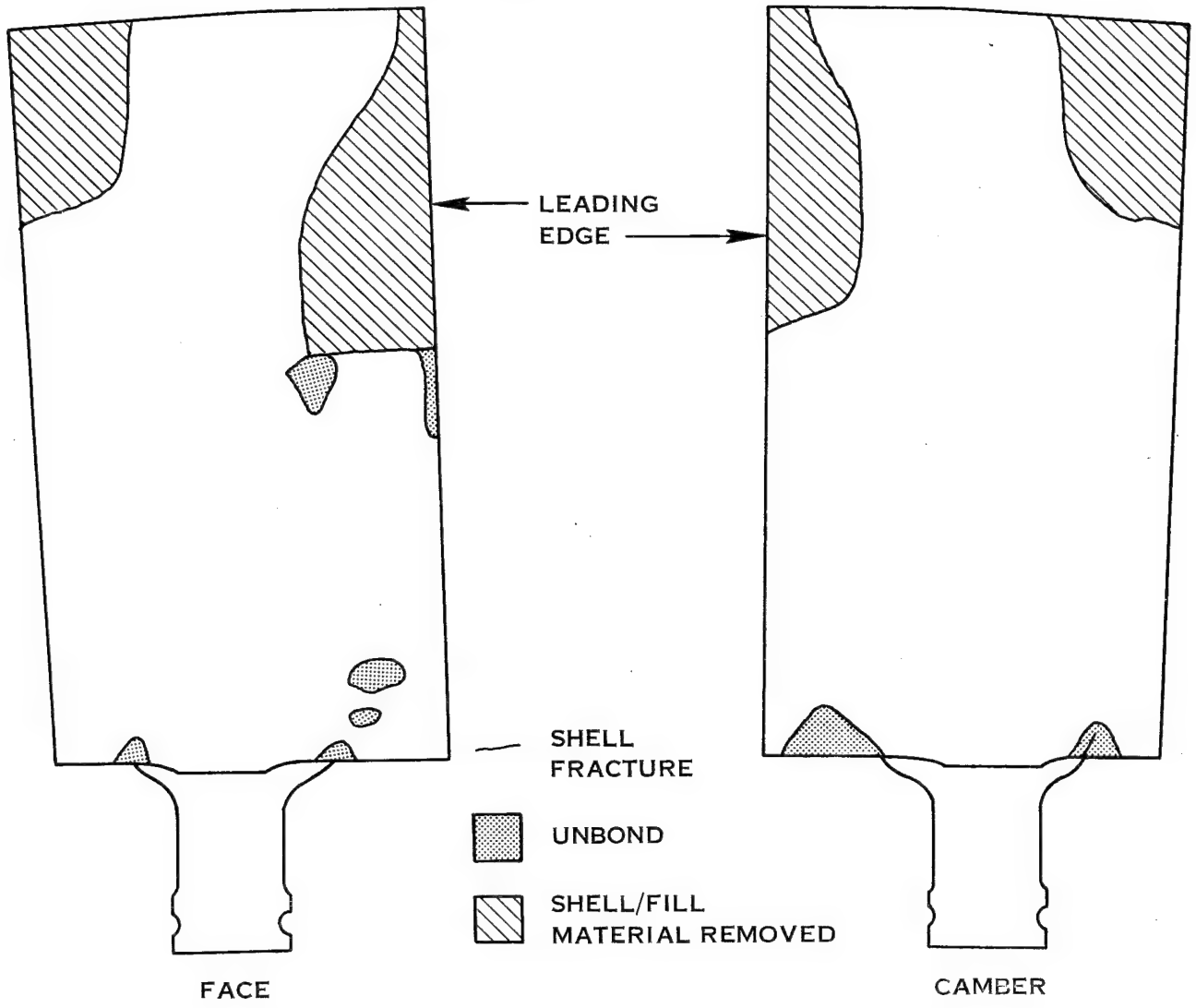

FIGURE 39. S/N 8 BLADE POST TEST CONDITION

The local blade response dynamic analysis gives spanwise bending and torsional stresses near the impact site during and immediately after the impact.

The local chordwise stress analysis is a dynamic analysis only in the sense that blade shell acceleration loads, obtained from the local blade response analysis, are applied to the leading edge in addition to the local pressure of the impact.

In particular, analyses employed in each of the above categories are described in more detail in the following paragraphs.

Three Degree-of-Freedom Gross Blade Response Dynamic Analysis

This gross blade response analysis assumes that the blade responds to an impact in its primary flatwise bending, edgewise bending, and torsional vibration modes. This analysis has been found to be accurate for impacts located between 35% and 85% of the blade span. The blade is represented as a spring-lump mass system in which the mass in each mode is located at the impact station and the spring rate for each mode is obtained by applying a static load at the impact station in the respective direction of motion. The mass for each mode is calculated so as to give the same frequency in each mode, in combination with the above respective spring rate, as the respective blade frequency. The analysis includes the effects of centrifugal stiffening, blade twist, retention stiffness and orientation, damping and blade motion on impact. Post-rocking behavior of blades that rock or exceed their retention moment capability can be determined by running the analysis in two stages. The analysis, has been used for all of the gross response analysis in the NASA-Lewis program.

Multi-Mode Dynamic Response Analysis

This is both a gross and a local blade response analysis and, in addition, generates impact pressure distributions for use in the local chordwise stress analysis. The analysis treats the impact as a series of incremental impacts of a multi-element missile, in which blade response is calculated after each time increment. The blade is assumed to respond in its normal beam modes; a typical case may use as few as four modes or as many af fifteen. The response in each mode is determined so as to minimize the strain energy of the blade. An elementary bird crushing analysis, which can be calibrated as test results become available, is applied to each missile element as it traverses the blade, providing pressure distribution data for use in the calculation of local stresses. In its present form this analysis is applicable to blades which are rigidly mounted or pinned at the shank and which do not have part span shrouds. This analysis does not as yet treat the post-rocking behavior of ball-retention blades.

At the present time, the analysis has not been fully verified and therefore the stress and deflection results it produces are somewhat uncertain. In the FOD fan blade program the analysis was used only for the purpose of obtaining very approximate impact load pressure distributions.

Perturbation Analysis

This analysis, which is a local blade response analysis, has recently been completed and programmed. It assumes that the deflection shape during impact is a perturbation from the primary bending mode shape. The deflection shape is determined so as to minimize the bending strain energy in the blade. Thus far, it has been applied to only the most severe of the test conditions.

Local Chordwise Stressing

This analysis assumes that the shell leading and trailing edges behave as cantilever beams built in at the spar leading and trailing edges, respectively, as shown in figure 40a. Incremental pressures, each of which acts over a different spanwise length, are obtained from the Multi-Mode Analysis. At any chordwise station, the effective spanwise length of the blade shell relative to a particular pressure increment is obtained by projecting 0.79 rad (45°) lines, as shown in Figure 40b. Section properties, bending moments and stresses are then obtained from simple beam theory. The method has been applied to the FOD fan blade design used in this program for a 50% slice of 1400 g (3 lb) bird impact condition.

Analysis of Test Conditions and Comparison of Theoretical and Experimental Results

Four fan blades were instrumented extensively to determine the blade gross and local stresses resulting from the impact. These blades were all tested at 0.56 rad (32°) angle of incidence. The test conditions for these blades were 700 g and 1400 g simulated birds, 1203 g (2.65#) real duck, and a 1400 g simulated bird with the blade fixed in its retention. These tests were designed to evaluate bird size effects, real bird versus simulated bird impact effects and fixed retention vs rocking retention. The instrumentation layouts are shown in figures 41 and 42. The data was recorded on a high speed tape system to obtain good resolution of the impact stresses. Gage 3 was eliminated when gages A and B were added and required the readout channel which had been provided for gage 3.

A summary of the test program data is given in table 1. The strain gage data were obtained in tests 4, 5, 10, and 11.

The peak stress values for each strain gage in each of these four tests are given in table VI. Theoretical stresses, obtained by means of the various analytical techniques described previously, are given in table VII for the test conditions and gage locations specified previously.

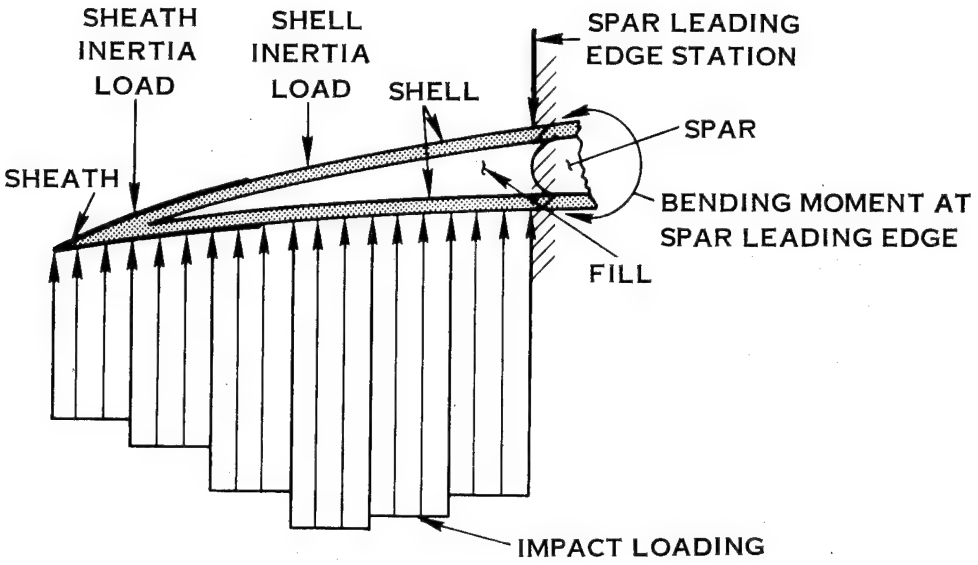

(A) CROSS-SECTION AT IMPACT STATION

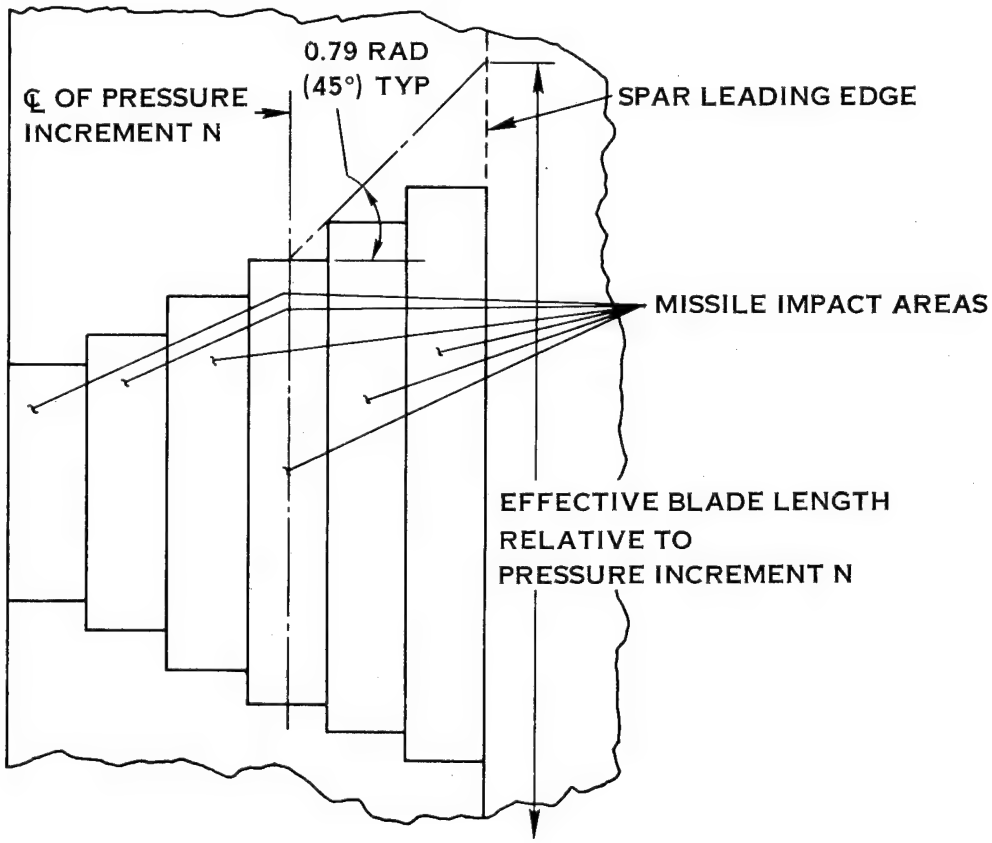

(B) PLAN VIEW OF BLADE AT IMPACT STATION

FIGURE 40. LOCAL CHORDWISE BENDING STRESS ANALYSIS MODEL

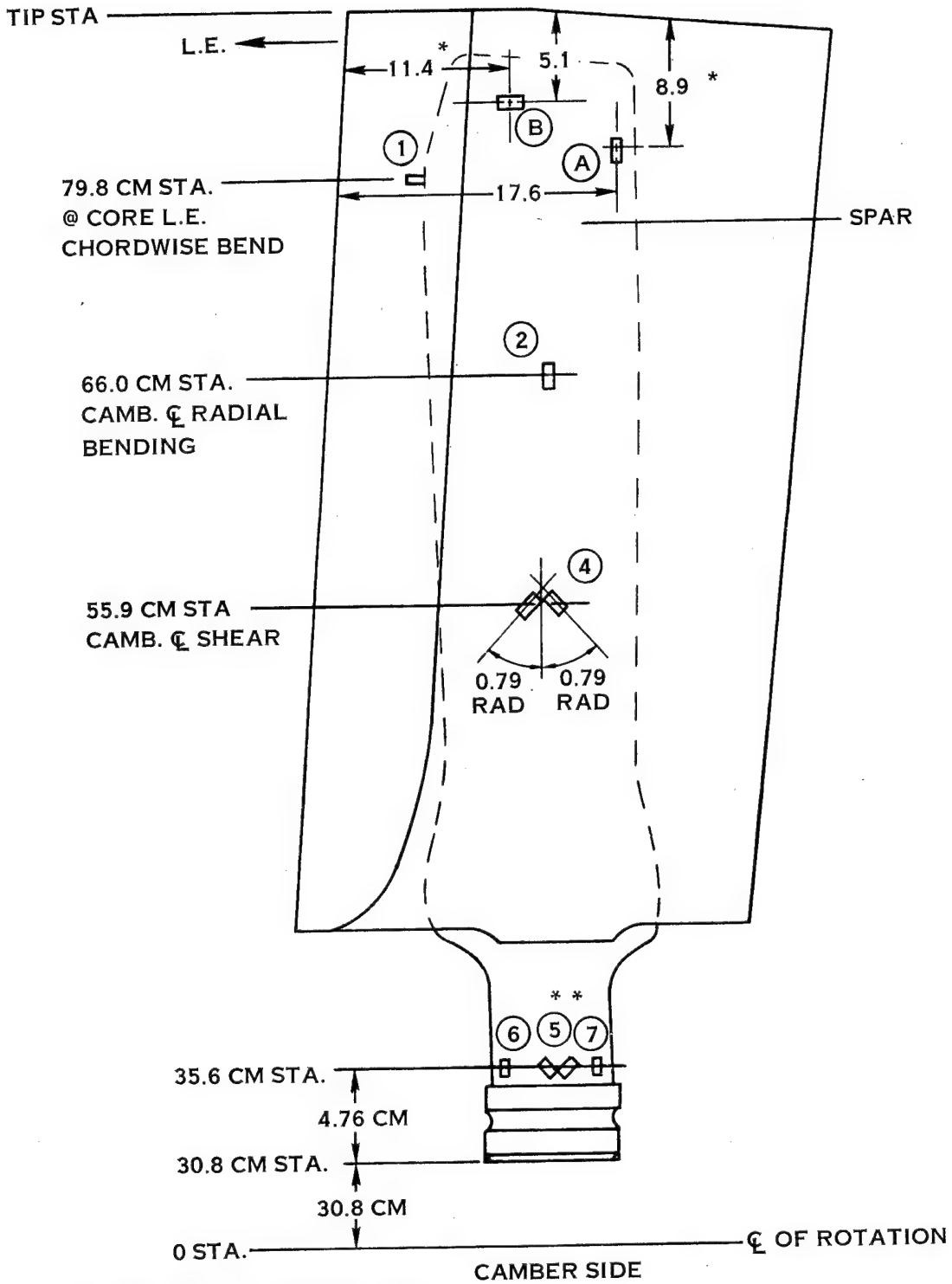

GAGE TYPE EA-06-250 BF-350

*FOR BLADE S/N 1, GAGE B DIM. IS 12.7 CM, GAGE A DIM. IS 7.6 CM

**GAGE (5) = 0.79 RAD ± SHEAR PAIR

FIGURE 41. FOD BLADE INSTRUMENTATION LAYOUT FOR BLADES S/N 1, 2, 8, 9

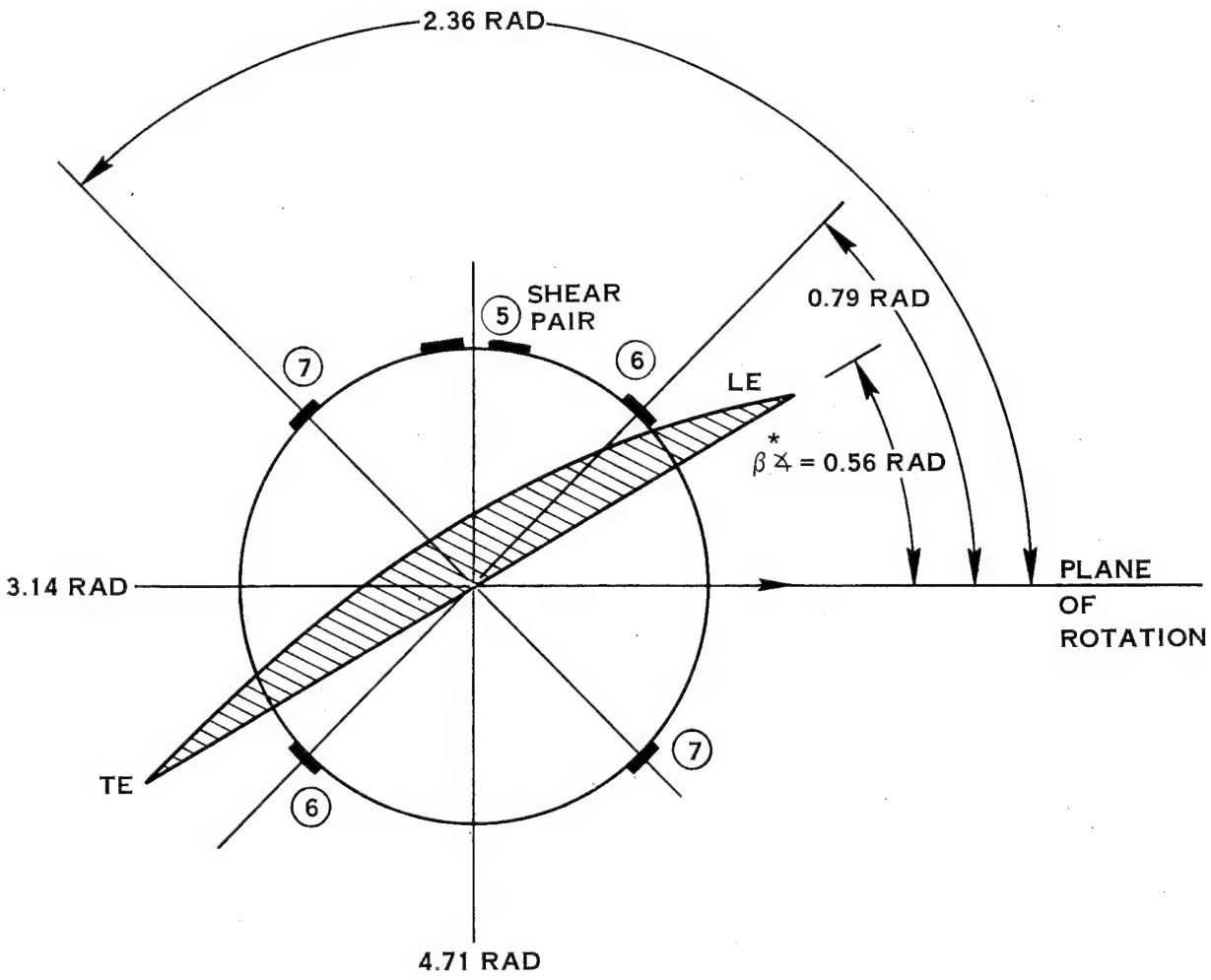

SHANK GAGE LOCATIONS
VIEW FROM TIP

* $\beta \measuredangle$ = 0.56 RAD @ 79.8 CM STA. REF.

FIGURE 42. FOD BLADE INSTRUMENTATION LAYOUT FOR BLADES S/N 1, 2, 8, 9

TABLE VI

EXPERIMENTAL RESULTS FROM INSTRUMENTED IMPACT TESTS

INTERNATIONAL SYSTEM OF UNITS

		Test #4	Test #5	Test #10	Test #11
Missile Impact Wt., g		440	763	788	650
Missile Type		Gelatin	Gelatin	Real Bird	Gelatin
Impact Angle (rad.)/Station	(m)	0.56/0.782	0.56/0.782	0.56/0.782	0.56/0.782
Stress at Strain Gage No. (See Figures 41, 42)	1	-125,400*	-215,100*	-268,900*	-394,400*
	2	-119,300	-153,800	-119,300	-158,600
	A	125,500*	138,600*	159,300*	106,200
	B	-80,700*	-114,800*	-120,000*	-71,700
(N/m^2)	4	37,400	46,100	46,100	28,800
	5	10,300	12,800	12,800	8,500
	6	30,900	25,400	22,100	33,100
	7	44,100	53,100	60,700	66,200
Resultant Stress, No. 6 and	7	52,400	57,400	63,000	70,300
Retention Type		Rocking	Rocking	Rocking	Fixed
Rocking Angle (rad.)		----	0.19	0.23	----

U.S. CUSTOMARY UNITS

		Test #4	Test #5	Test #10	Test #11
Missile Impact Wt. (oz.)		15.5	26.9	27.8	22.9
Missile Type		Gelatin	Gelatin	Real Bird	Gelatin
Impact Angle (deg.)/Station	(in.)	(32/30.8)	(32/30.8)	(32/30.8)	(32/30.8)
Stress at Strain Gage No. (See Figures 41, 42)	1	182,000*	-312,000*	-390,000*	-572,000*
	2	-173,000	-223,000	-173,000	-230,000
	A	182,000	201,000	231,000	154,000
	B	-117,000*	-166,500*	-174,000*	-104,000
(psi)	4	54,300	66,800	66,800	41,700
	5	14,900	18,600	18,600	12,400
	6	44,800	36,800	32,000	48,000
	7	64,000	77,000	88,000	96,000
Resultant Stress, No. 6 and	7	76,000	83,300	91,300	102,000
Retention Type		Rocking	Rocking	Rocking	Fixed
Rocking Angle (deg.)		----	11	13	----

*These are not true stresses; in some cases yielding has occurred giving erroneously high readings and in other cases fracture occurred at or near the gages, giving erroneously low stresses.

TABLE VII

THEORETICAL RESULTS FOR INSTRUMENTED IMPACT CONDITIONS

INTERNATIONAL SYSTEM OF UNITS

		Test #4	Test #5	Test #10	Test #11
Missile Impact Wt., (g)		440	763	788	650
Missile Type		Gelatin	Gelatin	Real Bird	Gelatin
Impact Angle (rad.)/Station (m)		0.56/0.782	0.56/0.782	0.56/0.782	0.56/0.782
Stress at Strain Gage No. (See Figures 41, 42)	1				-86,900(7)
	A		89,600(6)	89,600(6)	
(N/m^2)	4	32,400(3)	33,900(1)	33,900(1)	33,600(3)
	5	11,400(3)	12,000	12,000(1)	11,800(3)
Resultant Stress, No. 6 and	7	62,700(4)	62,700(4)	62,700(4)	102,700(3)
Retention Type		Rocking	Rocking	Rocking	Fixed
Rocking Angle (rad.)		----	0.18(5)	0.18(5)	----

U.S. CUSTOMARY UNITS

		Test #4	Test #5	Test #10	Test #11
Missile Impact Wt., (oz.)		15.5	26.9	27.8	22.9
Missile Type		Gelatin	Gelatin	Real Bird	Gelatin
Impact Angle (deg.)		32/30.8	32/30.8	32/30.8	32/30.8
Stress at Strain Gage No. (See Figures 41, 42)	1				-126,000(7)
	A		130,000(6)	130,000(6)	
(psi)	4	47,000(3)	49,200(1)	49,200(1)	48,700(3)
	5	16,500(3)	17,400(1)	17,400(1)	17,100(3)
Resultant Stress, No. 6 and	7	91,000(4)	91,000(4)	91,000(4)	149,000(3)
Retention Type		Rocking	Rocking	Rocking	Fixed
Rocking Angle (deg.)		----	10.3(5)	10.3(5)	----

(1) Data obtained with Multi-Stream version of Three Degree-of-Freedom Program.
(2) Data obtained with Single Stream version of Three Degree-of-Freedom Program.
(3) Estimated data based on Single Stream analysis and Multi-Stream analysis of Tests 5 and 10.
(4) Values limited by retention rocking.
(5) Obtained with single stream analysis of 700 gm missile.
(6) Obtained with perturbation analysis.
(7) Local chordwise bending analysis with 680 gm missile.

The theoretical impact stresses predicted in the shank region, where the FOD analyses are considered most accurate, are higher than the experimental values. However, the high speed movies show a great deal of bird crushing and spreading; and some of the missile material appears to have spread off the blade before the momentum transfer was complete. These occurrences are the likely reasons for the lower than predicted impact stresses.

As predicted, rocking occurred in tests, Nos. 4, 5, and 10. Reduction in shank bending moment, as indicated by the resultant of gages 6 and 7, was realized as compared to the fixed retention test, No. 11.

Gages A and B were placed near the fracture locations which had been identified in the early, non-instrumented tests. These fracture locations were found to recur very consistently in subsequent tests. Although it is difficult to determine from the movies where the fracture originated, it is clear from the traces of gages A and B that events occurred in the following sequence: the chordwise gage, B, responded first, being closer to the leading edge than gage A. Gage B responded in a negative or compression sense, indicating a decambering of the cross-section due to the beginning of the impact at the leading edge. Gage B passed through a compression peak successfully and began to give a positive reading as gage A began to respond. Gage A responded in a positive sense, indicating spanwise bending with the camber side in tension as expected. Fracture then occurred at gage A and shortly thereafter at gage B.

The local chordwise bending analysis, for gage 1, and the perturbation analysis, for gage A, both predicted stresses considerably lower than the respective test results. It is believed that the perturbation analysis does not include enough flatwise bending modes to accurately predict local stresses in the blade. The multi-mode dynamic response analysis, discussed earlier, includes as many modes as needed. When this analysis becomes fully operational it is believed that improved values of local spanwise stresses will be obtained. Accurate analysis of local chordwise bending stresses is a more difficult task, requiring knowledge of local pressure distributions and a more sophisticated description of local dynamic and structural behavior.

It is concluded that good experimental results have been obtained, and good agreement with theory is found for the impacts in the shank regions of the blade. More sophisticated methods are being developed for accurate prediction of stresses near the impact.

CONCLUSIONS

The following conclusions were drawn from observations and results of this test program:

1. Blades which were impacted by birds of 900 g (2 lb) or less, were judged capable of continued operation after impact at conditions specified by FAA AC33-1B for medium size birds.

2. All blades evaluated in the program were judged structurally capable of supporting a controlled engine shutdown after impact at conditions specified by FAA AC33-1B for large size birds.

3. Iceball impacts conducted in the test program resulted only in reworkable dents on the leading edge. The denting, however, is undesirable from an engine maintenance viewpoint.

4. Weight savings of 30% were demonstrated for the FOD resistant spar/shell blade in comparison to a titanium blade; weight savings in excess of 48% can be expected using a reduced weight titanium spar design.

5. The titanium spar and the structural bond joint between the spar and the blade airfoil displayed no distress after impact with the maximum bird size used in the program (1400 g).

6. Construction of the fan blade using a metal matrix composite, in place of the epoxy matrix composite used in the NASA FOD program in 1973, was successful in significantly increasing the impact capability of the fan blade.

7. Of the two angle ranges specified for test in the FOD program, impacts at 0.56 radians (32°) angle of incidence are much more severe than those at 0.38 radians (22°).

8. The flexible retention design appreciably improved the large bird blade FOD resistance.

9. Based on a comparison of real and simulated bird test results, the simulated bird comprised of modified gelatin, at a specific gravity of 0.69, is a very satisfactory simulation of the real bird.

RECOMMENDATIONS

The following recommendations are made based on the results of this program:

1. Further development be undertaken to further improve the Hamilton Standard "QCSEE" FOD blade by (1) reducing the weight of the blade while maintaining its current level of FOD resistance. (2) Improving the resistance of the leading and trailing edge tip areas to foreign object damage.

2. Design and fabrication of a direct replacement QCSEE blade be undertaken by Hamilton Standard, under NASA funds, for test in the QCSEE engine.

3. Leading edge modifications be designed and tested to develop improved resistance to ice ball denting.

4. Consideration be given to using gelatin/phenolic micro-balloons as a bird simulation in all FOD testing to provide a standard base of comparison.

REFERENCES

1. Turbine Engine Foreign Object Ingestion and Rotor Blade Containment Type Certification Procedures, FAA Advisory Circular AC-33-1B dated 4/22/70.

2. Graff, J., Stoltze, L. and Varholak, E.M. (1973). Impact Resistance of Spar-Shell Composite Fan Blades, NASA Report CR-134521.

3. Cornell, R. W., (1975). Elementary Three-Dimensional Interaction Rotor Blade Impact Analysis, Paper No. 75-WA/GT-15 presented at the Winter Annual Meeting of ASME.

APPENDIX A

PROCEDURE FOR MAKING ICEBALLS - 5.08 CM DIA.

Iceball Material: Supersaturated Carbonic Acid

Specific Gravity of Iceball: 0.80 - 0.85

PROCESS

1. Fill the mold cavities with supersaturated carbonic acid until the fluid overflows.

2. Place the molds in a freezer and freeze at approximately 244°K (-20°F) for a minimum of three hours.

3. Remove from the freezer and allow it to remain at room temperature 292 - 300°K (65 to 80°F) for five to ten minutes.

4. Remove and shape the overflow knob by rubbing the area against a smooth metal surface which is at room temperature.

5. Five to ten minutes after removing the setup from the freezer remove the balls from the mold. Caution: Handle the iceballs carefully and quickly to prevent breaking and melting.

After removal from the mold the iceballs should be maintained in the freezer.

ICEBALL CHECKS

1. In checking specific gravity, weigh iceball on gram scale. Weight should be 54-59 grams for a specific gravity of 0.80 to 0.85 for 5.08 cm (2 inch) diameter.

TRANSPORTING AND INSTALLING IN RIG

1. Transport iceballs to rig in an insulated container. Exposure of iceballs in insulated container outside of freezer should not exceed 45 minutes.

2. Iceball handling time between freezer and insulated container, and between insulated container and storage compartment of rig should be kept to a minimum.

3. Storage compartment of rig is to be below freezing before inserting iceball.

APPENDIX B

CONVERSION OF U.S. CUSTOMARY UNITS TO SI UNITS

The International System of Units (SI) was adopted by the Eleventh General Conference on Weights and Measures, Paris, October 1960. Conversion factors for the units used herein are given in the following table.

Physical Quantity	U.S. Cust. Units	Conversion Factor	SI Units
Length	in	0.0254	meters (m)
Temperature	(F° + 460)	5/9	degrees Kelvin ($^\circ K$)
Density	lbm/in^3	27.68×10^3	kilograms per cubic meter (Kg/m^3)
Load	lbf	4.448	newtons (N)
Modulus, stress	psi = lbf/in^2	0.6895	newtons per square meter (N/m^2)
Plane angle	degree$^\circ$	0.01745	radians (rad)
Mass	lbm	0.4536	grams (g)
Velocity	fps	0.3048	meter/second (m/s)
Speed	rpm	0.1047	radian/second (rad/s)

*Multiply value given in U.S. Customary Units by conversion factor to obtain equivalent value in SI Unit.

Prefix	Multiple
centi (c)	10^{-2}
Kilo (K)	10^3
Mega (M)	10^6

DISTRIBUTION LIST

NASA CR-135001, NAS3-17837

Fiber Composite Fan Blade Impact Improvement

Addressee	Number of Copies
1. NASA-Lewis Research Center 21000 Brookpark Rd. Cleveland, OH 44135	
Attn: Contract Section B, MS 500-313	1
Technology Utilization Office, MS 3-19	1
AFSC Liaison Office, MS 501-3	1
AAMRDL Office, MS 500-317	1
Library, MS 60-3	2
Report Control Office, MS 5-5	1
C. C. Ciepluch, MS 501-7	1
R. J. Denington, MS 501-7	1
R. H. Kemp, MS 49-3	1
R. H. Johns, MS 49-3	1
N. T. Saunders, MS 105-1	1
C. C. Chamis, MS 49-3	1
R. L. Lark, MS 49-3	1
J. R. Faddoul, MS 49-3	10
J. C. Freche, MS 49-1	1
2. NASA-Scientific and Technical Information Facility P.O. Box 33 College Park, MD 20740 Attn: Acquisitions Branch	10
3. NASA-Office of Aeronautics and Space Technology Washington, DC 20546	
Attn: RW/G. C. Deutsch	1
RWM/J. J. Gangler	1
RJS/L. A. Harris (Dr.)	1
4. NASA-Langley Research Center Hampton, VA 23365 Attn: Library	1

DISTRIBUTION LIST (Cont'd)

Addressee	Number of Copies
5. NASA- George C. Marshall Space Flight Center Huntsville, AL 35812 Attn: Library	1
6. NASA-Lyndon B. Johnson Space Center Houston, TX 77001 Attn: Library	1
7. NASA-Ames Research Center Moffett Field, CA 94035 Attn: Library	1
8. NASA-Flight Research Center P.O. Box 273 Edwards, CA 93523 Attn: Library	1
9. NASA-Goddard Space Flight Center Greenbelt, MD 20771 Attn: Library	1
10. Jet Propulsion Laboratory 4800 Oak Grove Dr. Pasadena, CA 91103 Attn: Library	1
11. Advanced Research Projects Agency Washington, DC 20525 Attn: Library	1
12. Air Force Office of Scientific Research Washington, DC 20333 Attn: Library	1

DISTRIBUTION LIST (Cont'd)

Addressee	Number of Copies
13. Air Force Materials Laboratory Wright-Patterson Air Force Base, OH 45433	
Attn: MBM/S. Tsai (Dr.)	1
MBC/T. J. Reinhart	1
LC/W. J. Schulz	1
MXE/J. Rhodehamel	1
MBC/G. E. Husman	1
LC/G. P. Peterson	1
14. Air Force Aeronautical Propulsion Laboratory Wright-Patterson Air Force Base, OH 45433	
Attn: TBP/T. Norbut	1
CA/Heiser (Dr.)	1
TBP/L. J. Obery	1
15. Air Force Flight Dynamics Laboratory Wright-Patterson Air Force Base, OH 45433	
Attn: C. D. Wallace (FBC)	1
P. A. Parmley	1
16. Defense Metals Information Center Butelle Memorial Institute Columbus Laboratories 505 King Ave. Columbus, OH 43201	1
17. Department of the Army U.S. Army Material Command Washington, DC 20315	
Attn: AMCRD-RC	1
18. Department of the Army U.S. Army Aviation Materials Laboratory Fort Eustis, VA 23604	
Attn: Library	1

DISTRIBUTION LIST (Cont'd)

Addressee	Number of Copies
19. Department of the Army U.S. Army Aviation Systems Command P.O. Box 209 St. Louis, MO 63166 Attn: Library	1
20. U.S. Army Materials and Mechanics Research Center Watertown Arsenal Watertown, MA 02192 Attn: Library	1
21. Department of the Army Watervliet Arsenal Watervliet, NY 12189 Attn: Library	1
22. Department of the Army Plastics Technical Evaluation Center Picatinny Arsenal Dover, NJ 07801 Attn: H.W. Pebly, Jr.	1
23. Department of the Navy Office of Naval Research Washington, DC 20360 Attn: Library	1
24. Director Naval Research Laboratory Washington, DC 20390	1
25. Commander Naval Air Systems Command Washington, DC 20360	1
26. Commander Naval Ordinance Systems Command Washington, DC 20360	1
27. Department of the Navy U.S. Naval Ship R&D Laboratory Annapolis, MD 21402 Attn: Library	1

DISTRIBUTION LIST (Cont'd)

Addressee	Number of Copies
28. Naval Ship Systems Command Code 03423 Washington, DC 20360 Attn: C. H. Pohler	1
29. National Science Foundation Engineering Division 1800 G. St., NW Washington, DC 20540 Attn: Library	1
30. U.S. Naval Ordinance Laboratory White Oak Silver Spring, MD 20910 Attn: F. R. Barnet	1
31. General Dynamics Convair Aerospace Division Ft. Worth Operation P. O. Box 748 Ft. Worth, TX 76101 Attn: C. W. Rogers	1
32. General Dynamics Convair Aerospace Division P.O. Box 80847 San Diego, CA 92138 Attn: J. E. Ashton (Dr.)	1
33. Materials Sciences Corp. 1777 Walton Rd. Blue Bell, PA 19422 Attn B. W. Rosen (Dr.)	1
34. E. I. Dupont DeNemours and Company Inc. 1007 Market St. Wilmington, DE 19898 Attn: C. H. Zweben (Dr.) Bldg. 262, Rm. 433	1
35. E. I. Dupont DeNemours and Company Inc. Experimental Station Wilmington, DE 19898 Attn E. A. Merriman (Dr.)	1

DISTRIBUTION LIST (Cont'd)

Addressee	Number of Copies
36. General Technologies Corp. 1821 Michael Faraday Dr. Reston, VA 22070 Attn: R. G. Shaver (Dr.) Vice Pres., Engineering	1
37. McDonnell-Douglas Astronatuics Co. 5301 Bolsa Ave. Huntington, Beach, CA 92647 Attn: R. W. Seibold, A3-253	1
L. B. Greszczuk	1
38. Union Carbide Corp. Carbon Products Division P.O. Box 6116 Cleveland, OH 44101 Attn: J. C. Bowman, Director Research and Advanced Technology	1
39. Structural Composites Industries, Inc. 6344 North Irwindale Ave. Azusz, CA 91702 Attn: E. E. Morris Vice President	1
40. The Garrett Corp. AiResearch Manufacturing Co. 402 South 36th St. Phoenix, AZ 85034 Attn J. G. Schnell	1
41. Fiber Science, Inc. 245 East 157th St. Gardena, CA 90248 Attn: L. J. Ashton	1
42. United Aircraft Research Laboratories United Aircraft Corp. East Hartford, CT 06108 Attn: M. DeCrescente (Dr.)	1

DISTRIBUTION LIST (Cont'd)

Addressee	Number of Copies
43. Pratt & Whitney Aircraft Division United Aircraft Corporation 400 Main St. East Hartford, CT 06108	
Attn: F. Ver Schneider	1
T. Zupnik	1
F. Mahler	1
T. Dennis	1
44. General Electric Co. Aircraft Engine Group Evendale, OH 45215	
Attn: M. Grandy	1
C. Salemme	1
A. Adamson	1
45. General Electric Co. Lynn River Works 1000 Western Ave. Mail Drop 34505 Lynn, MA 01910	
Attn: F. Erich	1
46. General Electric Co. Corporate Research and Development Center 1 River Rd. Schnectady, NY	
Attn: S. Levy	1
47. TRW, Inc. 23555 Euclid Ave. Cleveland, OH	
Attn: W. E. Winters	1
I. Toth (Dr.)	1
48. Bell Aerospace Division of Textron Buffalo, NY 14240	
Attn: Library	1
49. Massachusetts Institute of Technology Department of Civil Engineering Cambridge, MA 02139	
Attn: F. J. McGarry (Prof.)	1

DISTRIBUTION LIST (Cont'd)

Addressee	Number of Copies
50. Illinois Institute of Technology 10 West 32nd St. Chicago, IL 60616 Attn: L. J. Broutman (Prof.)	1
51. Purdue University West Lafayette, IN Attn: C. T. Sun (Prof.)	1
52. Drexel University Philadelphia, PA Attn: P. C. Chou (Prof.)	1
53. Northwestern University Evanston, IL Attn: J. D. Achenbach (Prof.)	1
54. Hercules, Inc. Wilmington, DE 19899 Attn: G. C. Kuebler	1
55. University of Florida Gainesville, FL Attn: R. L. Sierakowski (Prof.)	1
56. George Washington University St. Louis, MO 63130 Attn: E. M. Wu (Prof.)	1
57. University of California, Los Angeles School of Engineering and Applied Science Los Angeles, CA 90024 Attn: B. S. Dong (Prof.)	1
58. Grumman Aerospace Corp. S. Oyster Bay Rd. Bethpage, Long Island, NY 11714 Attn: R. N. Hadcock	1
59. North American Aviation Division Rockwell, Inc. International Airport Los Angeles, CA 90009 Attn: L. M. Lockman (Dr.)	1

DISTRIBUTION LIST (Cont'd)

Addressee	Number of Copies
60. Hughes Aircraft Co. Aerospace Group Culver City, CA 90230 Attn: R. W. Jones, (Dr.) Mail Stop D 132	1
61. Avco Space Systems Division Lowell Industrial Park Lowell, MA 01851 Attn: T. L. Moore	1
M. Salkind (Dr.)	1
62. Lockheed-Georgia Co. Marietta, GA 30060 Attn: W. G. Juveric	1
63. Vertol Division The Boeing Co. Philadelphia, PA 19142 Attn: R A Pinkney	1
64. Whittaker Corp. Research and Development Center 3540 Aero Ct. San Diego, CA 92123 Attn: R. K. Berg (Dr.)	1
65. Southwest Research Institute 8500 Culebra Rd. San Antonio, TX 78284 Attn: T. Anyos	1
66. IITRI 10 West 35th St. Chicago, IL 60616 Attn: I. M. Daniel (Dr.)	1
67. Lawrence Livermore Laboratory University of California P. O. Box 808, L-421 Livermore, CA 94550 Attn: T. T. Chiao	1

DISTRIBUTION LIST (Cont'd)

Addressee	Number of Copies
68. Boeing Aerospace Co. P.O. Box 3999 Seattle, WA 98124 Attn: J. T. Hoggatt, MS 47-01	1
69. Martin-Marietta Corp. Denver, CO Attn: A. Holston	1
70. Battelle Memorial Institute 505 King Ave. Columbus, OH 43201 Attn: L. E. Hulbert (Dr.)	1
71. Babcock and Wilcox Co. Advanced Composites Department P. O. Box 419 Alliance, OH 44601 Attn: R. C. Young	1
72. National Bureau of Standards Engineering Mechanics Section Washington, DC 20234 Attn: R. Mitchell (Dr.)	1
73. University of Dayton Research Institute Dayton, OH 45409 Attn: F. K. Bogner	1
74. University of Illinois Department of Theoretical and Applied Mechanics Urbana, IL Attn: H. T. Corten (Prof.)	1
75. Detroit Diesel-Allison Division General Motors Corp. Indianapolis, IN Attn: M. Herman (Dr.)	1

DISTRIBUTION LIST (Cont'd)

Addressee	Number of Copies
76. Sikorsky Aircraft Division United Aircraft Corp. Stratford, CT 06602 Attn: Library	1
77. Douglas Aircraft Company 3855 Lakewood Blvd. Long Beach, CA 90846 Attn: R. Kawai	1